ORNL/TM-7313

ornl

OAK RIDGE NATIONAL LABORATORY

UNION CARBIDE

Pyrolysis and Physical Properties of Coal Blocks

P. R. Westmoreland
R. C. Forrester
J. B. Gibson

Fossil Energy Program

OPERATED BY
UNION CARBIDE CORPORATION
FOR THE UNITED STATES
DEPARTMENT OF ENERGY

Printed in the United States of America. Available from
National Technical Information Service
U.S. Department of Commerce
5285 Port Royal Road, Springfield, Virginia 22161
NTIS price codes—Printed Copy: A09 Microfiche A01

ORNL/TM-7313
Dist. Category UC-90d

Contract No. W-7405-eng-26
Fossil Energy Program

PYROLYSIS AND PHYSICAL PROPERTIES OF COAL BLOCKS

P. R. Westmoreland,* R. C. Forrester,†
and J. B. Gibson††

Date Published: June 1981

Prepared for
Department of Energy/Fossil Energy
Division of Fossil Fuels Extraction

OAK RIDGE NATIONAL LABORATORY
Oak Ridge, Tennessee 37830
operated by
UNION CARBIDE CORPORATION
for the
DEPARTMENT OF ENERGY

---

*On leave of absence.
†Currently employed by Fluor Corporation, Irvine, Calif.
††Currently employed by Dow Chemical Company, Plaquemines, La.

ACKNOWLEDGMENTS

The support of our staff contributed significantly to the success of this research effort. The authors cite the valuable contributions of: technicians Leonard S. Dickerson, Ron L. Andrews, Gary D. Owens, Sherry M. Gibson, David A. McWhirter, and Kendall Ladd; co-ops and summer participants C. Joseph Golden, Fred H. Wilson, Jane Cohill, T. C. Scott, Carl F. Bertsch, and Alvin L. Thoma; secretarial staff members Deborah S. Brown, Janice T. Shannon, Pamela G. Valliant, Ogene V. Jennings, and Wanda F. Gilliam; and the editorial staff members Martha G. Stewart, Vivian A. Jacobs, Debbie P. Stevens, and Lydia S. Corrill.

TABLE OF CONTENTS

LIST OF FIGURES

LIST OF TABLES

PYROLYSIS AND PHYSICAL PROPERTIES OF COAL BLOCKS

P. R. Westmoreland,* R. C. Forrester,†
and J. B. Gibson††

ABSTRACT

Interactions between the various physical properties of coal and its pyrolysis were characterized by studying the heating of 150-mm-diameter cylindrical blocks of Wilcox lignite, Wyodak subbituminous coal, Hanna bituminous coal, and Pittsburgh bituminous coal. (Some samples of coal overburden were also tested.) In the various coals, block "pyrolysis" caused gasification and cracking reactions and changes in char reactivity and in swelling, none of which is observed in powder pyrolysis. These changes were interpreted as having resulted from internal temperature gradients and flow patterns. To aid in an evaluation of this interpretation, physical and transport properties of coals were reviewed, measured, and correlated; new data on thermal diffusivity and conductivity of lignite are of particular interest.

This research was conducted in support of underground coal gasification (UCG) technology. Implications of the results for UCG are described, but the mechanisms and property data also have broader applications within the field of coal conversion.

---

*On leave of absence.
†Currently employed by Fluor Corporation, Irvine, Calif.
††Currently employed by Dow Chemical Company, Plaquemines, La.

1. INTRODUCTION

The research described in this report focused on the physical and reaction phenomena observed when block coal was heated. An understanding of these phenomena is useful in modeling underground coal gasification (UCG).

To generalize, UCG may be distinguished from other coal conversion processes by the physical nature of the reacting coal. In other processes, coal is mined, broken into small pieces, cleaned, and sized before reaction. In UCG, reaction occurs within a coal seam, both in the wall of an underground cavity and on the surface of coal chunks that have fallen from the roof of the cavity. Temperature gradients and fluid-flow patterns within the coal result in behavior different from that ordinarily observed in powdered coal. These changes were studied in the laboratory by heating blocks of coal in controlled atmospheres.

The research reported here was directed specifically to support the field development of UCG by the U.S. Department of Energy (DOE) through Laramie Energy Technology Center (LETC), Lawrence Livermore National Laboratory (LLNL), Morgantown Energy Technology Center (METC), and others; it also was directed at support of UCG development overall.

To develop a perspective on the technology of UCG and to understand the potential contribution of laboratory research to it, some background knowledge of the process is necessary. This introduction provides a context for the detailed results discussed in Sects. 3 and 4.

1.1 History and Current Status of UCG

The UCG concept dates back to 1868, the year that Sir William Siemans of Great Britain first proposed the gasification of waste and slack coal in mined-out workings. Twenty years later, Mendeleev proposed gasification of seam coal by igniting it through shafts. Anson G. Betts of the United States was awarded a patent in 1907 for his

air-steam UCG concept, in which ignition occurs either at the end of a single well (or shaft) or between two wells (or shafts) as forward combustion.[1]

Not until 1912 in Great Britain did William Ramsey begin the first experimental work on UCG, work that was interrupted by the beginning of World War I and was not resumed until after Ramsey's death. News reports of Ramsey's work reached Russia and apparently intrigued Lenin as a way to enable coal miners to escape the dangers of the mine. His comments of approval in Pravda were acted on 20 years later in 1933, when the U.S.S.R. established a state trust for research and development of in situ gasification.[1]

By 1936, 1500 persons in the U.S.S.R. were involved on UCG development, and the gas produced was used for the first time (experimentally) to fire a boiler. Several billion cubic feet of low-Btu gas had been produced at five locations by 1941. Although Soviet UCG development was interrupted during World War II, it continued afterwards until full commercial-scale operations began in the 1950s.[1] These sites are currently the only production UCG facilities in use in the world.[2]

In the mid- to late-1940s, in situ gasification experiments were also conducted in Belgium, France, Italy, Poland, the United Kingdom, and the United States. Most of this work concluded unsuccessfully about 1950, except for British and U.S. work, which ended unsuccessfully about 1960. In each of these cases, the two basic problems were (1) insufficient thickness of seams (less than 1.5 m) and (2) poor control of the underground reaction zone (unstable flame fronts, excessive water influx, and gas losses), which results in low heating values. Product gas with poor heating value resulted. Nevertheless, useful development took place, such as, techniques (at Gorgas, Alabama) to fill the underground reaction cavity with solids, more efficient utilization of the coal, and the use of "roof collapse" to maintain good coal-oxygen contact.[1]

In 1971, Arthur D. Little, Inc., reviewed the accumulated experience with and knowledge of UCG in a document prepared for the

Bureau of Mines. Based on this appraisal, the Bureau of Mines funded western coal field testing, begun in 1973 in Hanna, Wyoming, by the Bureau of Mines facility at Laramie (now LETC). In turn, LETC success with the Hanna I and II field tests spurred UCG development in the United States by government and private industry. Table 1.1 summarizes this development. In addition, the Alberta (Canada) Research Council conducted a field test, and a joint Belgian and German field test is planned for the early 1980s.

Potentially, UCG could produce fuel or synthesis gas (1) from otherwise unrecoverable coal resources, (2) at lower cost than from surface gasification, (3) with greater occupational safety, and (4) with less environmental impact than can be achieved by other coal recovery techniques. Economic feasibility has yet to be proved because reliable, predictable operation has yet to be demonstrated and techniques for the measurement and control of the environmental impacts involved require further refinement.[3] Nevertheless, the potential of UCG technology as an energy supplement provides ample justification for the serious interest shown it worldwide.

1.2 Description of the Linked Vertical Wells Process

The linked vertical wells (LVW) process is a good example of how UCG is operated. Process chemistry and product-gas handling are very similar for UCG and above-ground gasification. However, UCG design and operation are radically different from those of surface gasifiers because permeable coal and rock comprise the underground reactor, as illustrated by the LVW process.

Figure 1.1 is a cross-sectional diagram of the LVW process. Because partial combustion is a principal step, air or O_2 must be piped into the coal seam [two (air) injection wells are shown]. The natural moisture of coal and the influx of groundwater into the seam will frequently provide sufficient water for steam gasification reactions; when O_2 is used additional steam may have to be injected.

Table 1.1 Current field development of UCG in the United States (July 1, 1980), in chronological order of original field tests

Developer	Sponsor	Site	Coal Seam	Status
Laramie Energy Technology Center, Wyo.	DOE	Hanna, Wyo.	Hanna No. 1 subbituminous	Campaigns since 1973; all use reverse combustion linkage and air injection
Lawrence Livermore National Laboratory, Calif.	DOE; Gas Research Institute	Gillette, Wyo.	Felix No. 2 subbituminous	Hoe Creek No. 3 conducted successfully in fall 1979; wells linked by directionally drilled horizontal hole; steam and O_2 injection
Basic Resources, Inc., and Air Products and Chemicals	Texas Utilities Co.	Tennessee Colony, Tex.	Wilcox lignite	Second campaign was conducted during the fall and winter 1978-1979; (Soviet technology) air-burn an 11-well, 2-channel pattern and to O_2-burn two 2-well tests
Texas A & M University	Industrial sponsors; DOE	Sandow, Tex.	Wilcox lignite	Second test was conducted in 1979; air and reverse combustion linkage
Atlantic Richfield Coal Co.	ARCO	Gillette, Wyo.	Roland (Wyodak) subbituminous	Rocky Hill No. 1 test conducted Apr.-Dec. 1978, deep coal (193 m) reverse combustion, air
Morgantown Energy Technology Center, W. Va.	DOE	Pricetown, W.Va.	Pittsburgh bituminous	Pricetown I test was conducted in 1979; reverse combustion, air
Gulf Research and Development Co., TRW	DOE; GR & DC	Rawlins, Wyo.	G-seam subbituminous	Rawlins I was conducted in the fall of 1979 in a steeply dipping bed of coal; air
Public Utility Company (PUCO) of New Mexico, University of New Mexico, Los Alamos National Scientific Laboratories	PUCO; DOE	Farmington, N. Mex.	Fruitland subbituminous	First field test is yet to to be conducted

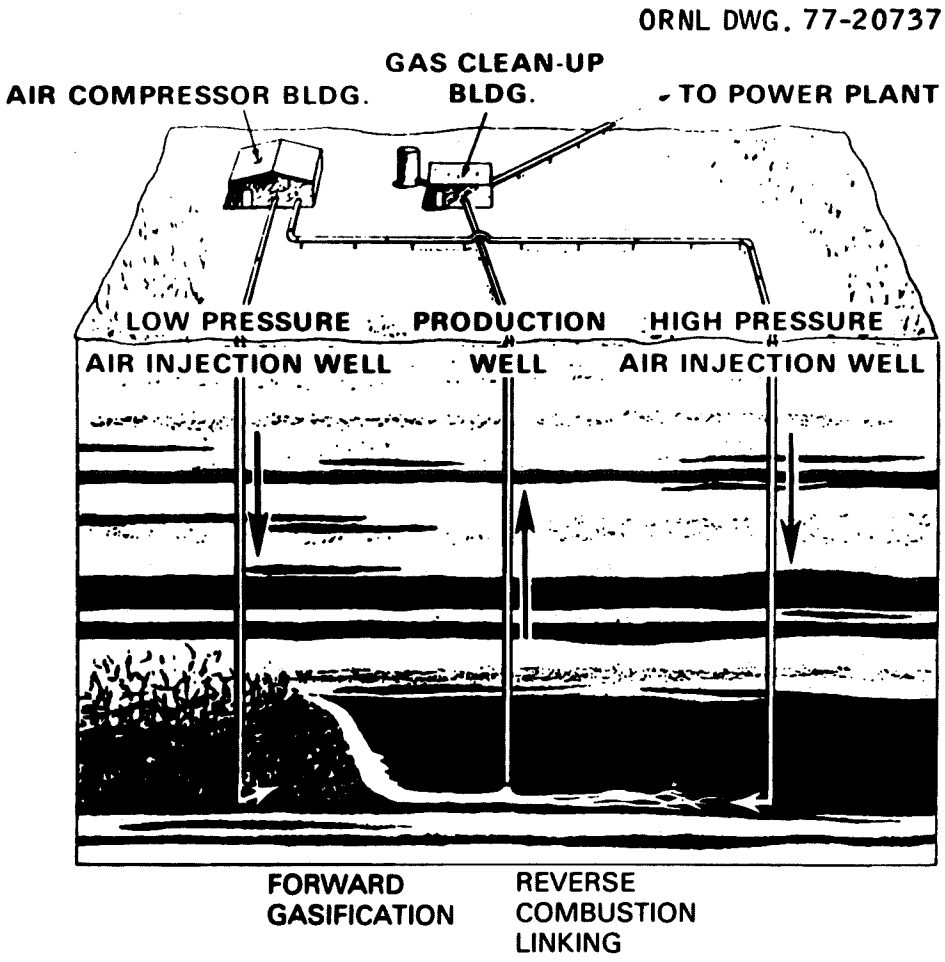

Fig. 1.1. Cross-section of the linked vertical wells process of UCG.

Gas must flow easily from the injection well to the production well. Because the natural permeability of most coals is low, the wells must be linked by a zone of enhanced permeability. Reverse combustion linkage is an important feature of the LVW process, as shown in Fig. 1.1. By this technique, a small flame front is drawn through the seam toward an air source, leaving behind it a porous, carbonized channel. An alternative method of linking the wells is to connect them by a horizontal hole, drilled from the surface.

Once ease of air flow at high rates is provided through the linkage, forward gasification is begun (Fig. 1.1). The reactor cavity grows predominately from the injection well (low-pressure, high-volume) toward the production well. Overall, the coal is simultaneously dried, pyrolyzed, gasified by steam and CO_2, and burned, producing a mixture of N_2, H_2, CO, CO_2, CH_4, H_2O, some tars, and other gases. These products are swept out by the gas flow through the linkage to the production well (Fig. 1.1).

The reaction cavity grows by the breakdown of its walls by incineration and by progressive collapsing of the roof. At the cavity wall or at the surfaces of fallen chunks of roof, heat from combustion moves into the coal seam, setting up a temperature gradient. Gasification of char and hydrocarbons occurs at temperatures >900 K, consuming H_2O and CO_2 to make H_2 and CO. Deeper into the coal seam, the coal pyrolyzes (thermally decomposes) at 500 to 900 K, forming char, CH_4, heavier hydrocarbons, and other gases. Deeper still, wet coal is dried at temperatures around 300 K. Thus, products of each region must escape against the temperature gradient (through hotter regions) in the coal seam.

1.3 Application of Block Data

We recognized that by heating coal blocks in the laboratory under controlled conditions, many ramifications of countercurrent heat and mass flux could be examined. In the experiments described herein, variables included coal type, heating rate, maximum temperature, and

surrounding atmosphere for the cylindrical blocks. Resulting data on product yields and internal time-temperature histories suggest mechanisms of physical and chemical change that may be applied to improve models of UCG processes. As an important example, steam generated inside the coal by drying was observed to gasify the block as it escaped (Sect. 3).

In addition, inclusion of data on various properties of coal and of overburden (strata overlying the coal seam) is important for good modeling. Swelling, shrinking, and spalling of these materials affect the flow of products and cavity growth. Information on the basic properties of coal and char — density, porosity, surface area, specific heat, enthalpy, thermal diffusivity, and thermal conductivity — is necessary for mechanistic modeling of UCG, but data for low-rank coals and for chars are frequently unavailable. As a part of this research, available data on these properties were reviewed, new data were gathered, and new correlations were developed (Sect. 4). Associated research on the heating and property measurement of overburden samples was included in Sect. 5.

Mathematical models have been applied to various aspects of UCG; each has been directed toward improving process monitoring, control, analysis, and, ultimately, predictability. For example, thermal models have been developed to monitor the growth of linkage paths and the cavity.[4,5] These models rely on an understanding of temperature profiles and accurate data on thermal conductivities. In addition, global models are being used to set air injection rates and to estimate coal usage during the progress of field tests. To improve such models, this research was conducted to better define those reactions and properties of coal that make UCG different from other coal conversion processes. (No UCG models were developed; model development was outside the scope of the project.)

Such research as we have begun must be undertaken with the realization that the ultimate "laboratory" for UCG must be the field. Process research in the laboratory may be categorized as (1) scaled

simulation, (2) study of individual process steps, or (3) characterization of materials involved in a process. As for the first category, the nature of UCG processes dictates that laboratory research cannot duplicate process conditions — complex flow patterns, geological stresses, and roof collapse cannot be scaled down. Nevertheless, field results do indicate process steps and materials that can be studied in the controlled environment of the laboratory and yield meaningful results. By judicious application of results like those reported here, the understanding of UCG can be increased, and the design, operation, and control of UCG can be ultimately improved.

1.4 References for Section 1

1. A. D. Little, Inc., A Current Appraisal of Underground Coal Gasification, U.S. Bureau of Mines, OFR 11-72, PB-209, p. 274 (1971).

2. B. R. Clements, "1977 Progress Report for the Texas Utilities UCG Program," Proceedings of the 3rd Annual Underground Coal Conversion Symposium, CONF-770652, Livermore, Calif., Lawrence Livermore National Laboratory, pp. 81-82 (1977).

3. P. R. Westmoreland, R. C. Forrester III, and A. P. Sikri, "In Situ Gasification: Recovery of Inaccessible Coal Reserves," Proceedings of the International Conference on Alternative Energy Sources, Miami Beach, Fla., Dec. 5-7, 1977, vol. 7, pp. 3113-3132 (1978).

4. P. J. Hommert, "Parameter Estimation Applied to Thermal Data," SPE 7524, presented at 53rd Annual Fall Technical Conference at SPE/AIME, Houston, Tex., Oct. 1-3, 1978.

5. R. W. Lyczkowski, C. B. Thorsness, and W. R. Aiman, A Simple Model for Locating the Front, Lawrence Livermore National Laboratory, UCRL-52461 (1978).

2. EXPERIMENTAL APPARATUS AND PROCEDURES

Cylindrical, 150-mm-diam blocks of coal were heated in a specially designed apparatus to temperatures as high as 1310 K (1040°C). Heating was controlled such that surface temperature could be increased at a constant rate, typically 3 K/min. As a result, a steep, moving temperature gradient could be set up and measured within the block. Throughout the experiment, a flow of purge gas maintained a controlled atmosphere around the block and purged products from the reactor. Product vapors were condensed and accumulated; noncondensible gases were sampled and metered.

Seventy-eight experiments were conducted in which different heating rates, maximum temperatures, coal ranks, and purge gases were used. The first series of 13 experiments was designated BP1 (experiment BP1-1, BP1-2, etc.). After the apparatus was rebuilt in a different building, a new series was started, BP2 (experiments BP2-1 through BP2-58). Details of the conditions and yields for the BP1 and BP2 series are included in Appendix 1, and interpretation of the results is presented in Sect. 3. Near the end of coal experiments, seven experiments (designated as OB experiments) were conducted using overburden samples from the Lawrence Livermore National Laboratory, Hoe Creek UCG site; details and discussion of these experiments are included in Sect. 5.

The purpose of this section, Sect. 2, is to describe in more detail the block "pyrolysis" apparatus, the coals and purge gases, experimental procedure, data analysis, and safety systems.

2.1 Block Pyrolysis Apparatus

A versatile apparatus for the heating of large coal samples was fabricated beginning in December 1974 (Fig. 2.1). This "block pyrolysis" apparatus was designed to heat samples that were as large as 200 mm in diameter and 350 mm long (8-in. diameter and 14 in. long). A temperature programmer permitted surface temperature of the sample to be raised at constant rates of 0.1 to 10 K/min to temperatures as

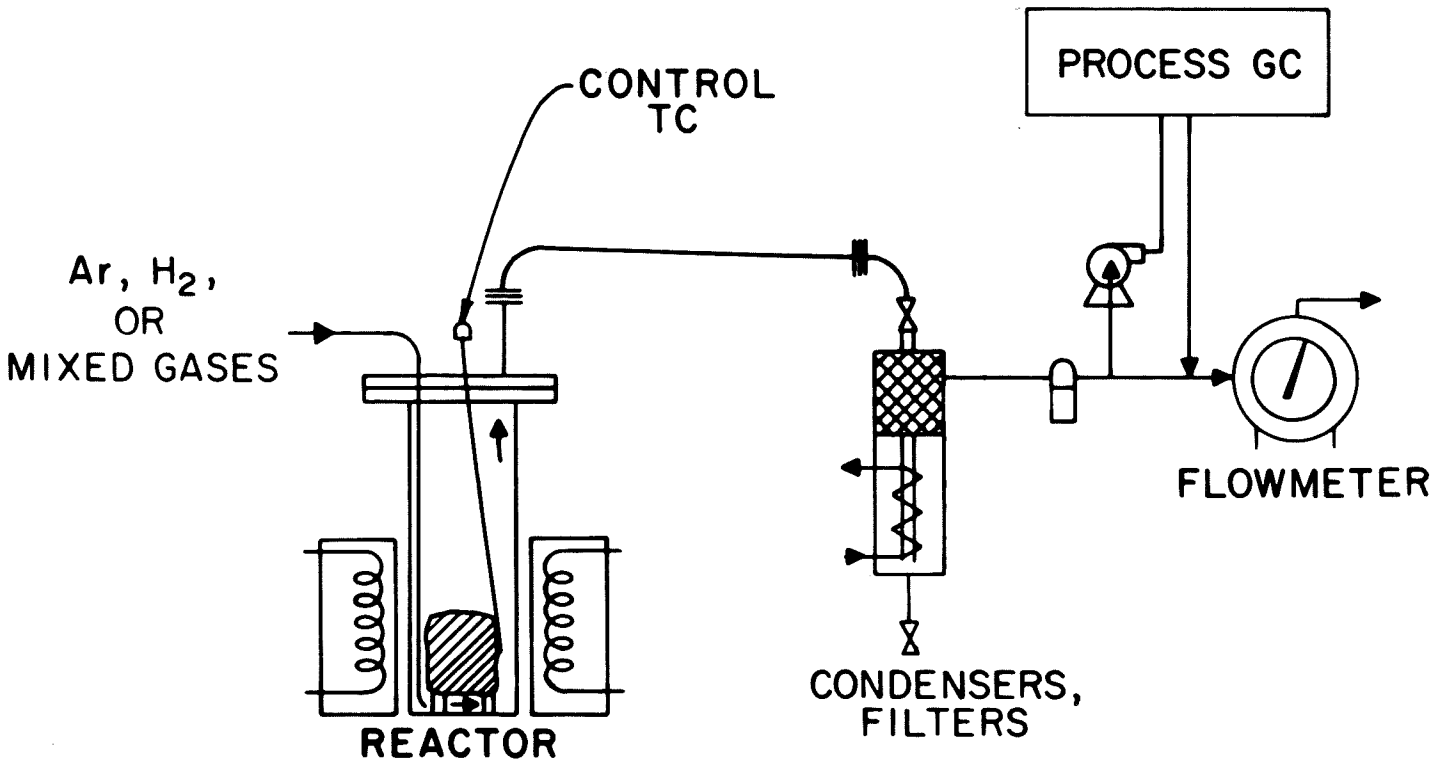

Fig. 2.1. Simplified schematic diagram of the block heating apparatus.

high as 1373 K (1100°C). The apparatus consists of the (1) purge gas metering and supply system; (2) reactor and heating system; (3) condenser and filter system; (4) gas sampling, analysis, and metering system; and (5) computer data collection system.

2.1.1 Purge gas supply and metering

Both inert gas (Ar) and reducing gases (H_2 or mixed gases) have been used as purge gases in the block pyrolyzer. The proportions of Ar, H_2, CO_2, CO, CH_4, and H_2O in the mixed gases are listed in Table 2.2, Sect. 2.2.

Two gas-feed systems were available for inert gas supply, each with a high-pressure regulator and connections for three, 264-mol (225-scf) cylinders. A separate header and regulator for reducing gas supply had connections for four cylinders of dry reducing gas and one of inert gas so that lines could be purged of O_2 before the experiment and of reactive gas following the experiment. These headers were located outside the building to permit adequate ventilation.

The feed system was such that steam could be injected into the reactor along with the purge gas. In the two experiments purged by mixed purge gases, water was metered into the purge gas line at approximately 0.25 g/min from an 800-cm^3 reservoir. No water was introduced until the reactor temperature exceeded 398 K (125°C), so that when entrained water entered the reactor, it was instantly converted to steam.

2.1.2 Reactor and heating system

For all experiments, a cylindrical reactor was heated inside an electrical furnace. The reactor was fabricated of 8-in., sched 10, 304L stainless steel pipe; the inside diameter was 211.6 mm (8.329 in.), and the inside depth was 610 mm (24 in.). A plate of 304L stainless steel was welded to the cylinder bottom, and a 150-lb slip-on flange was welded to the top. For protection against high-temperature oxidation, the reactor wall was coated by a commercially prepared nickel-chromium-aluminum coating (METCO No. P443-10).

All connections to the reactor came through the removable reactor top. Connections were provided for a 1/4-in. purge gas line; a 2-in. heated pipe for carrying off-gas to the condenser; three thermocouples used for monitoring and controlling the reactor temperature; a 0.35-psig pressure gauge; a 70-kPa (10-psi) pressure relief valve; and four internal-block thermocouples. These 1.02-mm-diam (0.040-in.) chromel-alumel thermocouples were inserted through a Conax lava-sealed Multihole Packing Gland. Although as many as 37 internal thermocouples were used for special experiments, 5 to 12 thermocouples were normally used to measure internal temperature profiles.

The large coal blocks were mounted upright (on the end of the cylinder) near the bottom of the reactor on four small cubes of firebrick, which rested on a horizontal platform of steel mesh. This platform was suspended from the underside of the reactor top by long, thin steel rods welded to the periphery of the platform. (Small cores of coal or overburden were placed on a single piece of firebrick.) If the blocks were positioned carefully, all faces of the cylinder received about the same radiant heat flux from the reactor walls.

The box furnace used in most experiments was fabricated by Oak Ridge National Laboratory (ORNL). Four flat-plate elements were used (Lindberg Hevi-Duty Model 50874, Type 56-KTS), each rated for 1350 W and a maximum temperature of 1478 K (1205°C). By wiring two elements in parallel to each of two Variac power supplies, a total furnace power of 5400 W was achieved at 230 V. The furnace was 460 mm (18 in.) high with a heated length of 360 mm (14 in.). Because of the box shape, the distance from the flat furnace element to the curved reactor wall varied from 10 to 60 mm.

A cylindrical furnace was used in the final two experiments of this series to provide more even heating around the circumference of the reactor. Four quarter-circular elements (Lindberg Hevi-Duty Model 50842, Type 8716-KSP) were used in this furnace and were strapped onto the reactor. Each element was rated for 2100 W and

1478 K (1205°C); the combined power of 8400 W was achieved at 230 V. The length of the heated section was 406 mm (16 in.).

To control the furnace temperature, an ORNL-fabricated temperature programmer was developed. It generated a linearly increasing set point for a modified Leeds and Northrup temperature controller; the temperature sensor was a thermocouple positioned alongside or just above the top edge of the cylinder. By using the temperature programmer, heating rates of 0.1, 0.2, 0.3, ..., 0.9, 1.0, 2, 3, ..., 9, or 10 K/min could be generated. This temperature ramp could be started at any temperature in the operating range; this capability permitted predrying of a sample or other special experiments.

The insulated reactor and furnace are pictured in Fig. 2.2. An insulated, horizontal 2-in. pipe connected the reactor to the condenser; in this photograph the pipe is hidden behind the thermocouples.

2.1.3 Condenser and filter system

Water and condensible organic vapors in the product gas were separated from noncondensibles by a water-cooled condenser and by several demisters (Fig. 2.1).

In the glass-walled primary condenser, hot gas was delivered to the condenser bottom by an axially positioned 2-in. pipe (uninsulated). The gas flowed upward between the delivery pipe and the condenser wall, contacting a copper coil that contained cooling water flowing countercurrently. Most of the liquid condensed on the coil or condenser wall and accumulated in the bottom of the condenser. A ball valve on the condenser bottom allowed collection of condensibles of low viscosity after the experiment; any remaining material was scooped out or wiped onto weighed rags.

Glass wool was packed into the upper part of the condenser and into the 1-in. exit pipe to knock out remaining tar/water mist. Next, a cotton-string filter was used to remove the last of the mist. To improve mist collection during the experiments that tested overburden cores, the string filter was cooled with dry ice. Finally, in the last two experiments,

ORNL Photo 1090-75

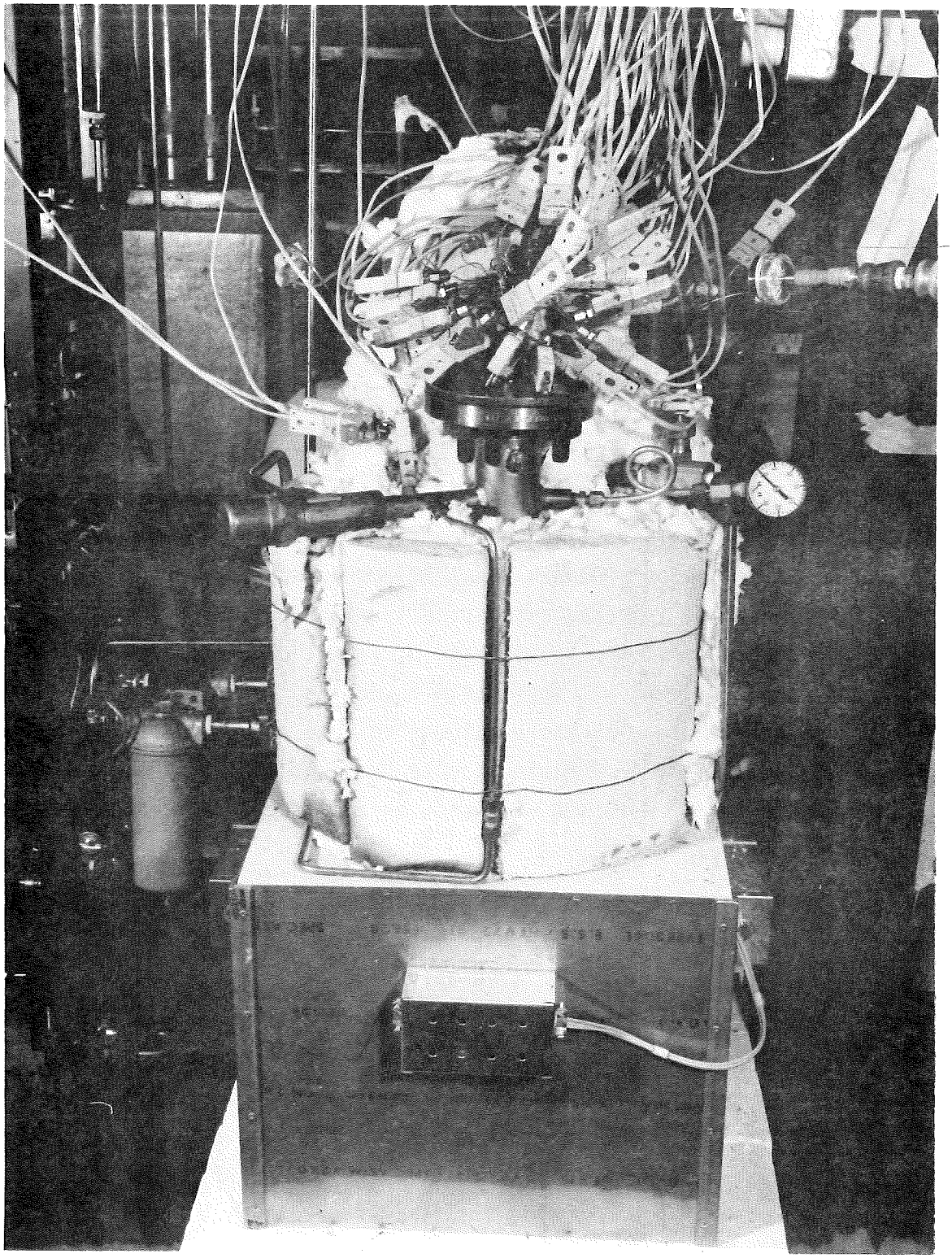

Fig. 2.2. Furnace and insulated top of the block reactor.

BP2-57 and BP2-58, a cyclonic knockout pot was installed upstream of the string filter and both were immersed in ice water.

2.1.4 Gas sampling, analysis, and metering

Once condensibles were removed, noncondensible gases were periodically sampled for composition analysis.

Through experiment BP2-39, grab samples were taken in 250-cm^3 glass sample bottles (Fig. 2.3); 4 to 50 samples were taken per run. Analysis was by mass spectrometry (MS); separate analysis by gas chromatograph (GC) was used to measure the N_2/CO ratio, which is not easily resolved by MS because both molecular weights are 28.01.

For experiment BP2-39, a process gas chromatograph was installed to provide better, more frequent analysis of gas composition. A slip stream was drawn from the cleaned, noncondensible product gas and metered into the sampling valves of a Bendix Model 7170 process GC. In this system, a 40-mm^3 sample was injected automatically with N_2 into Porapak Q and 5A molecular-sieve columns to separate H_2 from the other components. A second sample (1 cm^3) was injected with He into a valved set of Porapak Q and 5A molecular-sieve columns to resolve CO_2, CO, H_2S, C_2H_4, C_2H_6, C_3H_6, C_3H_8, and Ar. Minimum cycle time was 8 min. A single thermal conductivity detector was used; sweep gases for the two columns are N_2 and He, respectively.

Gas flow rate was measured by a 28.32-cm^3 (1-ft^3) wet-test meter. By attaching a magnet to the pointer tip and a stationary magnetic reed switch to the meter face, time between revolutions could be monitored by computer and converted to average liters per min. During early experiments, rotameters were used to measure flow rates, and for some experiments a smaller, 7.080-cm^3 (0.25-ft^3) wet-test meter was used. A Hastings-Raydist thermal mass flowmeter (0-0.669 mol/min H_2 equivalent) was installed for experiments BP2-57 and BP2-58 and was tied to computer data monitoring for improved accuracy.

ORNL Photo 1798-75

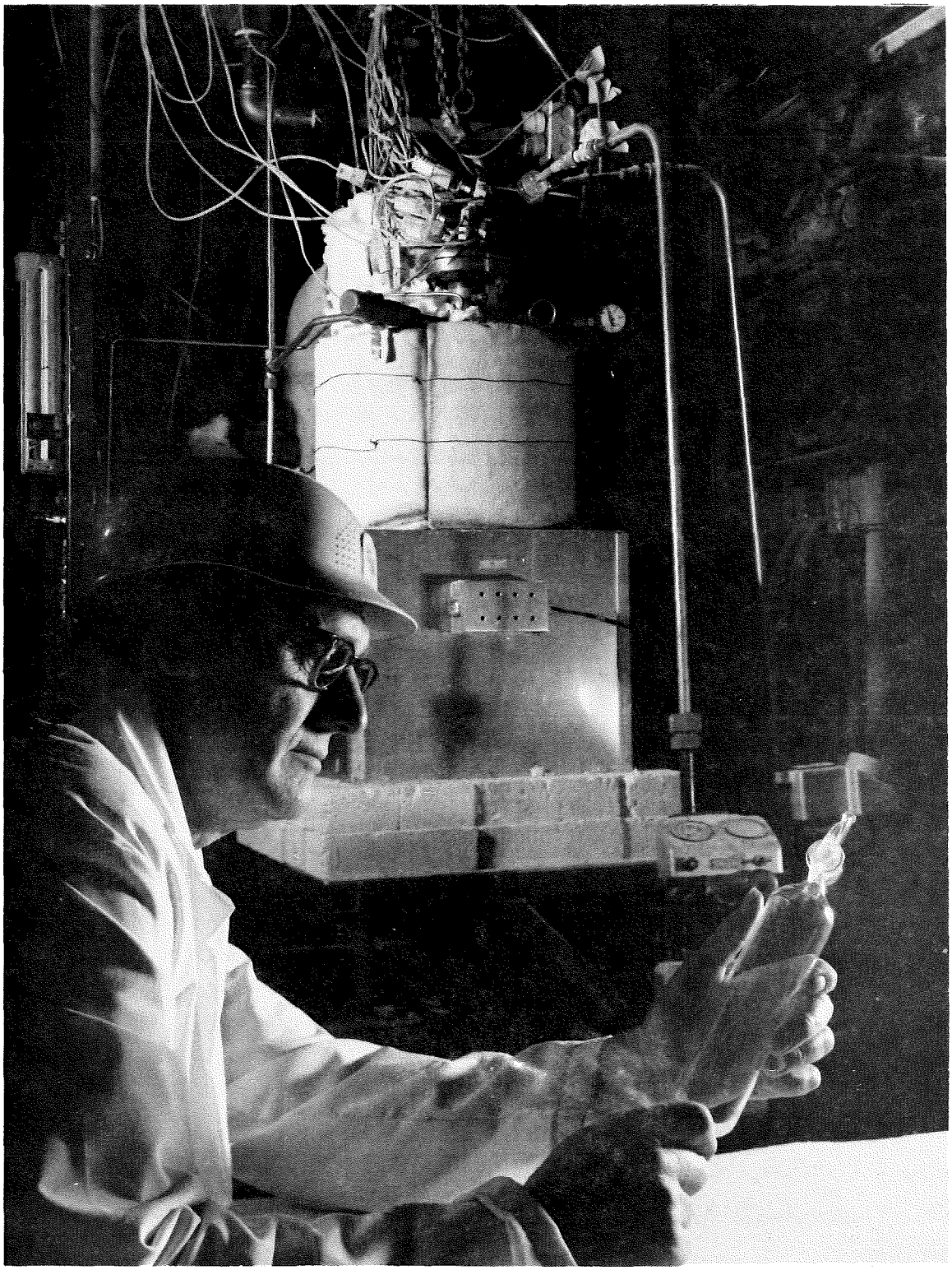

Fig. 2.3. Examining a gas sample bottle; block reactor in background.

After sampling was complete, product gas passed through a vapor trap before being vented. Approximately 1 kg of activated charcoal served to trap H_2S and the remaining hydrocarbon vapors.

2.1.5 Computer data collection

Starting with experiment BP2-48, temperatures and effluent flow rates were logged by a PDP 11/40 minicomputer. Although the computer was time-shared, 16 analog-to-digital converters were dedicated for use in this experiment. Logged data are stored on DECTAPE magnetic tapes and on disk.

Data provided by 12 chromel-alumel thermocouples were simultaneously recorded on 12-point Brown recorders and monitored by the computer. Ice-water reference junctions were used on the computer thermocouple circuits. To facilitate interpretation of temperature data, temperature profiles and heating-rate (K/min) distributions within the blocks could be plotted on a visual display (CRT with copier).

Flow measurements by wet-test meter and thermal mass flowmeter were described in Sects. 2.1.1 and 2.1.4. The signal from the wet-test meter was one 1.5 VDC pulse per cycle, lasting approximately 5 s; time of the start of the pulse was determined with 0.1-s accuracy. The mass flowmeter produced a 0 to 5 VDC signal proportional to the scale of the instrument. For the mass flowmeters, data on the composition of the gas was also required to calculate flow rate.

2.2 Raw Materials

2.2.1 Coals

Four coals were tested in the block pyrolyzer — a lignite (Wilcox), a subbituminous coal (Wyodak), a shrinking bituminous coal (Hanna), and a swelling bituminous coal (Pittsburgh). Analyses for each coal are presented in Table 2.1. Cored samples of overburden were also tested; descriptions of these samples will be deferred to Sect. 5.

Table 2.1. Standard analyses of coals used in ORNL block pyrolysis experiments and in UCG field tests

Seam	Wilcox lignite	Wyodak[a]		Felix No. 2[b]	Hanna No. 1 For UCG[c]	Hanna No. 1 ORNL samples	Pittsburgh bituminous
Moisture, wt %	37.5	33.6	(0.05)	30.11	8.62	9.9	1.77
Proximate analysis, wt % dry							
Ash	14.0	5.34	(0.63)	5.80	31.65	3.5[d]	5.8
Volatile matter	54.7	47.0	(1.80)	45.96	34.65	40.3	37.5
Fixed carbon (by difference)	31.3	47.6		48.24	33.7	56.2[d]	56.7
Ultimate analysis, wt % maf[e]							
Carbon	73.4	73.3	(0.97)	72.15	72.59	75.5	84.2
Hydrogen	6.1	5.22	(0.52)	5.46	5.89	6.0	5.9
Nitrogen	1.38	1.12	(0.10)	1.51	1.83	1.85	1.60
Sulfur	1.9	0.59	(0.03)	0.51	1.10	0.42	3.2
Oxygen (by difference)	17.2	19.8		18.54	18.59	16.2	5.1
Heating value							
kJ/kg maf	30,100	29,200	(610)	29,300	31,800	30,500	35,400
Btu/lb maf	12,930	12,650	(265)	12,700	13,770	13,230	15,350
Btu/lb, mmf[f]	7,770	8,560		8,740	12,525	11,910	14,610
Rank	lig A	sub C		sub C	hvCb	hvCb	hvAb

[a] Average and standard deviation for eight samples.
[b] Source of data: Fischer, D. D., J. E. Boysen, and R. D. Gunn, "Energy Balance for Second Underground Coal Gasification Experiment, Hanna, Wyoming," Trans. SME, AIME 262, 341 (December 1977).
[c] Source of data: LLL In Situ Gasification Program Quarterly Progress Report, January through March 1978, UCRL-50026078-2, Lawrence Livermore National Laboratory, Livermore, Calif., October 1978.
[d] Despite differences from nominal analysis of seam for UCG, samples used in the two ORNL experiments also came from the UCG field site.
[e] Moisture- and ash-free.
[f] Moist, mineral-matter-free.

All coal samples were obtained and preserved as carefully as possible to minimize drying and oxidation. The Wilcox lignite, taken from the Calvert Bluffs formation of the Wilcox group, was obtained in chunks from freshly exposed, strip-mined coal (Sandow Mine, ALCOA/ Industrial Generating Co.; Rockdale, Milam County, Texas). Wyodak subbituminous coal came from the Roland-Smith seams, also at a fresh strip-mine face (Wyodak Mine, Wyodak Resources Development Corp.; Gillette, Campbell County, Wyoming). Two cored samples of Hanna No. 1 coal were provided by LETC staff from the Hanna UCG field site (Hanna, Carbon County, Wyoming). Finally, chunks of freshly mined Pittsburgh seam coal were selected by METC staff from the conveyor belt of a local mine (Conoco Coal Co.; Monongalia County, West Virginia). All of these samples were sealed in plastic bags and shipped in rigid containers. At ORNL the wet, low-rank coals were removed and stored underwater in 55-gal drums; Pittsburgh coal was kept wrapped in plastic.

2.2.2 Purge gases

Cylinders of pure Ar (99.998%) or H_2 (99.9%) were used to supply purge gas in nearly all the experiments. Argon was used rather than N_2 because gas yield calculations can be complicated by pyrolysis-generated N_2.

For experiments BP2-57 and BP2-58, a mixed purge gas was prepared to simulate the product gas of UCG (Table 2.2). Dry gas composition was selected on the basis of Hanna and Hoe Creek field data; cylinders of the mixed gas were prepared by Matheson Gas Products. As described in Sect. 2.1.1, distilled water was introduced into the metered dry gas; the compositions of Table 2.2 were produced when the water vaporized in the reactor.

2.3 Experimental Procedure

The general procedures for block pyrolysis, overburden testing, and thermal property measurement were basically the same: a cylindrical sample was heated by increasing its surface temperature at a constant

Table 2.2. Composition of simulated UCG sweep gas in experiments BP2-57 and BP2-58

Gas	Composition (mol %)			
	BP2-57		BP2-58	
	Dry	Wet	Dry	Wet
H_2	16.70	14.2	16.70	15.4
CH_4	3.89	3.3	3.87	3.6
CO	13.92	11.8	13.84	12.8
CO_2	13.78	11.7	13.77	12.7
Ar[a]	51.71	43.9	51.82	47.7
H_2O		15.2		7.9

[a]Substituted for N_2, which is present in UCG product gas.

rate to some maximum temperature and the temperature held constant until the interior of the sample reached thermal equilibrium with the surface.

Chunks of coal or sealed cores of overburden were first shaped, if necessary, and then instrumented with thermocouples. Sample shaping, which took place just before an experiment began, involved selection of a piece of coal, cutting an approximate 150-mm-diam (6-in.), right circular cylinder with a band saw and smoothing and evening the cylindrical face with a sander. These machinery operations were conducted under a water spray, again to prevent drying or oxidation. Overburden samples needed no machining, but a slice approximately 20-cm-thick was cut off one end for physical property testing and chemical analysis.

Holes 1.2-mm (3/64-in.) in diameter were drilled into the samples to accept 1.02-mm-diam (0.040-in.) chromel-alumel thermocouples. During drilling, the coal cylinders were held underwater and the sealed cores of overburden were exposed only on one end. Several placement patterns (Fig. 2.4) were used to study and minimize any perturbations of the temperature profiles that might be caused by the thermocouples themselves. The most satisfactory procedure was to place holes no closer than 12 mm (1/2 in.) on one or more radii. Holes were generally drilled only to mid-height of the coal block, although for some experiments holes were drilled to different heights near the axis of symmetry (see Fig. 2.4). As shown in Fig. 2.5, radial positions of the thermocouple junctions were indirectly determined by measuring radial positions of the holes drilled at the top of the coal block. Clearly, this was only an approximation to the junction position because the long drill bits that were used can veer in the coal. Depth of thermocouple penetration was also measured. For BP2-57, BP2-58, and overburden tests, the cylindrical samples were x-rayed to establish precisely the position of the thermocouple tips.

The coal block was placed on the suspended mesh platform and was instrumented with thermocouples. Two or three strands of wire were normally wrapped around the coal sample to provide structural support; thermocouples were often held between these wires and the block. Except for bituminous coal tests, the furnace control thermocouple was positioned

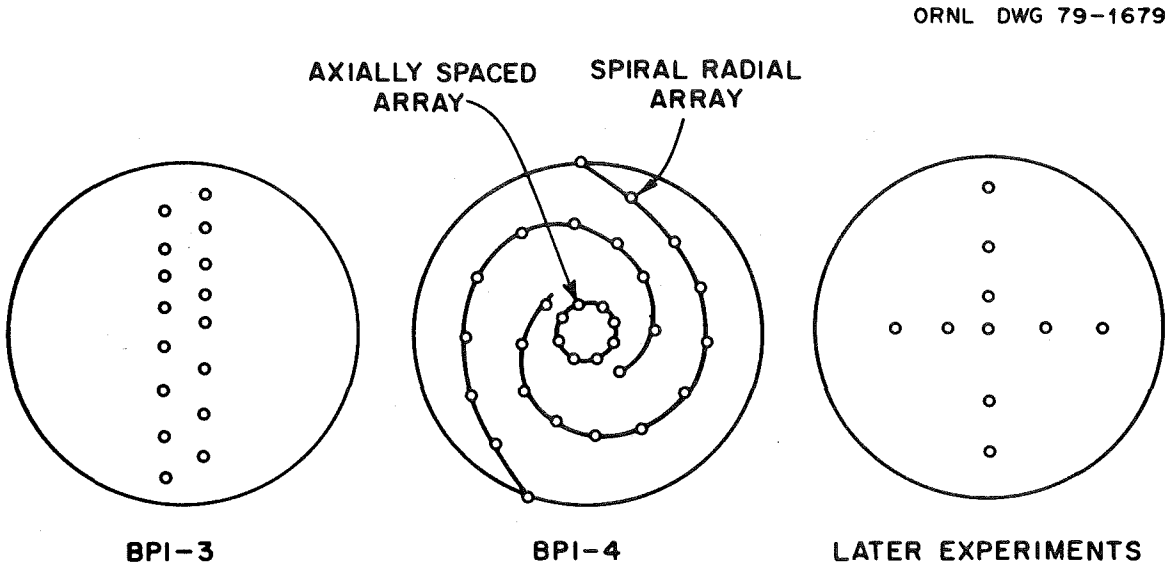

Fig. 2.4. Thermocouple patterns used to instrument coal blocks (typically 152-mm or 6-in. diameter) — top view.

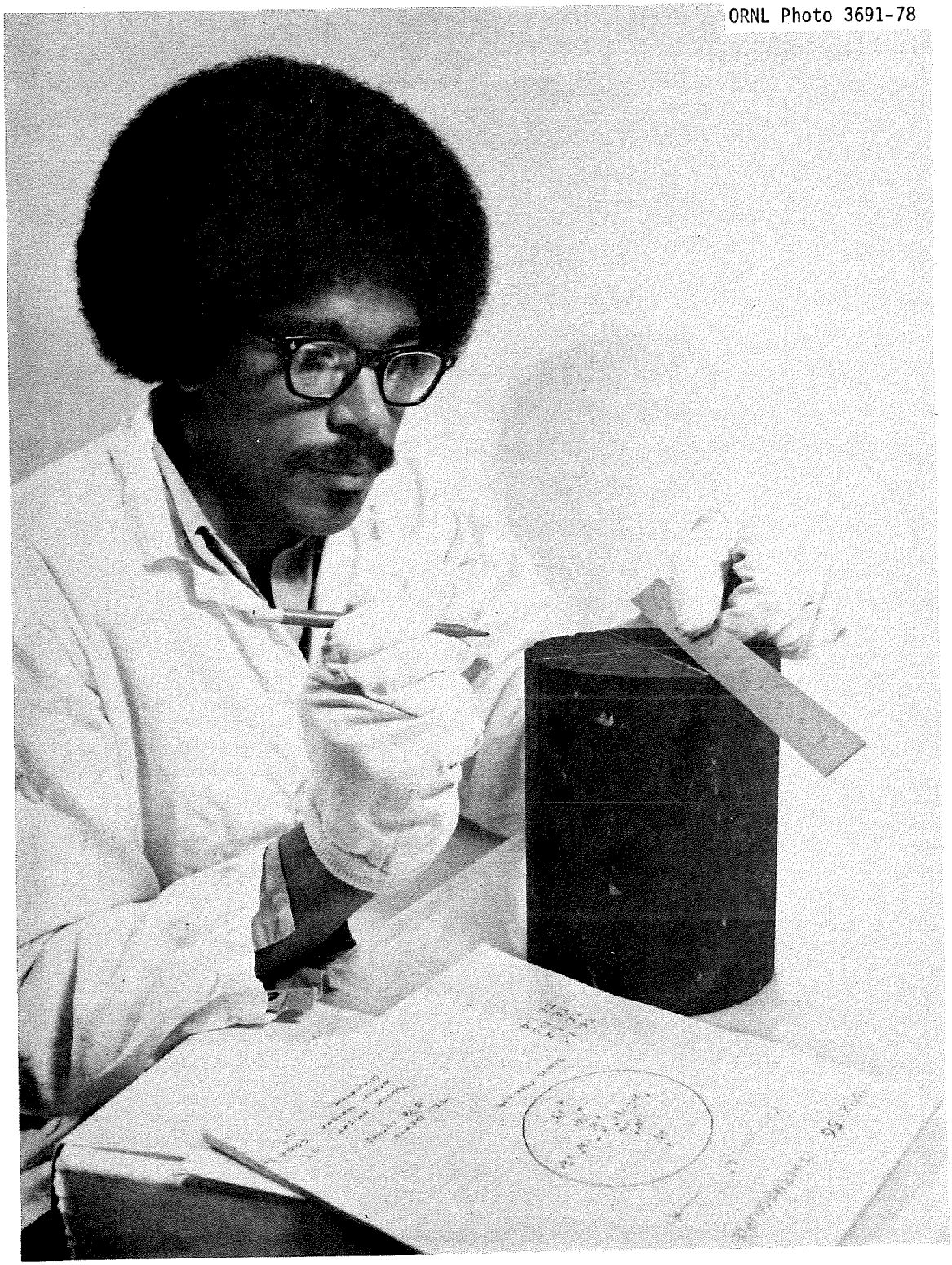

Fig. 2.5. Measuring positions of thermocouple holes in a block of Wilcox lignite.

alongside the cylinder. The swelling bituminous coal tended to engulf the control thermocouple, ruining our attempt to control temperature. In those experiments, the thermocouple was placed just above the top edge of the block.

As final steps of preparation, the reactor was sealed, leak-tested, insulated, and purged of air with inert gas. When the purge gas for the experiment was reactive, the reactive gas was used to purge the inert gas from the system. Three experiments (BP2-18, BP2-19, and BP2-52) used coal that had been predried in vacuum or in inert gas before the ramped heating began. These blocks were heated until internal temperatures were nearly uniform and above 378 K (105°C) but less than 423 K (150°C).

Next, steady flow of purge gas was established and heating began; the temperature programmer set heating rates at 0.3, 3, or 10 K/min. Gas flow rates and liquid levels in the primary condenser were periodically logged, and system temperatures and pressures were monitored. When the maximum temperature for the experiment was reached (between 773 K to 1273 K or 500 to 1000°C), the programmer was put on hold and temperatures within the sample were allowed to equilibrate with the surface. Based both on achievement of temperature equilibration and the termination of gas evolution, heaters were shut off and the continuously purged system was cooled to room temperature over about 36 h. (This shutdown procedure was slightly modified if the purge gas was H_2 because the purge was switched to Ar when temperatures equilibrated. For mixed purge gas experiments, the switch to Ar occurred when maximum surface temperature was reached. These modifications were necessary from safety and cost considerations to limit consumption of the char block by the reactive purge gases after the planned termination of the experiment.)

Following the experiment, the reactor was unbolted and the top was lifted, exposing the instrumented char sample to air (Fig. 2.6). For low-rank coals, temperatures had to be monitored during this step. Pyrophoricity (spontaneous heating and oxidation) was frequently observed when the low-rank chars were exposed to air; bituminous char was not pyrophoric. To characterize the relative levels of pyrophoricity, an initial rate of self-heating (K/min) was measured for lignite and

Fig. 2.6. Examining a charred cylinder of Wilcox lignite.

subbituminous chars. The temperature that the char reached was also recorded, and oxidation was quenched by reimmersion in Ar. Char samples (15 g each) were selected from the top, center, bottom, side, and half-radius positions of the cylinder.

Solids and liquids were removed from the system and weighed. Liquids were drained as thoroughly as possible (Fig. 2.7) from the string filter and condenser. Remaining condensibles (mostly tars) were scraped or wiped from the condenser walls and coils and, occasionally, from the string filter shell and reactor-to-condenser pipe. Materials trapped in the glass wool demister or string filter were weighed.

2.4 Procedures for Data Analysis

Principal data from these experiments were temperature (as a function of time and position in the block) and the yields of gas, char, organic liquids, and water. Other data included relative pyrophoricity (described above), char surface areas (Sect. 3.7.2), and dimensional changes of the block (swelling or shrinking).

Temperatures were logged on recorder charts for all experiments and on computer disk and tape for all experiments beginning with BP2-48. Data in computer files could be plotted either as temperature or point heating rate (K/min) vs radial position. Using these data and the conduction equation, thermal diffusivity and conductivity could be determined for specific samples, as described in Sect. 4.3.1.

Gas yields were determined either from the base flow rate of an inert purge gas (the tie element) or from total flow rate minus the base flow. These rates were effluent rates rather than evolution rates because the system did not operate in plug flow. Thus, a more meaningful comparison between block and powder yields, cumulative yields of gas components, are reported. Data for mass yields are reported in Table A-1.2 (in kg and in wt % maf), for molar yield in Table A-1.3 (mol/kg maf), for higher heating value or HHV in Table A-1.8 (Btu/scf), and for percent thermal efficiency in Table A-1.8 (J of the gas HHV vs J of the starting coal HHV). As additional information, effluent flow rates from selected

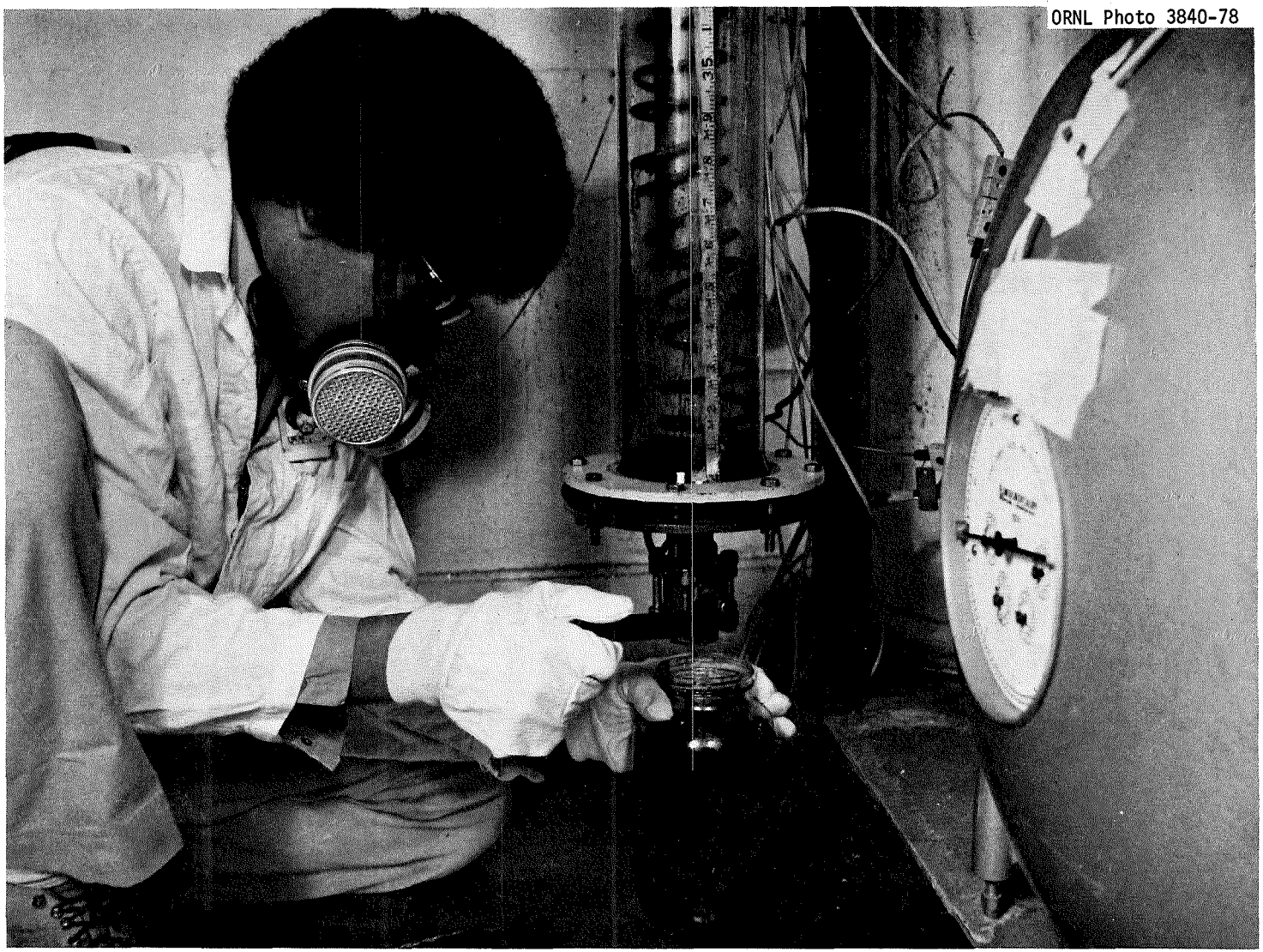

Fig. 2.7. Draining organic condensibles and water from primary condenser.

experiments are reported in Tables A-1.4 through A-1.7; system flow characteristics are described in the introduction to the Appendixes.

Char yields (reported in Table A-1.2 in kg and in wt % maf) are corrected to an ash-free basis by subtracting the amount of ash in the coal, as calculated from the coal analysis, from the gross char weight. A small additional correction was necessary for some of the subbituminous chars because pyrophoric combustion had been permitted to continue until either a temperature maximum or 300°C was reached. The correction (1.5 wt % maf at most) was based on the approximate heat release by combustion.

Organic liquids were resolved from H_2O for lignite and bituminous coal but were included in the "total condensibles" yield from experiments on subbituminous coal. Resolution was effected by a combination of decanting, analyzing of the aqueous condensate for total carbon, azeotropic distillation (with benzene) of concentrated tar fractions, and drying of cleaning rags in air. Oil yields are reported in Table A-1.2 (in kg and in wt % maf), and some ancillary data on distillation and composition were produced (see Tables 3.4, 3.5, and 3.7).

Total yields of condensibles and of H_2O are reported on a net basis; that is, not including the calculated moisture of the original coal. Water from the block pyrolysis experiments was produced (or consumed) by drying, by pyrolysis, and by gas-gas and gas-solid reactions. To make H_2O yields from block pyrolysis comparable to the H_2O yields from pyrolysis of dry powders, coal moisture was calculated and subtracted from block yields to give a net H_2O of reaction.

2.5 Safety Systems

The primary safety hazards that were presented by this experiment are potential accumulations of explosive and toxic gases and researcher contacts with carcinogenic coal tars.

Gas hazards were controlled by enclosing the apparatus in a closed, ventilated cell, by purging the apparatus, and by monitoring for hydrogen. Except for the cylinder station, the apparatus was fully enclosed in a thick-walled, 44-m^3 cell, 2.4 m deep by 4.3 m wide by

4.3 m high (8x14x14 ft). Two doors with air inlet dampers sealed off the room, which was ventilated at 2100 mol/min (1800 scfm). Pressure drop through the ventilation system filter was monitored with an audible alarm, as was reactor pressure. A hydrogen monitor sampled air at several locations; an alarm was to be sounded at 50% of the lower explosive limit (at 2% H_2 by volume). Also, careful purging of the system and use of a critical-orifice flow restrictor in the gas inlet helped prevent the development of hazardous conditions.

Coal tars contain polynuclear aromatic hydrocarbons and other potential carcinogens. Apparatus cleaning and tar sampling was conducted in the cell or in a ventilated hood; both procedures were monitored by the industrial hygiene department by using air samplers. To prevent skin contact, individuals cleaning the system were dressed in company-issued clothes and wore respirators and gloves. The health of each individual involved in the project was checked periodically by means of skin examinations, skin photographs, sputum cytology, and conventional physical examinations. Results of this careful program of industrial hygiene have been satisfactory.

3. RESULTS FROM HEATING OF COAL BLOCKS

The rationale for heating coal blocks in these experiments was that pyrolysis reactions, which are conventionally studied by heating powdered coal, could be experimentally coupled with drying and heat transfer phenomena and the escape of drying and reaction products. In in situ coal gasification such coupled processes occur simultaneously in the walls of the UCG reaction cavity and in chunks of roof coal that fall into the cavity.

Dry, powdered samples of coal have been used intentionally in pyrolysis research because the particles can be heated uniformly and the rapid escape of powders is facilitated. With powders, only pyrolysis reactions are considered to occur. In contrast, pyrolysis in UCG is coupled with the phenomena cited in the previous paragraph. Also during UCG, gasification and combustion occur as reactants penetrate into the coal; surfaces are eroded away by collapsing or burning. All of these phenomena were examined in coal block research except for combustion and erosion.

The experimental approach of coal block research applied the equipment and procedures described in Sect. 2. Lignite, subbituminous coal, and bituminous coals were studied (see Table 2.1) at pressures of approximately 100 kPa (1 atm).

For the block size normally used (150-mm in diameter), heating of the surface at 3 K/min caused significant temperature gradients within the block, successfully coupling the phenomena described above. Decoupling was approximated in different experiments by (1) comparing with powder pyrolysis data; (2) predrying blocks at low temperatures before further heating; (3) using small blocks, which dried more rapidly; or (4) using a heating rate of 0.3 K/min, which caused early drying and more uniform internal temperature. Also, higher heating rates (9 to 14 K/min) were applied in some experiments to intensify the coupling. (Use of different heating rates was an experimental technique to produce the different types of internal temperature gradients that can occur in UCG, not to produce a duplication of in situ heating rates, which would require much larger pieces of coal.)

Maximum temperature of experiments and type of purge gas were the other independent variables. Each block was heated to some maximum temperature 773 to 1300 K, and heat input was maintained until internal temperatures equilibrated with the surface temperature. Several maximum temperatures were used to facilitate the comparison of cumulative yields with data from powders and from the other blocks. Inert gas (Ar) was purged through the reactor in most experiments, as is conventional in pyrolysis research. However, to examine the effects of reactive gases on block pyrolysis, hydrogen or a simulated UCG product gas was used as in some cases.

Results of the coal block research may be summarized by these statements:

1. Drying and low thermal conductivities contribute to cause steep temperature gradients within the coal, as has been observed in UCG (Sect. 3.1).
2. Yields from block experiments at 3 to 14 K/min were different from the yields measured at lower heating rates when coupled phenomena were minimal (Sect. 3.2).
3. Oil, tar, and methane, which were generated by pyrolysis of the coal, were cracked as they escaped from the block (Sect. 3.3).
4. Steam, which was generated by drying and pyrolysis of the coal, participated in gasification reactions (Sect. 3.4).
5. When hydrogen was purged past the coal block during heating, methane yields increased; when a simulated UCG product gas containing H_2, CO, CO_2, CH_4, steam, and inert gas was used, steam gasification, water-gas shift, and increased methane yield were observed (Sect. 3.5).
6. Changes in char reactivity (as measured by pyrophoricity) and changes in char yields indicated that reactive carbon deposited by cracking reactions was a carbon source for steam gasification and hydrogasification (Sect. 3.6).

7. Swelling of bituminous coals at UCG-like conditions was less than expected from data based on conventional swelling tests on powders (Sect. 3.7).

Observations and implications have already been discussed.

3.1 Temperature Gradients and Drying

Temperature gradients similar to those observed in UCG were produced by heating blocks of coal at 3 K/min. These gradients were related to the couplings among the many physical and chemical phenomena produced in the experiment. In wet and dry coal blocks, low thermal conductivity helped cause the gradients, but in wet coal, drying and transpiration cooling were also important factors. Together with the flow direction of escaping products, the temperature data were suggestive of mechanisms for the side reactions of secondary cracking (Sect. 3.3) and self-gasification (Sect. 3.4). In addition, the amount of swelling in bituminous coal was affected by the gradients (Sect. 3.7). Similarity in block and UCG temperature data was demonstrated, which was a verification of the importance of this research in modeling UCG phenomena.

Instrument monitoring of seams during UCG of wet Hanna coal[1] produced the data shown in Fig. 3.1. Initially, temperatures rose slowly to a steam plateau. This plateau was observed at temperatures of 405 to 415 K, corresponding to the boiling point of water at 240 to 380 kPa in the seam. Before moving beyond the steam plateau permanently, measured temperatures in the instrumentation well increased and decreased twice, suggesting that drying and collapsing of roof coal may have occurred near the well. When drying was complete, temperature rose rapidly. These temperature changes may be interpreted as the results of a thermal wave moving through the coal, influenced by roof coal falling in the cavity.

Time-temperature data for a cylindrical block of wet Wyodak subbituminous coal (Fig. 3.2), compared to the UCG data (Fig. 3.1) were limited by a finite geometry and a maximum temperature. Nevertheless,

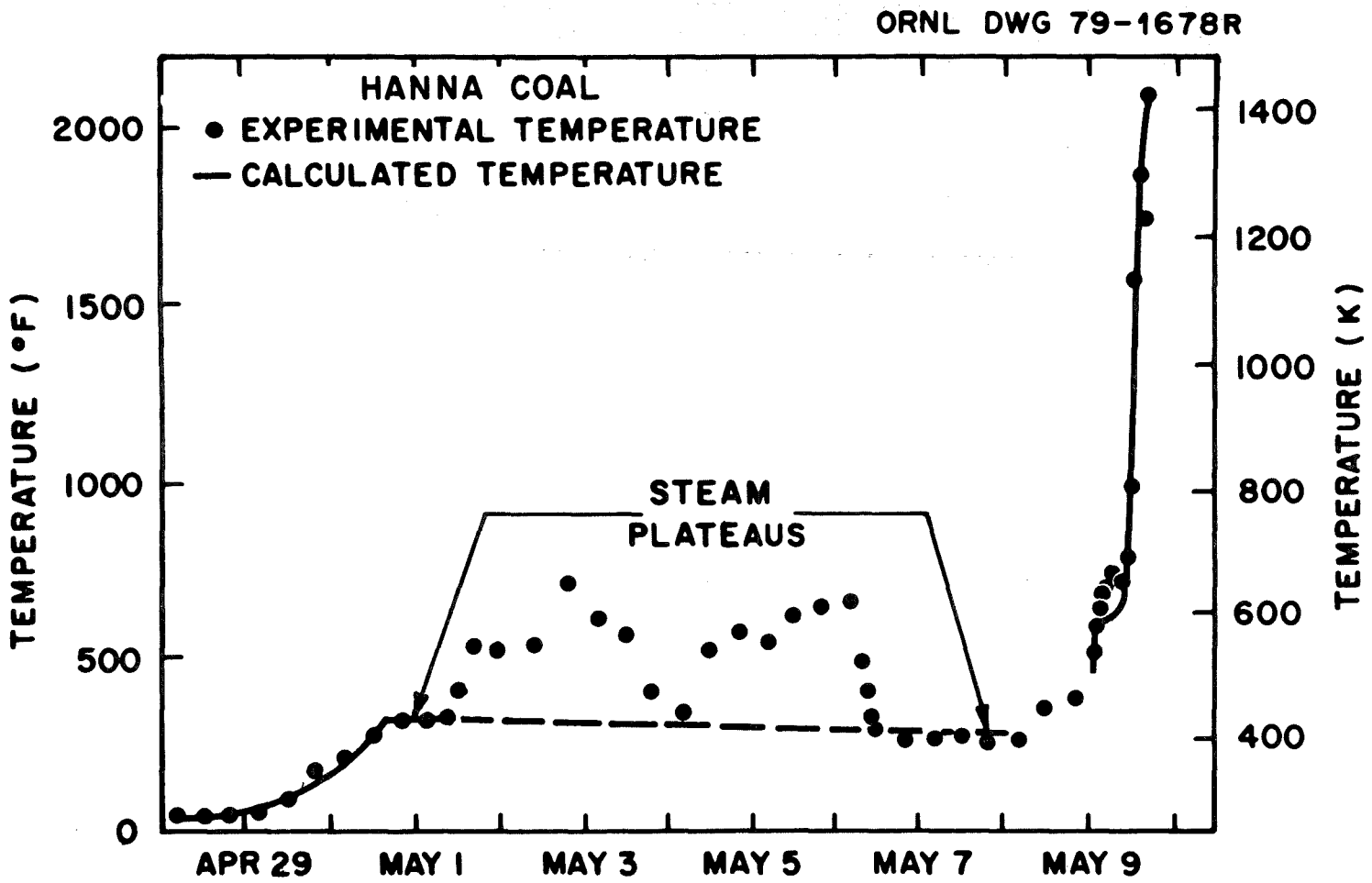

Fig. 3.1. Temperature history of a thermocouple during the Hanna 2, Phase 2, UCG field test (well B, 4 m or 13 ft above the coal seam's bottom). Source: R. D. Gunn, D. L. Whitman and D. D. Fischer, "A Permeation Theory for In Situ Coal Gasification," SPE J. (5), 300-314 (October 1978).

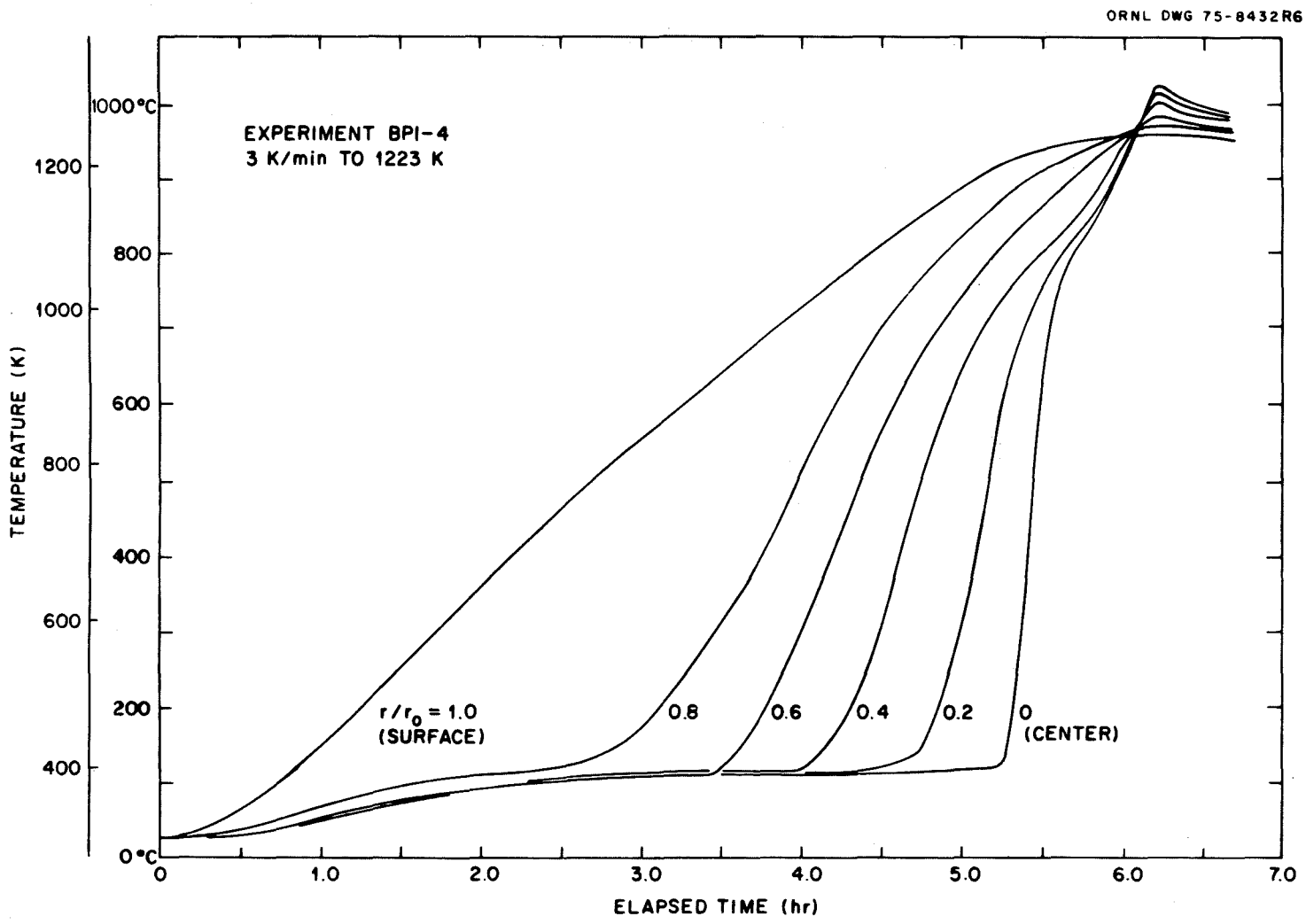

Fig. 3.2. Temperature histories at different radii during experiment BP1-4, heating of a cylinder of wet Wyodak subbituminous coal. An unusual exotherm was observed inside the block near the end of the experiment.

the same slow rise to a boiling point, the steam plateau, and the subsequent rapid rise were observed as in the UCG data.

Temperature-radius plots were more useful for interpreting the regions of heat transfer. In Figs. 3.3 and 3.4, data from the same experiment as in Fig. 3.2 were replotted four times as temperature vs dimensionless radius and as point heating rate $(\partial T/\partial t)_r$ vs dimensionless radius. (The instrumentation pattern of 26 thermocouples was shown in Fig. 2.4.) The steam plateau at those times was observed to occupy the entire center of the block (Fig. 3.3) and to heat very slowly with respect to the surface (Fig. 3.4). Note that temperature was not strictly constant at 373 K in the steam plateau region; over a radial thickness of 100 mm, the temperature varied approximately 2 K. Thus, the gradient and point heating rate were too small to be shown in Fig. 3.3. Similar profiles were plotted from the heating of blocks of Wilcox lignite (Fig. 3.5) and Pittsburgh bituminous coal (Fig. 3.6).

From such plots, trends in temperature profiles were seen to be the results of up to three moving regions of heat transfer. Heat transfer mechanisms can be described for each of the regions; for example, note a profile in wet Wilcox lignite (time t_3 in Fig. 3.5, isolated on a separate graph in Fig. 3.7).

First, in the wet coal region, heat transfer was assumed to be by conduction from the edge of the steam plateau into the cooler core. Coal moisture was assumed to be immobile, although capillary action may have drawn some water through macropores to the drying zone. Thermal conductivity of wet Wilcox lignite was low for a solid — 0.31 $\pm$ 0.03 W/m·K (see Sect. 4.1.1), or about half the conductivity of water. However, the probable reason that the core was so slow in heating was that little heat penetrated to it. Conduction would have been the only mechanism available for heat transfer through the steam plateau into the core, and the driving force for conduction (the temperature gradient) was quite small in the plateau.

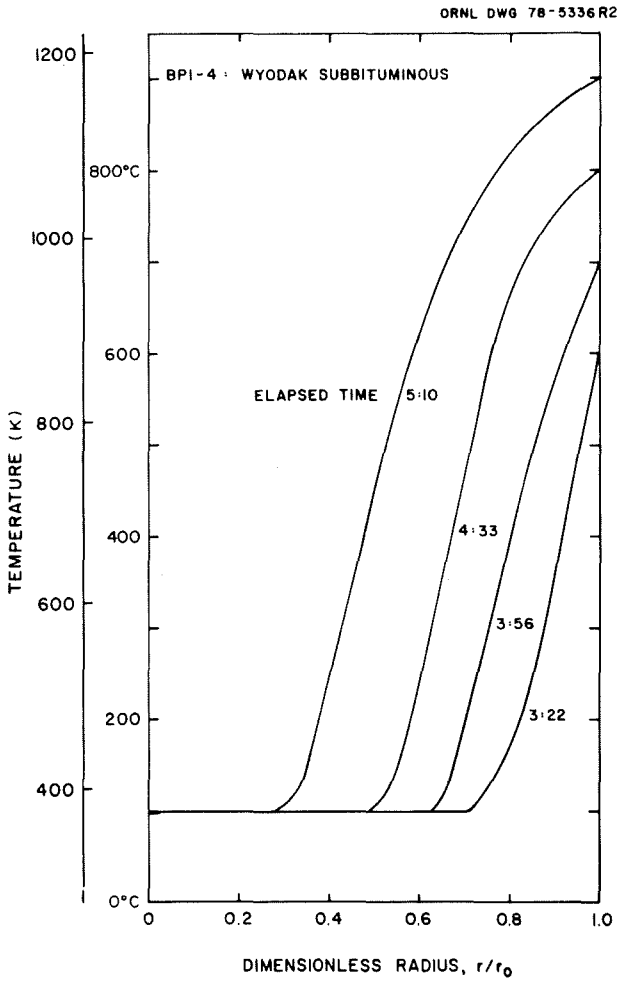

Fig. 3.3. Radial profiles of internal temperature during heating of Wyodak subbituminous coal at 3 K/min in experiment BP1-4; the profiles are based on 26 data points; r_0 = 157 mm.

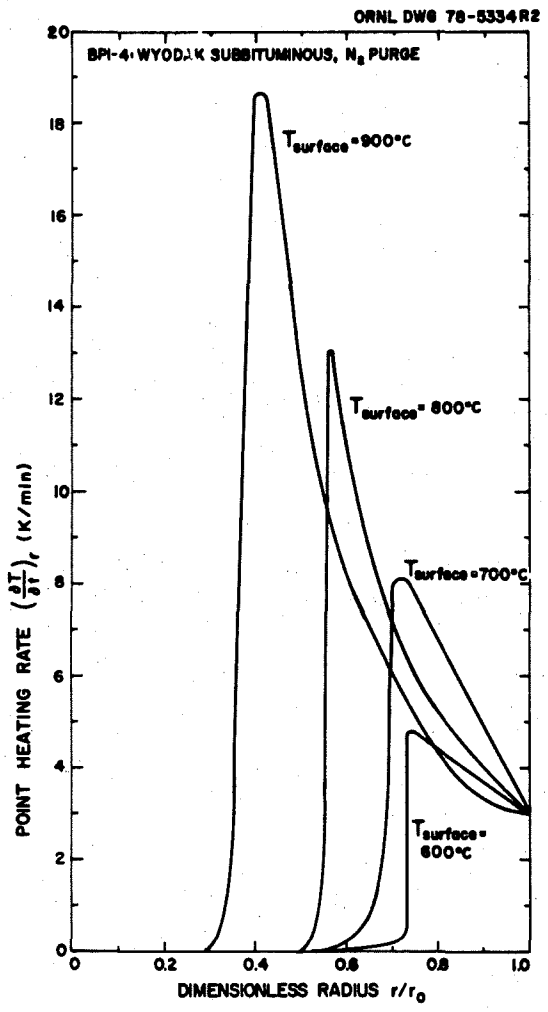

Fig. 3.4. Radial profiles of internal heating rate ∂T/∂t during heating of Wyodak subbituminous coal at 3 K/min in experiment BP1-4; profiles are based on 26 data points; r_o = 157 mm.

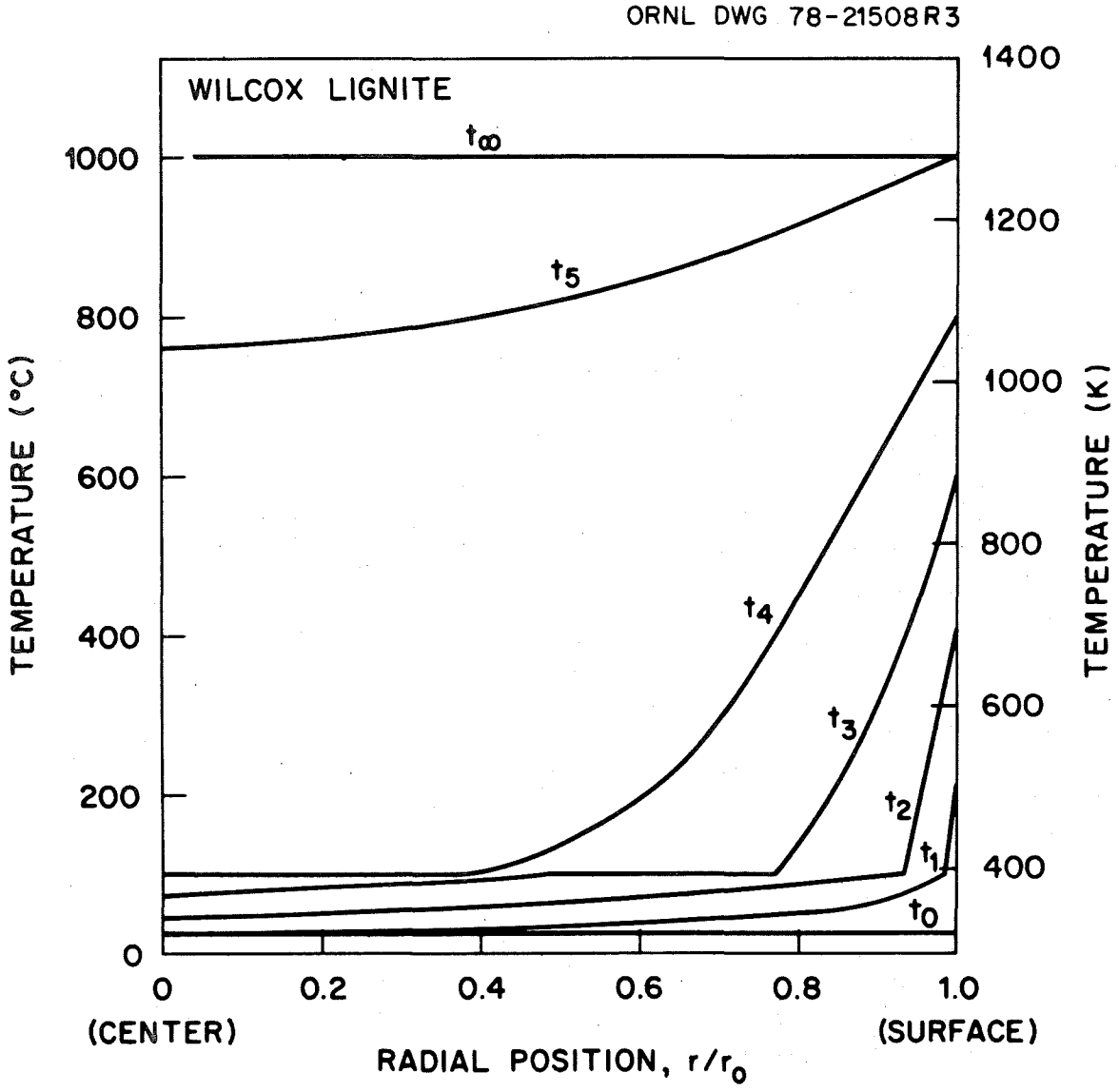

Fig. 3.5. Time series of radial temperature profiles in Wilcox lignite during heating at 3 K/min to 1273 K (1000°C). Composite data from 12 thermocouples from experiments BP2-48 and BP2-55.

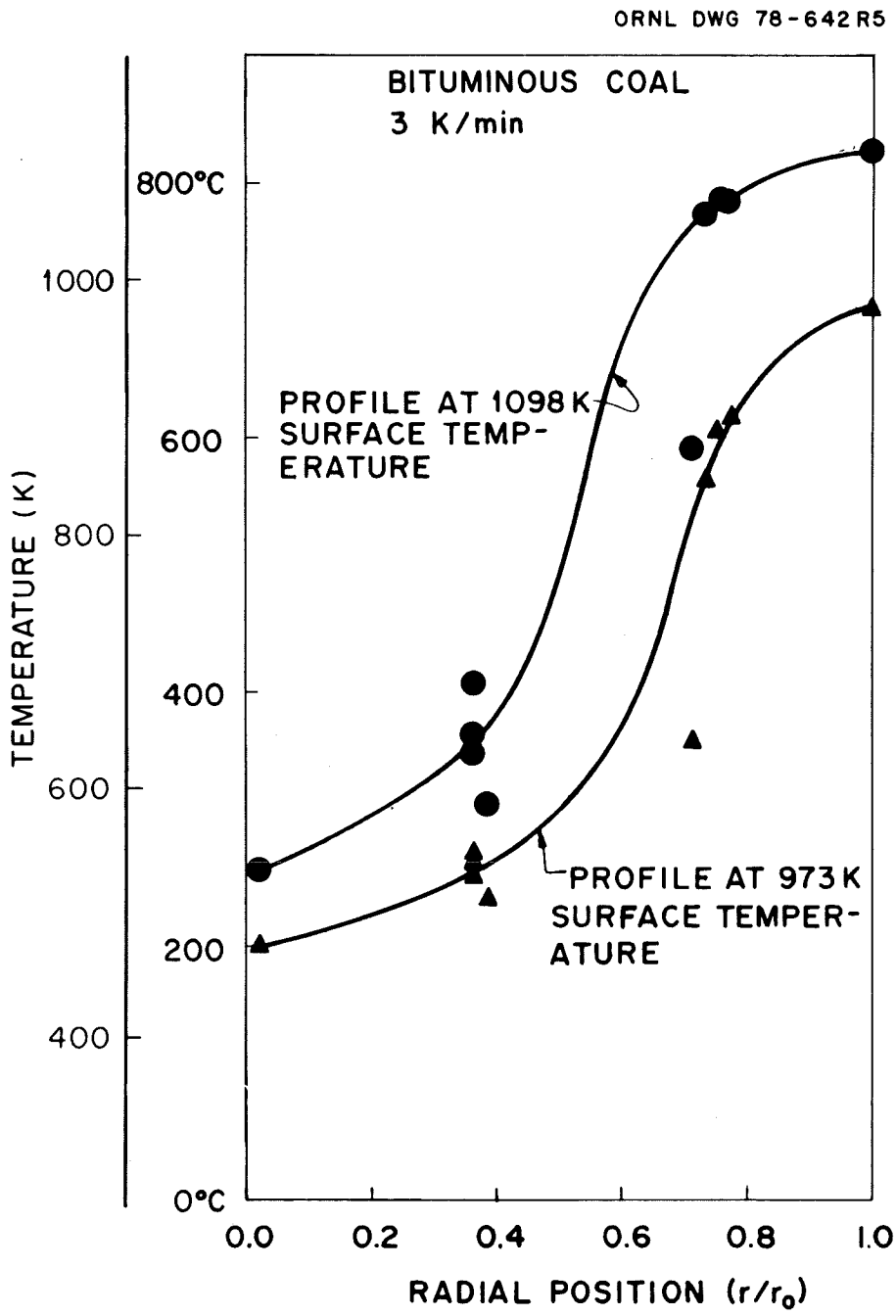

Fig. 3.6. Radial temperature profiles during heating of Pittsburgh bituminous coal (experiment BP2-32). Radial position of points hotter than 673 K (400°C) are slightly underestimated because of swelling; block radius at end of experiment had expanded approximately 30%.

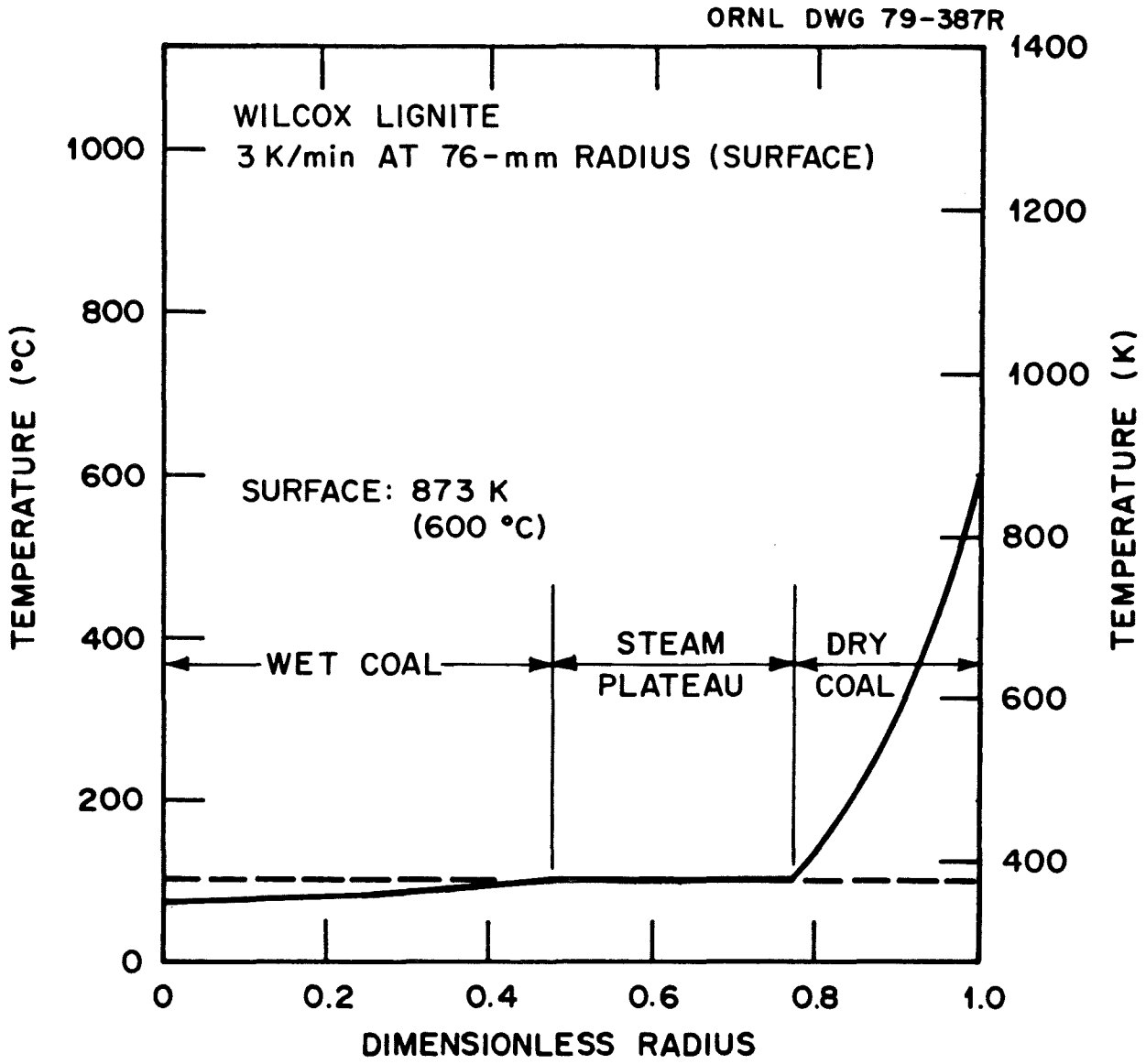

Fig. 3.7. Temperature profile in a block of Wilcox lignite when surface reached 873 K (600°C); heating at 3 K/min at the surface.

In the steam plateau, heat was conducted through the solid matrix but was consumed in vaporizing moisture. Lyczkowski[2] has modeled the plateau, treating it as a case of two-phase drying (steam and water) in a porous medium. Mechanistically, the drying process could be interpreted by relating it to the pore size distribution. The boiling point of water in pores is higher than the normal boiling point and is inversely related to pore size. Because of pore size distribution, the drying zone can be envisioned as having contained dried, drying, and water-filled pores simultaneously and only a small temperature gradient. Thus, the fraction of voidage volume filled by steam varied from zero at the wet edge of the plateau to 1.0 at the dry edge. Such a model was consistent with the greater thickness of the steam plateau in Wyodak and compared favorably to the wetter Wilcox lignite (33.6 vs 37.5% moisture, Fig. 3.3 vs Fig. 3.5). Measurement of pore size distribution of Wyodak coal has revealed a higher proportion of micropores,[3] so that the steam plateau would have been spread over an even broader region.

In the third region, a steep gradient was caused in the dry coal by low thermal conductivity and transpiration cooling. Thermal conductivity of dried lignite was measured to be 0.14 ± 0.03 W/m·K (see Sect. 4.1.1), about half that of wet lignite and comparable to insulation. However, when a wet block was heated, steam was escaping through the dry coal countercurrently to conduction. Transpiration cooling of the coal occurred as the steam was superheated by the hotter coal, steepening the temperature gradients. Because of this combined conduction and convection, gradients as large as 60 K/mm were measured in the Wilcox lignite; heating rates $(\partial T/\partial t)_r$ near the steam plateau were higher than those at the surface (e.g., Fig. 3.2). The latter result was attributed to the higher linear velocities of steam (and thus the fastest convective heat transfer) occurring at the smallest radii.

Radial temperature profiles became less steep near the block surface at temperatures above 800 K. If conduction only had occurred, a parabolic

profile would have been measured (see Sect. 4.1.1). The flattening was probably caused by the onset of appreciable radiation heat transfer within the coal. In addition, heats of reaction and poorer transpiration cooling (lower steam velocities) may have flattened the profile.

Pittsburgh bituminous coal contained little moisture (1.7%), so drying effects were not apparent. Profiles sketched from point temperature data on a block heated at 3 K/min (Fig. 3.6) showed the typical steep temperature gradients, resulting in this case from low thermal conductivity. Locations of points hotter than 670 K were distorted by swelling, which increased the block radius by 30%. Effects of the temperature gradients on swelling will be discussed in Sect. 3.7.

The implication for UCG is that block data on temperature gradients can be related to important physical and chemical mechanisms in UCG. While escaping into the reaction cavity, pyrolysis products like tars and methane can be cracked (Sect. 3.3) and internally generated steam can gasify the coal and tars (Sect. 3.4). Also, reactivity of the char (Sect. 3.6) and solid structure (Sect. 3.7) can be changed, affecting the propagation rate of gasification. Because of transpiration cooling in UCG of wet coals, drying would not necessarily be speeded up by faster heat input (by higher air injection rates or the injection of oxygen). If drying rates were increased, transpiration cooling would also increase and convective heat transfer from the dry coal would be improved. These effects would limit the rate of heat transfer to the drying zone and narrow the char reaction zone by steepening the temperature gradient.

That high moisture content in the coal would have had the same effect is a hypothesis supported by material balance estimates[4] from UCG field tests. In the Hoe Creek 2 UCG field test, the width of the char zone was estimated to be narrow and the coal used contained 30% moisture. In contrast, char zones in UCG of Hanna coal (9% moisture) were estimated to be much broader. Extremely wet coal cannot be gasified at all because steam generation begins upon ignition, creating such a steep temperature gradient that the combustion would soon die out.

As noted previously, the extent of these interactions in kinetics experiments on powders is minimal. Generally, dry powders have been used; particle size is usually such that the entire particle is uniformly heated. However, powder data are easier to obtain and are readily available. Understanding of block data can make possible the satisfactory application of powder data to UCG modeling, in which temperature gradients and drying do occur.

3.2 General Trends in Yield Data from Blocks

Heating rate markedly affected yields from coal blocks by changing the temperature profiles inside the coal. In particular, yields from wet blocks heated at 3 K/min or faster were observed to be different from yields from dry powdered coal, predried blocks, or slowly heated wet blocks. As described in the introduction to Sect. 3, interactions between internally generated steam and hot char were minimized in the latter two types of block experiments because the block was dried before hot char was present. [The hottest char present was 670 K (400°C) maximum and was recorded in the case of wet blocks of lignite heated at 0.3 K/min.]

Yield data were the primary means of determining changes in the reactions. Complete tables of experimental conditions and yields are presented in Appendix 1, but trends were not as apparent as when the numerical data were plotted as in Figs. 3.8–3.21.

The graphs presented in these figures generally have maximum temperature of the experiment as the abscissa of the graph. As a result, the yields are comparable to yields from powders heated to different temperatures. Again it must be emphasized that these yields are cumulative yields, not partial yields at a temperature during heat-up. As a result, they reflect heating of the *entire* block or powder to a given temperature.

Graphs are grouped by type of coal. For Wilcox lignite, yields of gas, oil, net water, and char were plotted as functions of temperature and heating rate. Where possible, block yields from lignite were compared to the pyrolysis yields from dry powder as published by Goodman et al.[5]

Yields of gas, net condensibles, and char from blocks of Wyodak coal were plotted against temperature endpoints from experiments at 0.3 and 3 K/min; powder data were reported by Campbell.[6,7] Finally, gas, oil, water, and char yields from Pittsburgh coal were plotted. All yields were reported as wt % of maf coal, and calculated ash and moisture contents of the coal blocks tested were subtracted from the char and water (or condensibles) yields, respectively.

These graphs demonstrated that synergisms were occurring among heat transfer, drying, pyrolysis, and escape of products. The changes and trends in yields will be discussed here, and the mechanistic causes will be discussed in subsequent sections.

Heating blocks of Wilcox lignite to 870 K (600°C) or above at 3 K/min produced more gas, less oil and tar, less water, and approximately the same amount of char as from simple pyrolysis of dry powdered lignite. As shown in Fig. 3.8, more gas was produced from wet blocks than from dry powder or a predried block; the use of hydrogen as purge gas instead of inert purge gas increased gas yields further. Oil and tar yields from dry blocks (Fig. 3.9) were nearly 40% below yields from powder and from wet blocks, 50 to 80%; no effect of purge gas composition was observed. Net moisture (water) yield from coal blocks, derived by subtracting the known moisture content from gross water yield, was comparable to yield from dry powder. Net yields of water from blocks (Fig. 3.10) were lower than yields from powder. In fact, net yields were negative in higher-temperature experiments on wet blocks, indicating that less water was produced than if the block had simply been dried (i.e., that some steam generated by drying had been consumed). Yields of char (Fig. 3.11) were highest from the predried block. Wet blocks produced char yields that were the same or greater than the yields from powder.

The various yields from lignite blocks heated at 3 K/min or faster showed much the same relationship to yields from blocks heated at 0.3 K/min as they did to powders. All yields from block experiments that were run to 1073 K (800°C) were plotted in Fig. 3.12 against surface heating rates. As heating rates were increased (or as internal temperature gradients became steeper), gas yields increased, oil yields were unchanged, water

ORNL DWG 79-368 R2

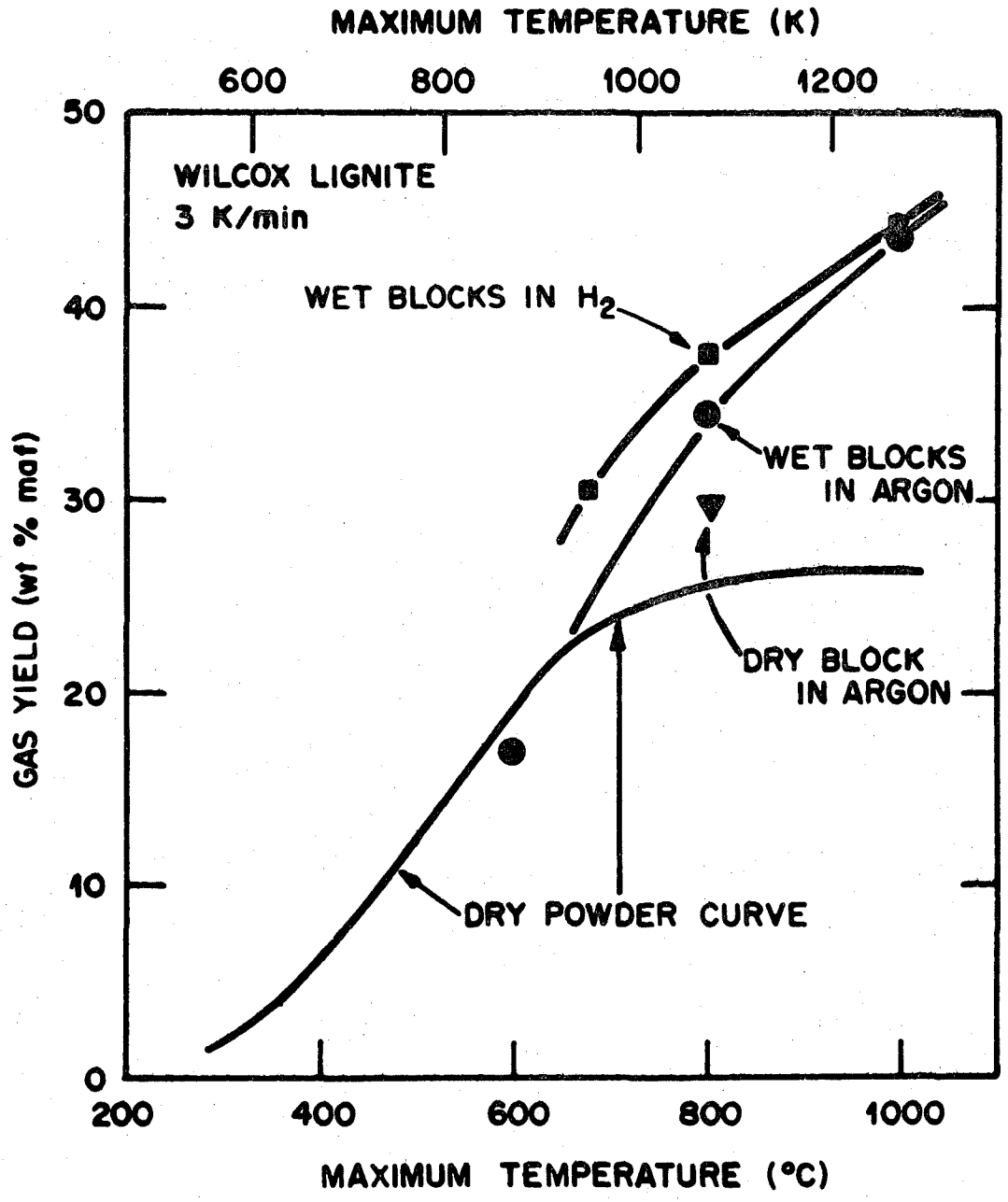

Fig. 3.8. Gas yields from heating of Wilcox lignite at 3 K/min. Circles represent wet blocks which were heated in inert purge gas; squares represent wet block heated in hydrogen; and the triangle represents a predried block which was heated in inert gas. (Source: J. B. Goodman, M. Gomez, and V. F. Parry, Laboratory Carbonization Assay of Low-rank Coals at Low, Medium, and High Temperatures, RI-5383, U.S. Bureau of Mines, January 1958.)

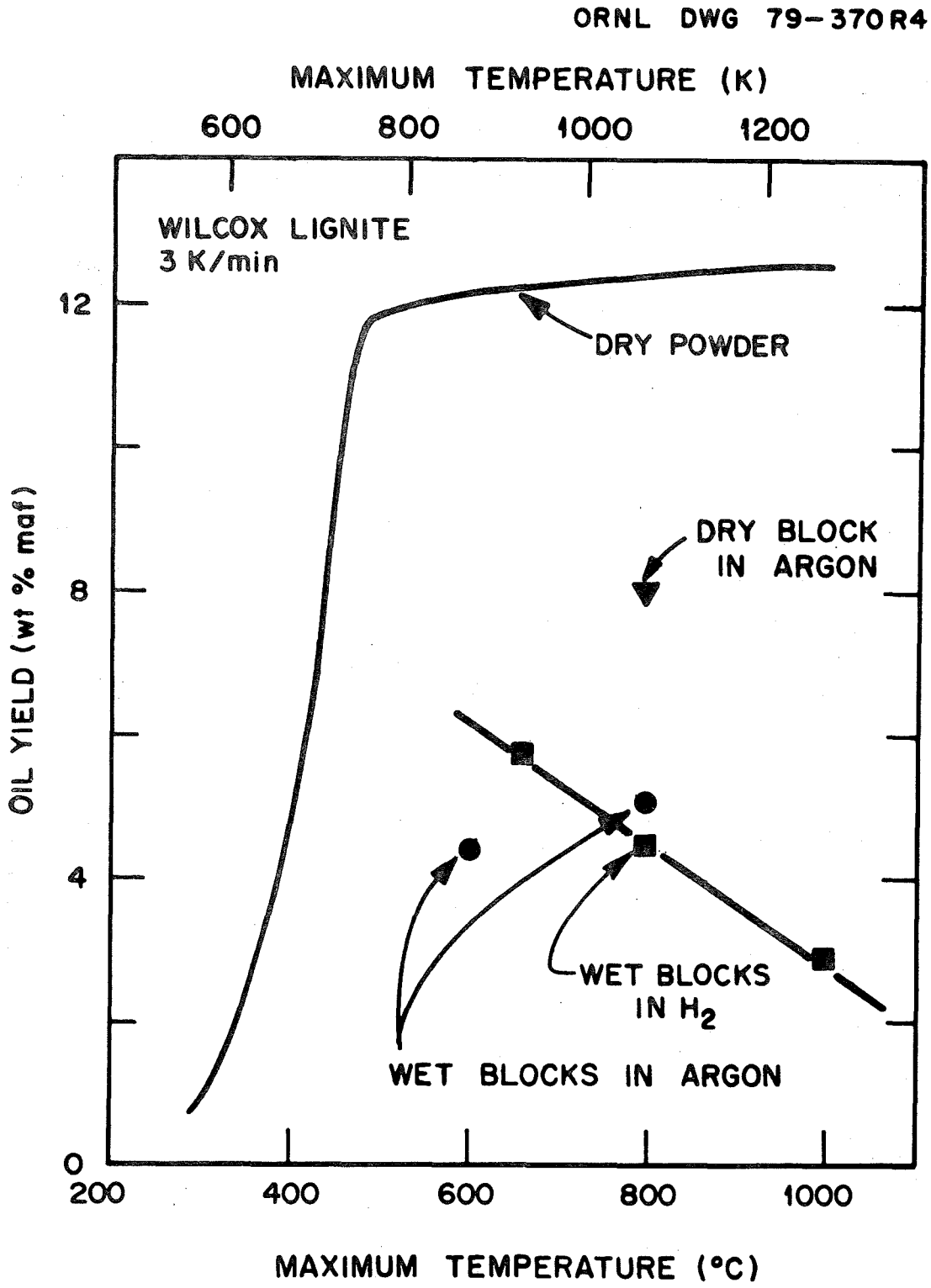

Fig. 3.9. Yields of condensible organics from heating of Wilcox lignite at 3 K/min. Data represent wet blocks that were heated in inert purge gas; squares represent wet blocks heated in hydrogen; and triangle represents a predried block heated in inert gas. (Dry powder data source: J. B. Goodman, M. Gomez, and V. F. Parry, Laboratory Carbonization Assay of Low-rank Coals at Low, Medium, and High Temperatures, RI-5383, U.S. Bureau of Mines, January 1958.)

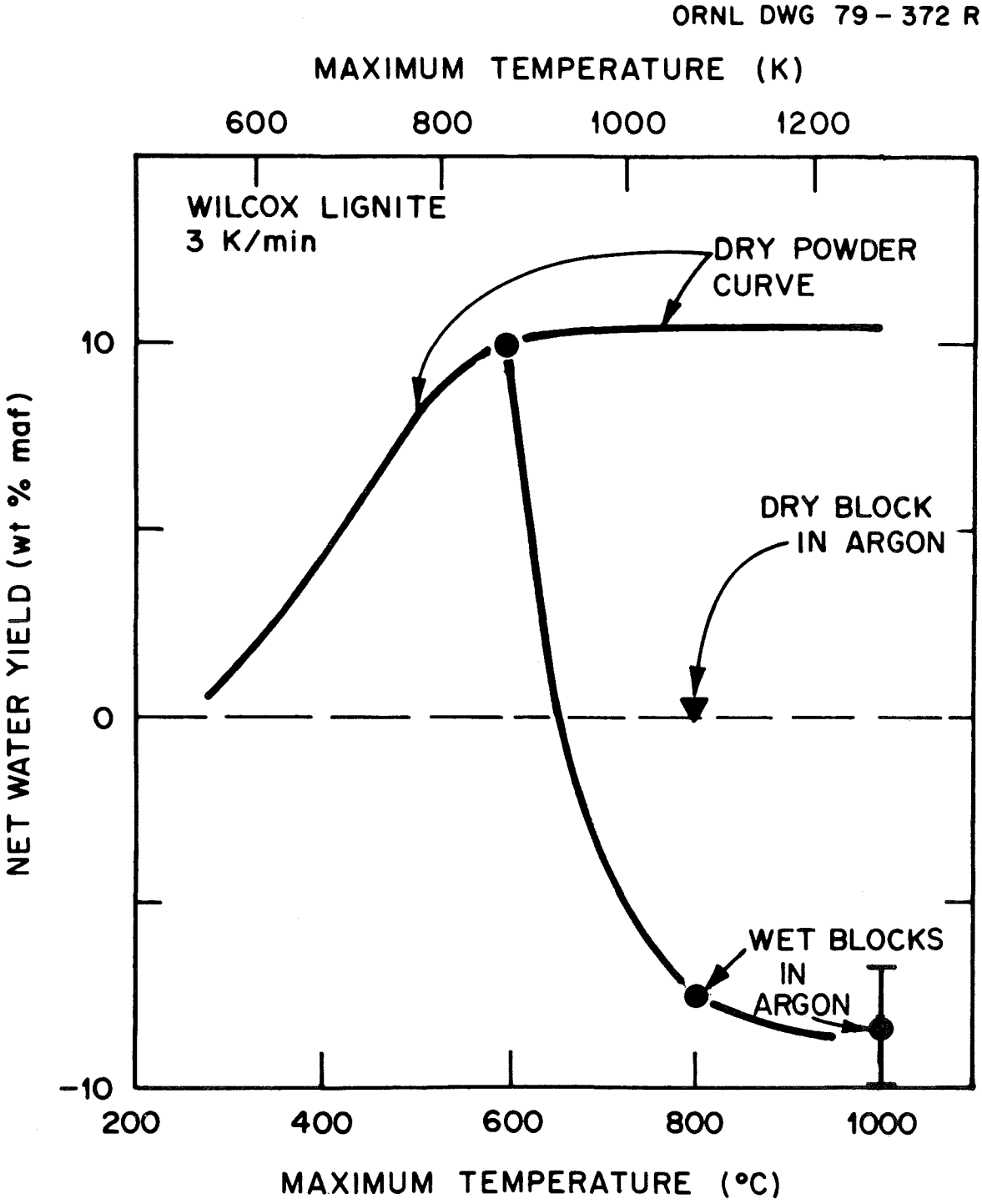

Fig. 3.10. Net yields of water from heating of Wilcox lignite at 3 K/min in inert purge gas. Dots and the error bar represent wet blocks and the triangle represents a predried block. (Dry powder data source: J. B. Goodman, M. Gomez, and V. F. Parry, Laboratory Carbonization Assay of Low-rank Coals at Low, Medium, and High Temperatures, RI-5383, U.S. Bureau of Mines, January 1958.)

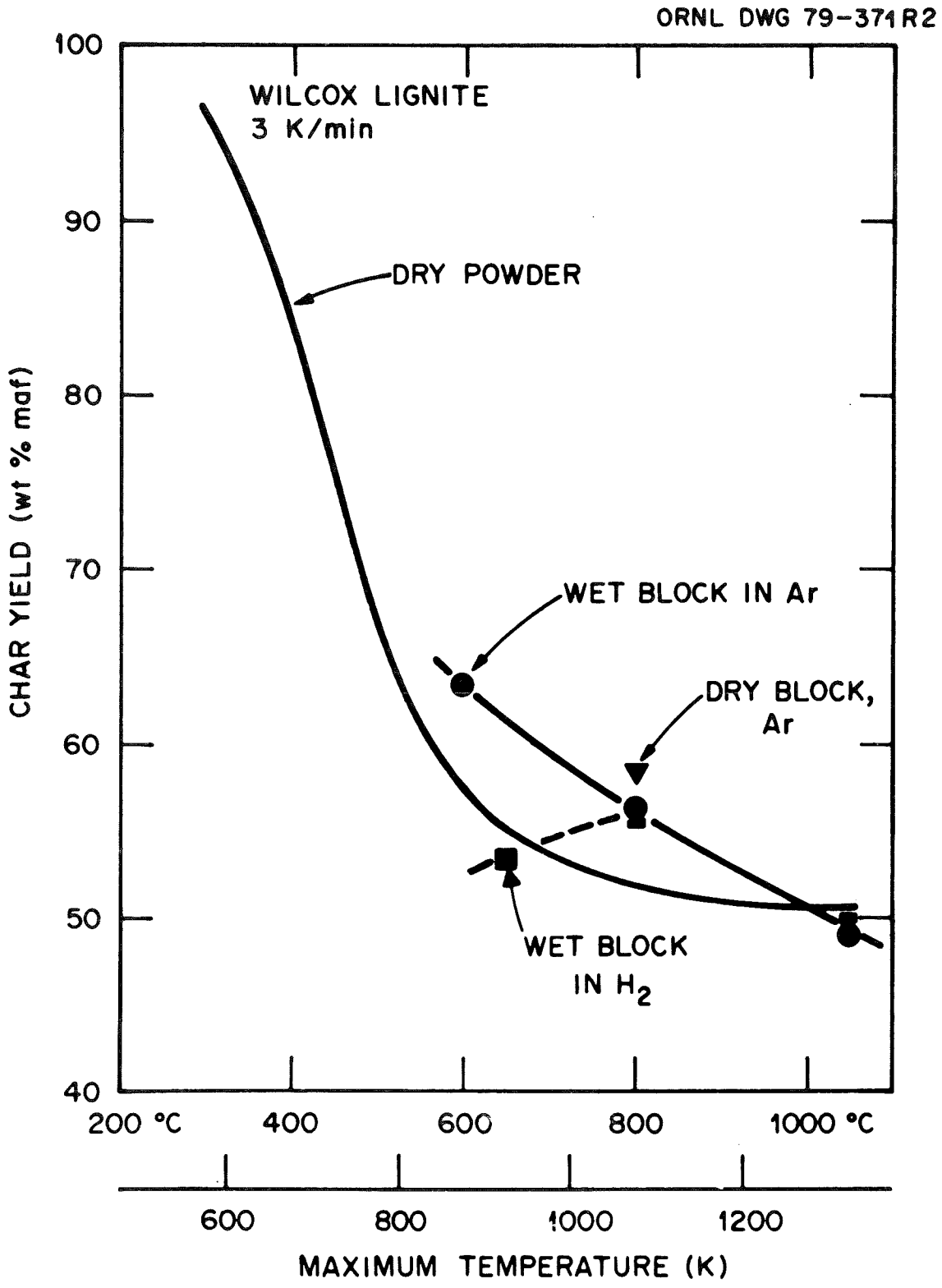

Fig. 3.11. Char yields from heating of Wilcox lignite at 3 K/min. Circles represent blocks that were heated in inert gas; squares represent wet blocks heated in hydrogen; and the triangle represents a predried block that was heated in inert gas. (Powder pyrolysis data source: J. B. Goodman, M. Gomez, and V. F. Parry, Laboratory Carbonization Assay of Low-rank Coals at Low, Medium, and High Temperatures, RI-5383, U.S. Bureau of Mines, January 1958.)

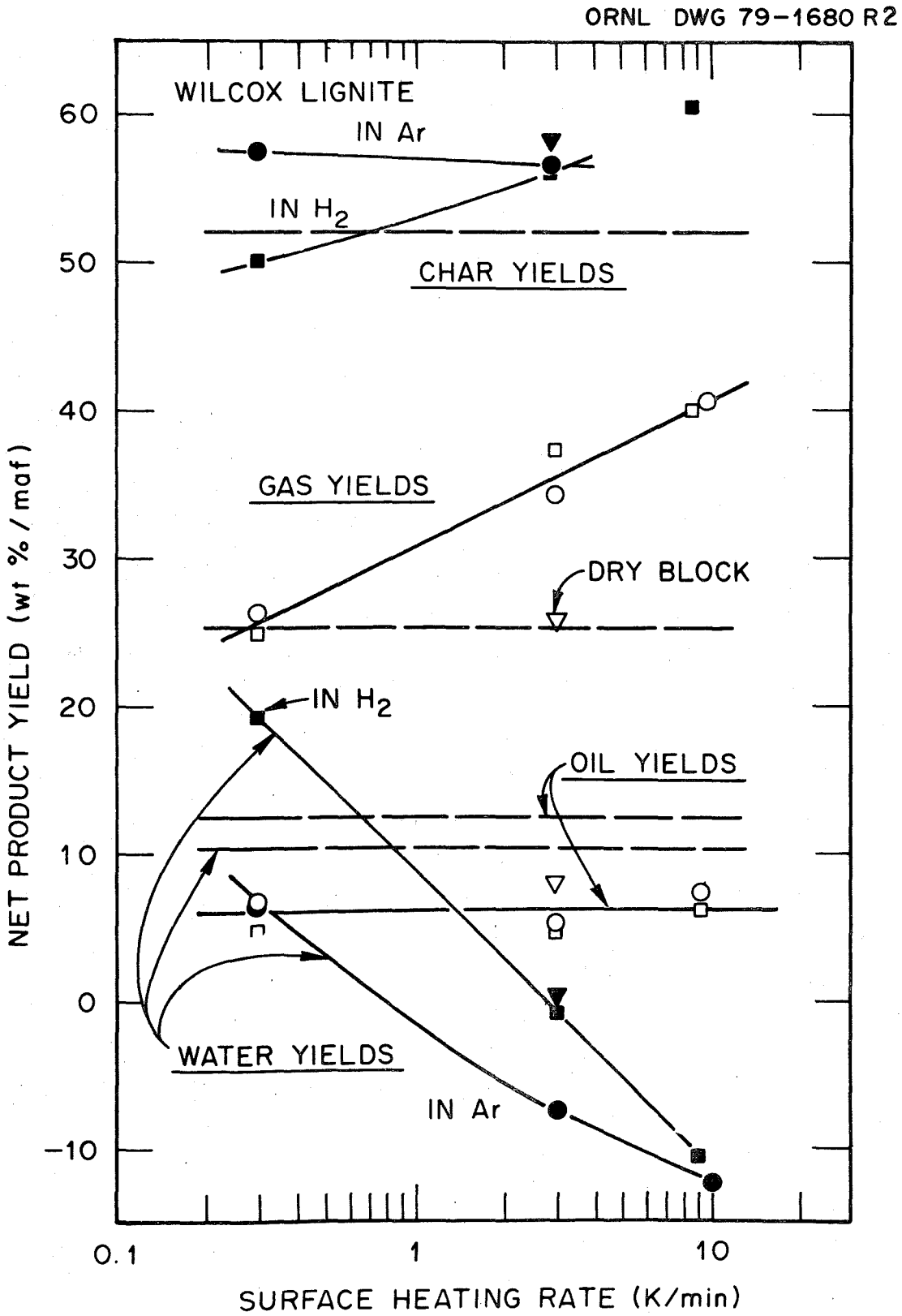

Fig. 3.12. Product yields from heating of blocks of Wilcox lignite to 1073 K (800°C). (Circles represent inert gas, squares represent H_2, and triangles represent inert gas using a predried block; dashed lines represent yields from powder.)

yields decreased, and no definite trends in char yields were observed. Nearly all char and gas yields were higher than yields from powder (52.1 and 25.2 wt % maf, respectively[5]). In contrast, nearly all oil and water yields were lower than the 12.3 and 10.3 wt % maf yields from powder. The notable exception was a net water yield of 19.1 wt % maf from a wet block heated in H_2 at 0.3 K/min, indicating that water had been produced.

Many of the same trends were observed with Wyodak subbituminous coal as with Wilcox lignite. Yields of gas (Fig. 3.13) from dry powders, from predried blocks, and from wet blocks heated at 0.3 K/min were similar, whereas yields from wet blocks heated at 3 K/min were higher. Water and oil products were not physically separated, but the combined (net) yield of condensibles (Fig. 3.14) at 3 K/min showed the same decreasing trends as would the graphical sum of Figs. 3.8 and 3.9. At 0.3 K/min, net yields of condensibles from blocks were lower than yields from powder by a constant offset. Char yields (Fig. 3.15) from predried blocks or from blocks heated at 0.3 K/min were higher than yields from powders or blocks heated at 3 K/min.

Yields from Pittsburgh bituminous coal (1.7% moisture) did not show the same trends as yields from wet, low-rank coals. Gas yields (Fig. 3.16) were higher at higher heating rates, but the effect of heating rate was greater when hydrogen purge gas was used. Oil and tar yields (Fig. 3.17) were unaffected by purge gas composition but decreased as heating rates were increased from 0.3 to 3 to 14 K/min. Net water yields (Fig. 3.18) were higher at higher heating rates, in contrast to water yields from lignite. Hydrogen as purge gas may have increased the water yield in one experiment (3 K/min to 910 K), but no other effects of purge gas composition were observed. Finally, char yields (Fig. 3.19) at a given temperature decreased in the order: inert-gas-purged experiments at 0.3 K/min, hydrogen-purged experiments, and inert-gas-purged experiments at 3 K/min.

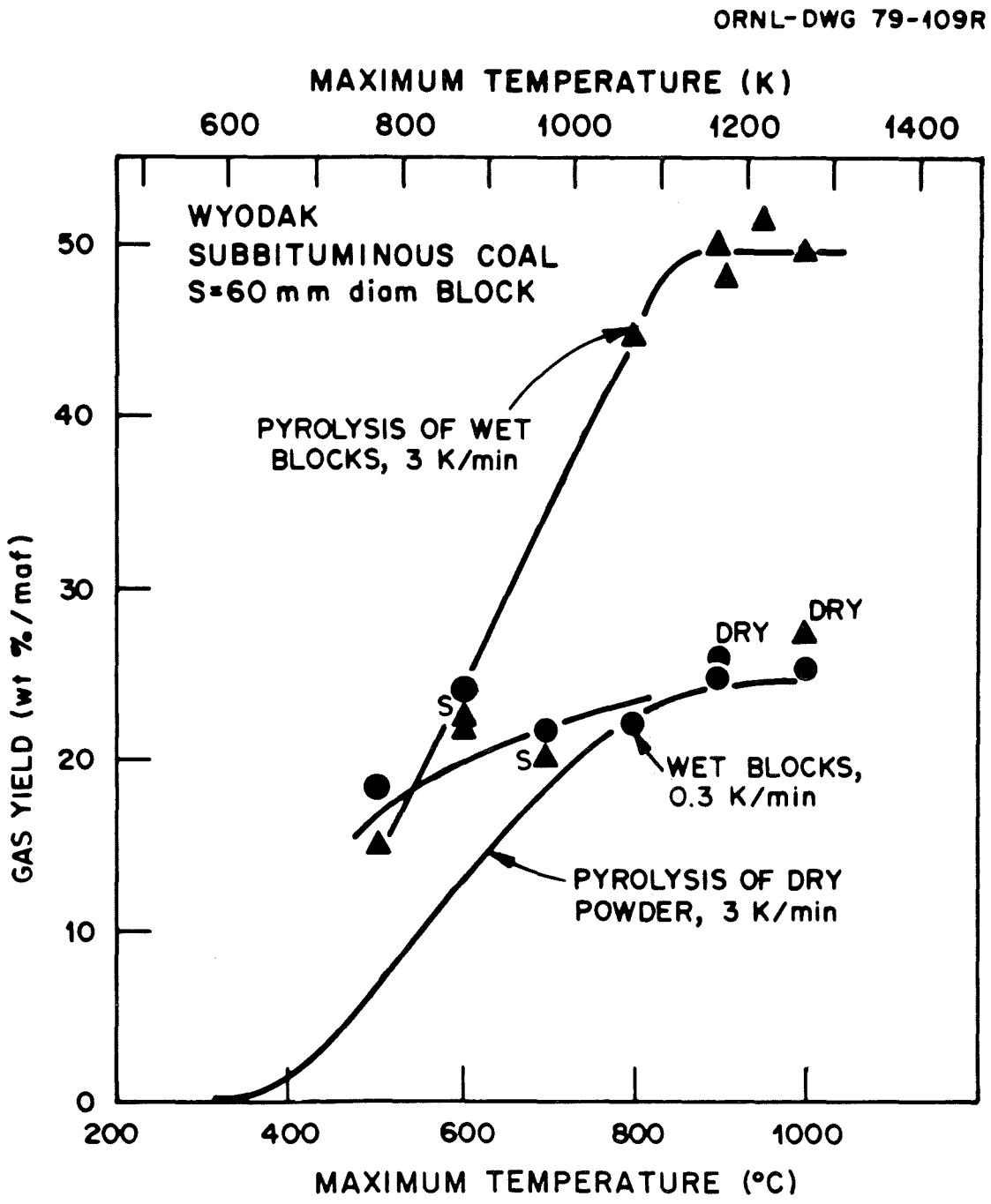

Fig. 3.13. Gas yields from heating of Wyodak subbituminous coal in inert gas (S designated small, 60-mm-diam blocks). Triangles represent blocks heated at 3 K/min; circles represent blocks heated at 0.3 K/min. [Powder pyrolysis data source: J. H. Campbell, Pyrolysis of Subbituminous Coal as It Relates to In Situ Gasification (Part 1: Gas Evolution), UCRL-52035, Lawrence Livermore National Laboratory, March 1976; (Part 2: Characterization of Liquid and Solid Products), UCRL-52035 Part 2, Lawrence Livermore National Laboratory, June 1976.]

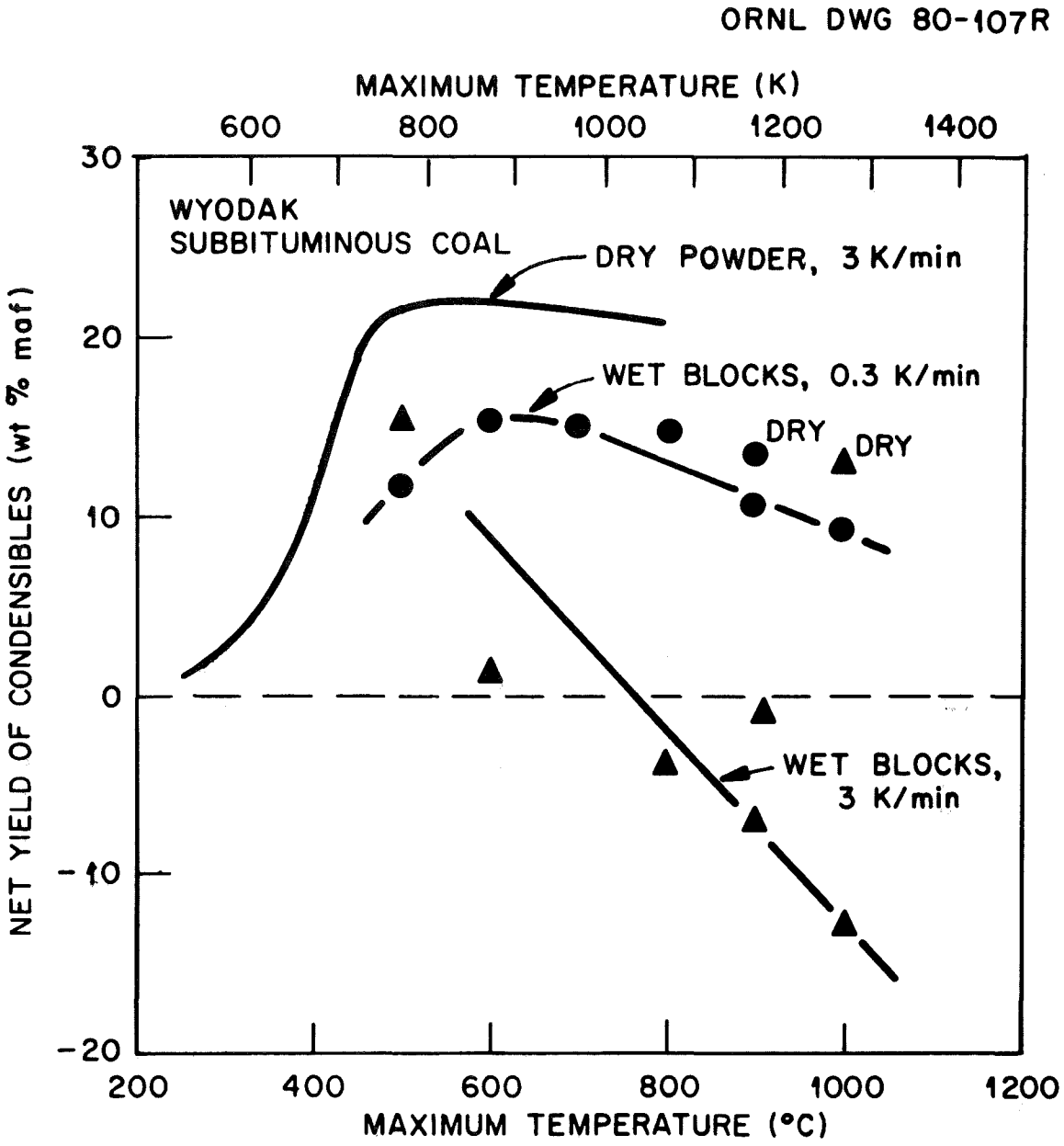

Fig. 3.14. Net yields of condensibles from heating of Wyodak subbituminous coal in inert gas. Triangles represent blocks heated at 3 K/min while circles represent blocks heated at 0.3 K/min. [Dry powder data source: J. H. Campbell, Pyrolysis of Subbituminous Coal as It Relates to In Situ Gasification (Part 1: Gas Evolution), UCRL-52035, Lawrence Livermore National Laboratory, March 1976; (Part 2: Characterization of Liquid and Solid Products), UCRL-52035 Part 2, Lawrence Livermore National Laboratory, June 1976.]

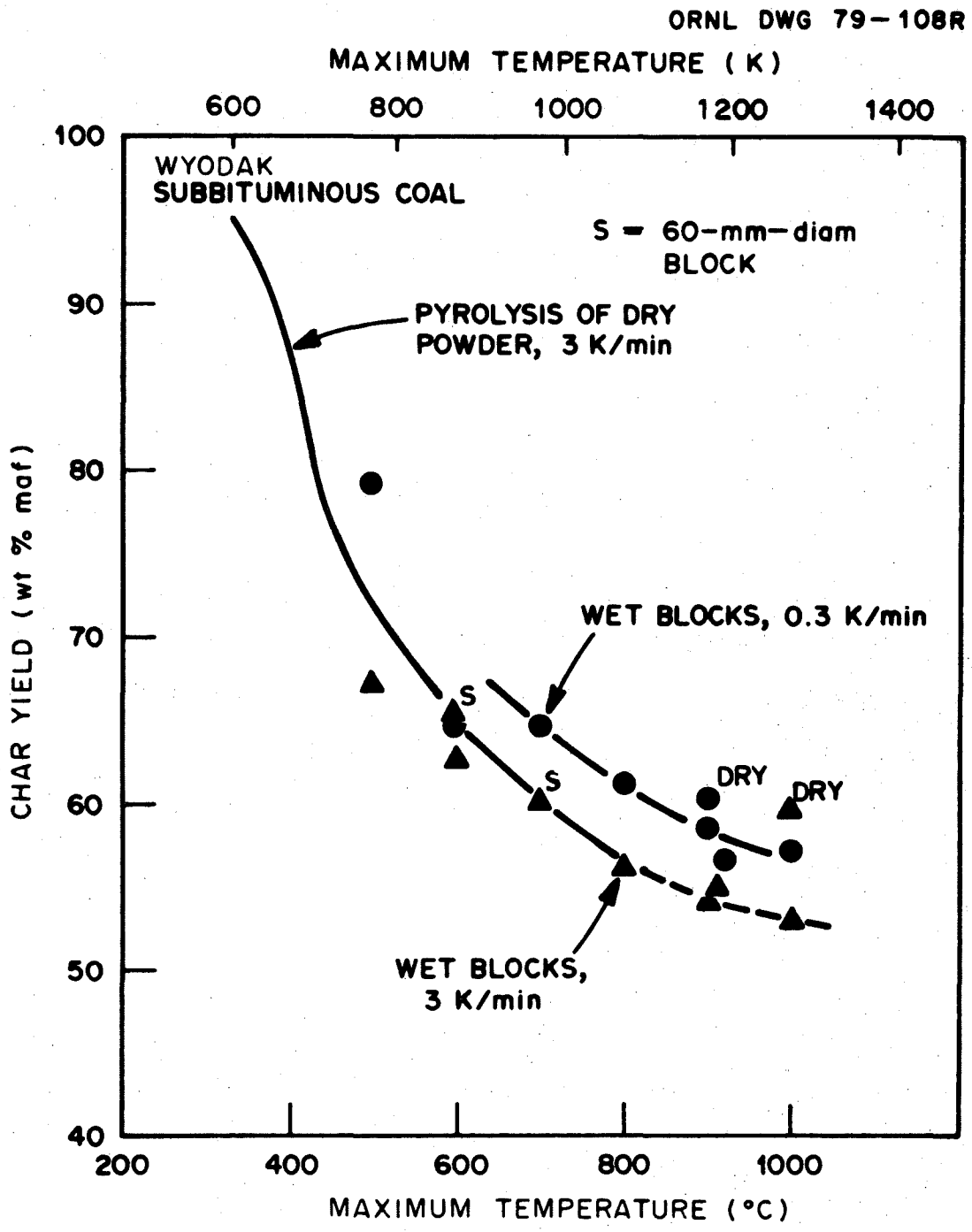

Fig. 3.15. Char yields from heating of Wyodak subbituminous coal in inert gas. Triangles represent blocks heated at 3 K/min; dots represent blocks heated at 0.3 K/min. (Dry powder data source: J. B. Goodman, M. Gomez, and V. F. Parry, Laboratory Carbonization Assay of Low-rank Coals at Low, Medium, and High Temperatures, RI-5383, U.S. Bureau of Mines, January 1958.)

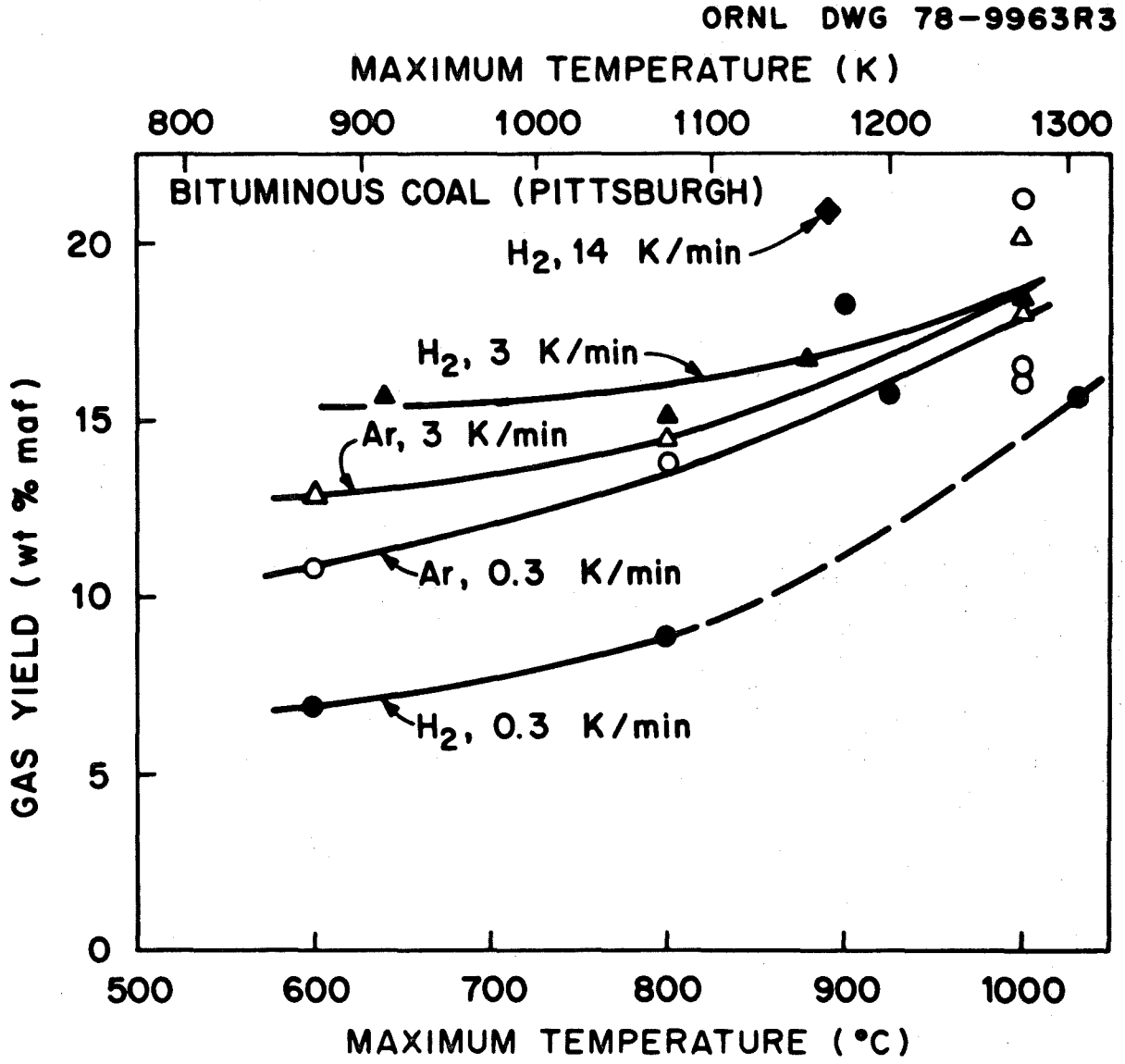

Fig. 3.16. Gas yields from heating of Pittsburgh bituminous coal. (Open symbols represent Ar runs, solid symbols represent H_2; circles represent 0.3 K/min, triangles represent 3 K/min, and squares represent 14 K/min.)

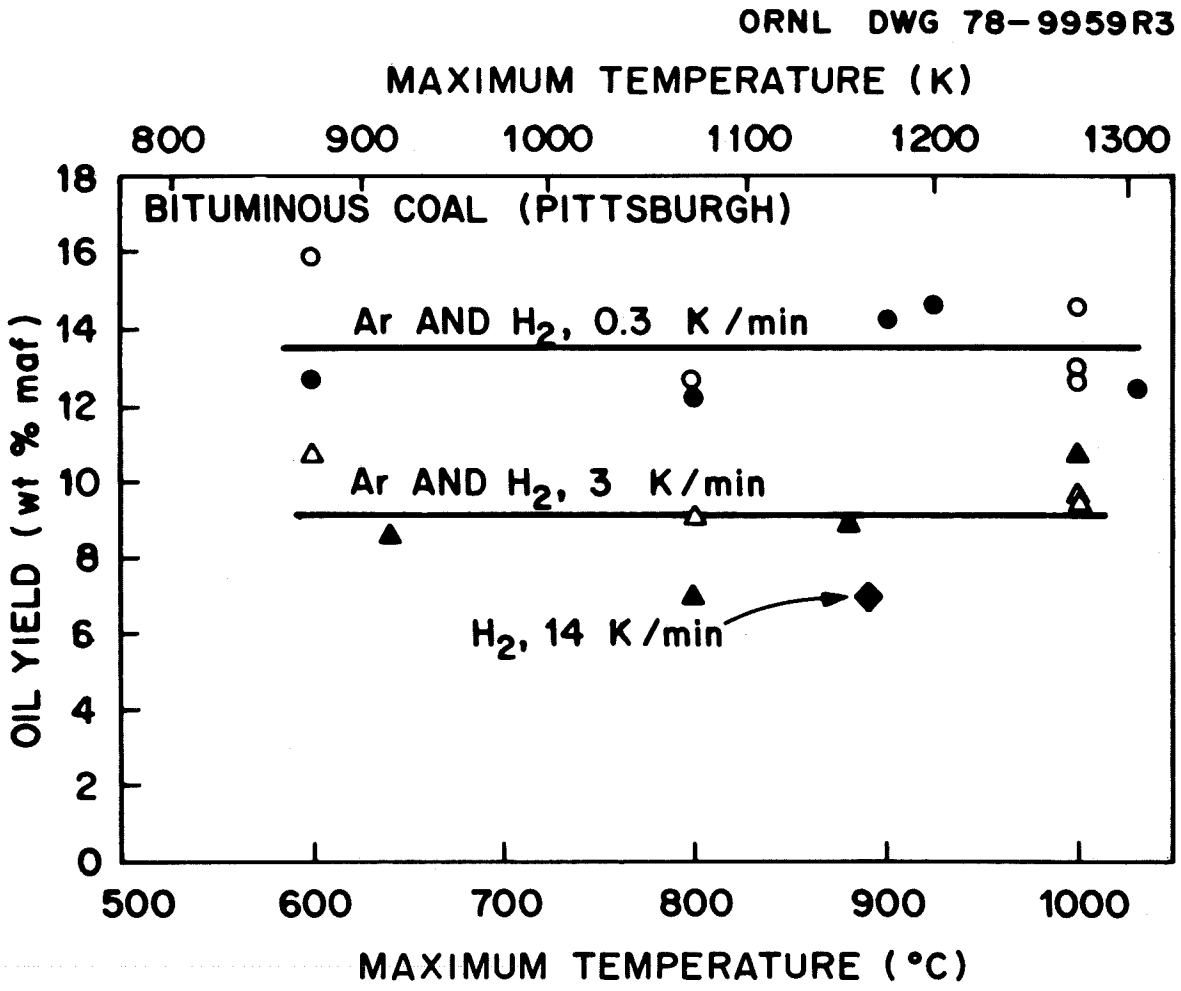

Fig. 3.17. Yields of condensible organics from heating of Pittsburgh bituminous coal. (Open symbols for Ar runs, solid symbols for H_2; circles represent 0.3 K/min, triangles represent 3 K/min, and squares represent 14 K/min.)

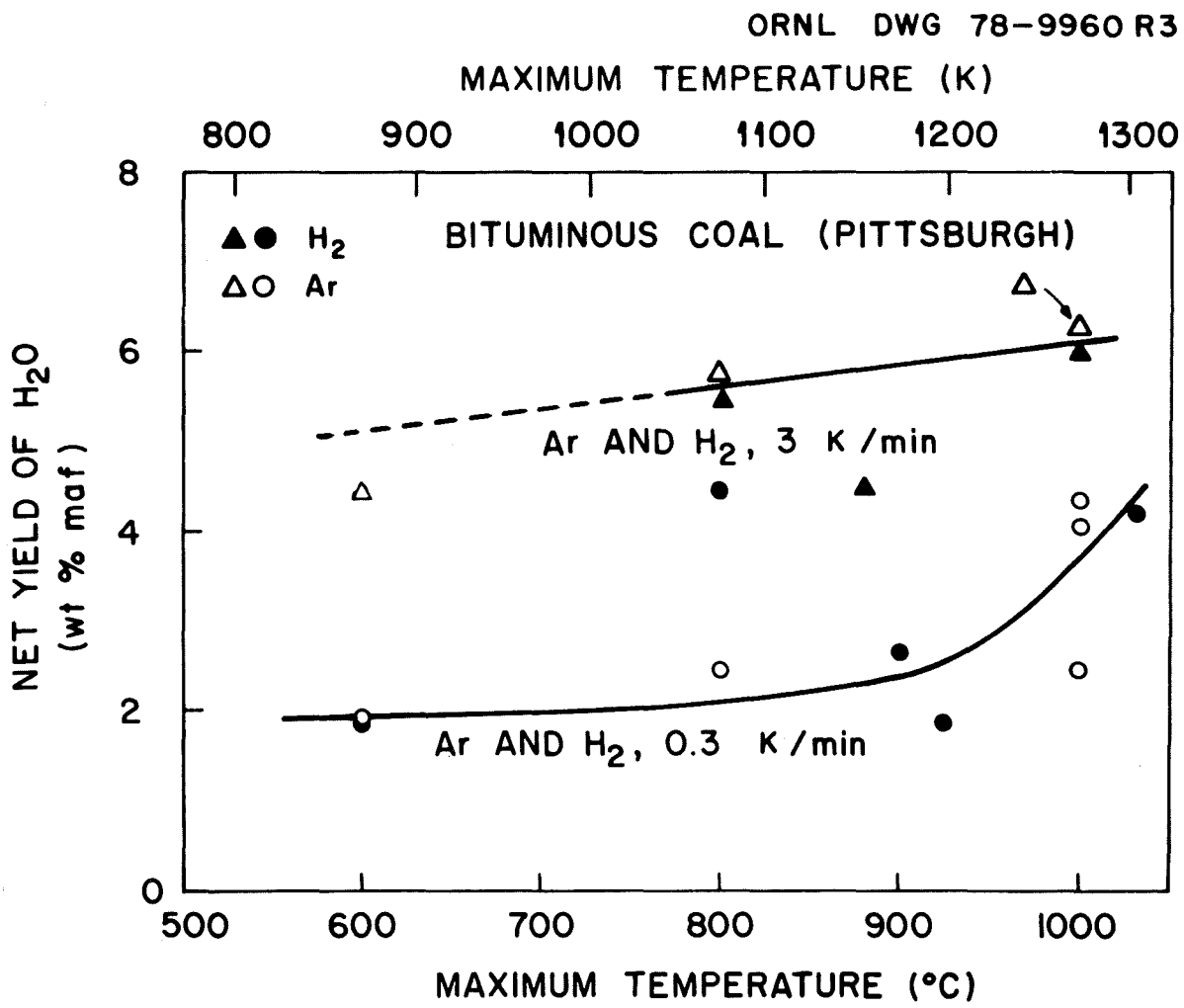

Fig. 3.18. Net yields of water from heating of Pittsburgh bituminous coal. (Open symbols for Ar runs, solid symbols for H_2; circles represent 0.3 K/min, triangles represent 3 K/min.)

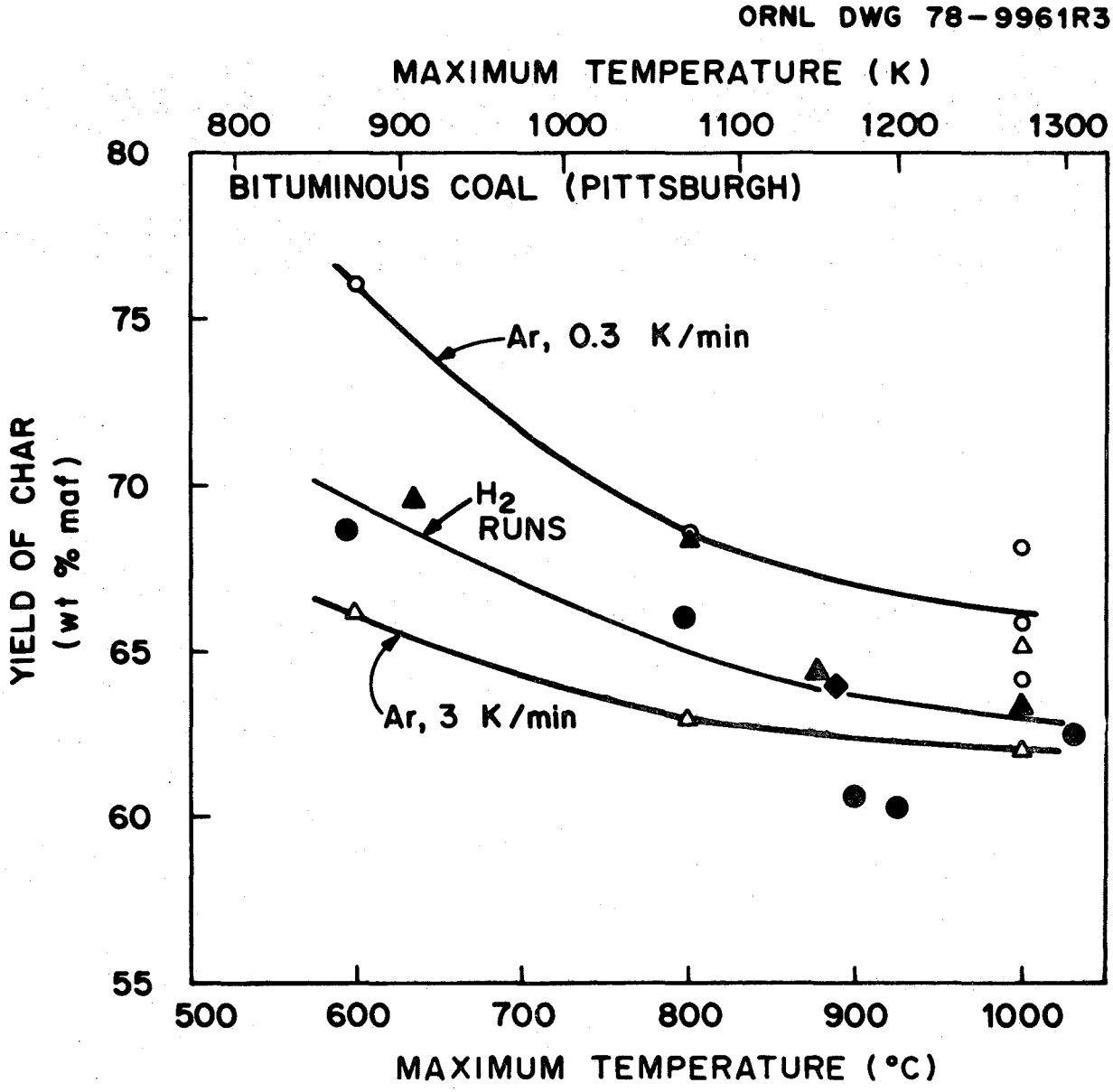

Fig. 3.19. Char yields from heating of Pittsburgh bituminous coal. (Open symbols for Ar runs, solid symbols for H_2; circles represent 0.3 K/min, triangles represent 3 K/min, and squares represent 14 K/min.)

In summary, changes in cumulative yields occurred as rank, "particle" size (block vs powder), coal moisture content, surface heating rate, and maximum temperature were changed. In conventional pyrolysis experiments using powdered coal, at heating rates used in our experiments, no changes are observed except those resulting from rank and temperature. However, analyses of the temperature and yield data from block experiments indicated what mechanisms may account for the measured differences between results from block vs powder pyrolysis experiments. Modeling of drying and pyrolysis of UCG may be improved as a consequence of the new understanding of the synergism among heat transfer, drying, and pyrolysis phenomena and the escape of products through the coal.

3.3 Secondary Cracking of Pyrolysis Products

Secondary cracking of oils, tars, and methane was observed when blocks of Wilcox lignite, Wyodak subbituminous coal, and Pittsburgh seam bituminous coal were heated. Simply, the mechanism consists of the products of coal pyrolysis themselves being pyrolyzed or thermally cracked into lighter oils, gases, steam, and carbon deposits as they escaped from the coal. Anthony and Howard[8] had studied this phenomenon in the rapid heating of coal powders; but in experiments in which large pieces of coal were heated slowly, the effect was also important. If such cracking occurred in UCG, a portion of the pyrolysis tars would be destroyed and would leave behind carbon deposits that could be gasified.

3.3.1 Mechanism of secondary cracking

Organic vapors and gases are formed from coal by pyrolysis, typically at temperatures of 570 to 870 K (300 to 600°C).[5] As these pyrolysis products escaped from the block, as in UCG, they passed through hot char where pyrolytic cracking could occur:

$$\text{organic vapors} \xrightarrow{\Delta} \text{lighter organic vapors} + H_2, CH_4, C_2H_4, \text{other gases} + \text{steam} + \text{carbon deposits.} \qquad (3.1)$$

Research and review of pyrolysis by Anthony and Howard[8] treated such cracking of organic vapors as the principal secondary reaction in their experiments with dry powders in which particle sizes were small (1-mm-diam maximum, and more typically 53 to 88 μm), but heating rates were very high (6,000 to 720,000 K/s). Within these particles, the intrinsic pyrolysis kinetics were modeled as first-order reactions that have a Gaussian distribution of activation energies and produce the same intrinsic yields of primary products regardless of heating rate. Thus, actual yields were determined by the relationship between the kinetics of secondary cracking and the residence time of escaping products. Differences in powder yields were interpreted as being only indirectly caused by different heating rates or particle sizes.

Secondary cracking occurred in the coal block experiments because residence times of vapors were appreciable and because the escape was through progressively hotter char as heating rates increased (i.e., before equilibration occurred). The intrinsic yields measured by Anthony and Howard were based on near-instantaneous release of pyrolysis products from very small particles. In the blocks, residence times of vapors escaping through 75 mm of coal (or more if swelling occurred) had to be appreciable. Also, the escaping vapors followed paths that increased in temperature, as shown in the temperature profiles of Sect. 3.1. Higher heating rates, by causing steeper temperature gradients, would make the vapors move within extreme temperature gradients, causing more extensive cracking.

In summary, heating rates applied in coal block research were much lower than in the powder experiments of Anthony and Howard. However, the use of larger chunks of coal caused significant in-coal residence times for escaping vapors, as in UCG. Consequently, cracking of condensible organics occurred for coal of all ranks in this block pyrolysis study.

3.3.2 Secondary cracking in low-rank coals

Because of interferences from steam, secondary cracking in low-rank coals was most reliably identified by comparing yields from dry blocks and from dry powders. Two types of dry blocks were studied: predried blocks, which were dried at 378 K in vacuum or at 405 K in an inert purge gas, and blocks slowly heated at 0.3 K/min, which dried out before surface temperature reached 680 K (410°C). All of the blocks to be discussed were heated in an inert purge gas (Ar).

Predried blocks of Wilcox lignite and Wyodak subbituminous coal were heated at 3 K/min. As shown in Table 3.1, oil and tar yield from the lignite block was 34% lower than from dry powder; conversely, gas and char yields from blocks were higher than from powder. The lower oil and tar yield is consistent with increased cracking, although steam reforming also occurs (Sect. 3.4). In a Wyodak block, 3.3 wt % maf of oil and tar were produced as compared to 5.8 wt % maf from a powder, 43% less. Again, gas and char yields were higher from predried Wyodak blocks than from powder (Figs. 3.13 and 3.15).

Data from pyrolysis of predried blocks must be used cautiously, taking into account the possibility that interferences from gasification may have occurred. In powders, water was generated by pyrolysis (see Fig. 3.10). Because the predried blocks were heated at 3 K/min, slight steam gasification of the organic vapors or carbon deposits could have occurred, as will be discussed in Sect. 3.4. However, blocks heated at 0.3 K/min were probably free of this interference. Pyrolysis data from powders (Fig. 3.10) indicated that generation of water was nearly complete at 870 K (600°C). When the center reached 870 K in a lignite block heated at 0.3 K/min, the surface of the block was only at 900 K, lower than temperatures at which gasification is significant.

Yields from blocks heated at 0.3 K/min showed the effects of secondary cracking. Again referring to Table 3.1, a block of Wilcox lignite produced 42% less oil and tar than did the dry powder. Also, gas and char yields from the block were higher. The differences in yields of condensibles (Fig. 3.14) between Wyodak blocks heated at

Table 3.1. Occurrence of secondary cracking in blocks of Wilcox lignite heated to 1070 K (800°C)

Sample type	Surface heating rate (K/min)	Yields (wt % maf)		
		Oil and tar	Gas	Char
Dry powder[a]	6	12.3	25.2	52.1
Predried block	3	7.9	28.7	58.3
Block dried during heating[b]	0.3	7.1	26.3	57.5

[a]Source of data: J. B. Goodman, M. Gomez, and V. F. Parry, Laboratory Carbonization Assay of Low-rank Coals at Low, Medium, and High Temperatures, RI-5383, U.S. Bureau of Mines, January 1958.

[b]Dried out before surface temperature reached 680 K (410°C).

0.3 K/min and dry powders were apparently caused by lower oil and tar yields. Gas yields from Wyodak blocks (Fig. 3.13) were marginally higher and char yields (Fig. 3.15) were definitely higher than from powders.

Secondary cracking also occurred in the heating of wet blocks at 3 K/min, possibly in addition to steam reforming of the vapors. Oil and tar yields from blocks of Wilcox averaged approximately 50% less than yields from powders (Figs. 3.9 and 3.12). Net yields of condensibles from Wyodak coal suggest the same sort of decrease. However, without further evidence, these decreases could just as well have been attributed to consumption of the oil and tar by steam reforming.

Differences in ethylene yields and char reactivity as compared to powders further indicated that secondary cracking had occurred in the wet blocks. Ethylene and ethane yields were resolved by mass spectrometry for experiments using Wyodak coal. Ethane was not cracked further; its yield, unaffected by heating rate or maximum temperature, averaged 0.56 ± 0.095 wt % maf. In contrast, despite a scattering in the data, an increase in ethylene yield was observed when higher heating rates were used (Fig. 3.20). If ethane yields were constant from Wilcox lignite blocks, an increase in ethylene yield was indicated by a 70% increase in C_2 yield (ethane and ethylene) when heating rate was increased from 0.3 to 10 K/min (wet blocks, 1073 K). Ethylene is a characteristic product of cracking, and its higher yield suggested an increase in secondary cracking. Changes in char reactivity also indicated that secondary cracking had occurred in wet lignite. Section 3.6 discusses these changes.

3.3.3 Secondary cracking in bituminous coal

Secondary cracking was the principal side reaction observed when blocks of Pittsburgh seam bituminous coal were heated in inert gas. Natural moisture content was only 1.8 wt %, so that steam interactions were not important. Because powders of this coal agglomerate when heated, no suitable data for powders were available in this range of heating rates. Changes in heating rate of the blocks were used to

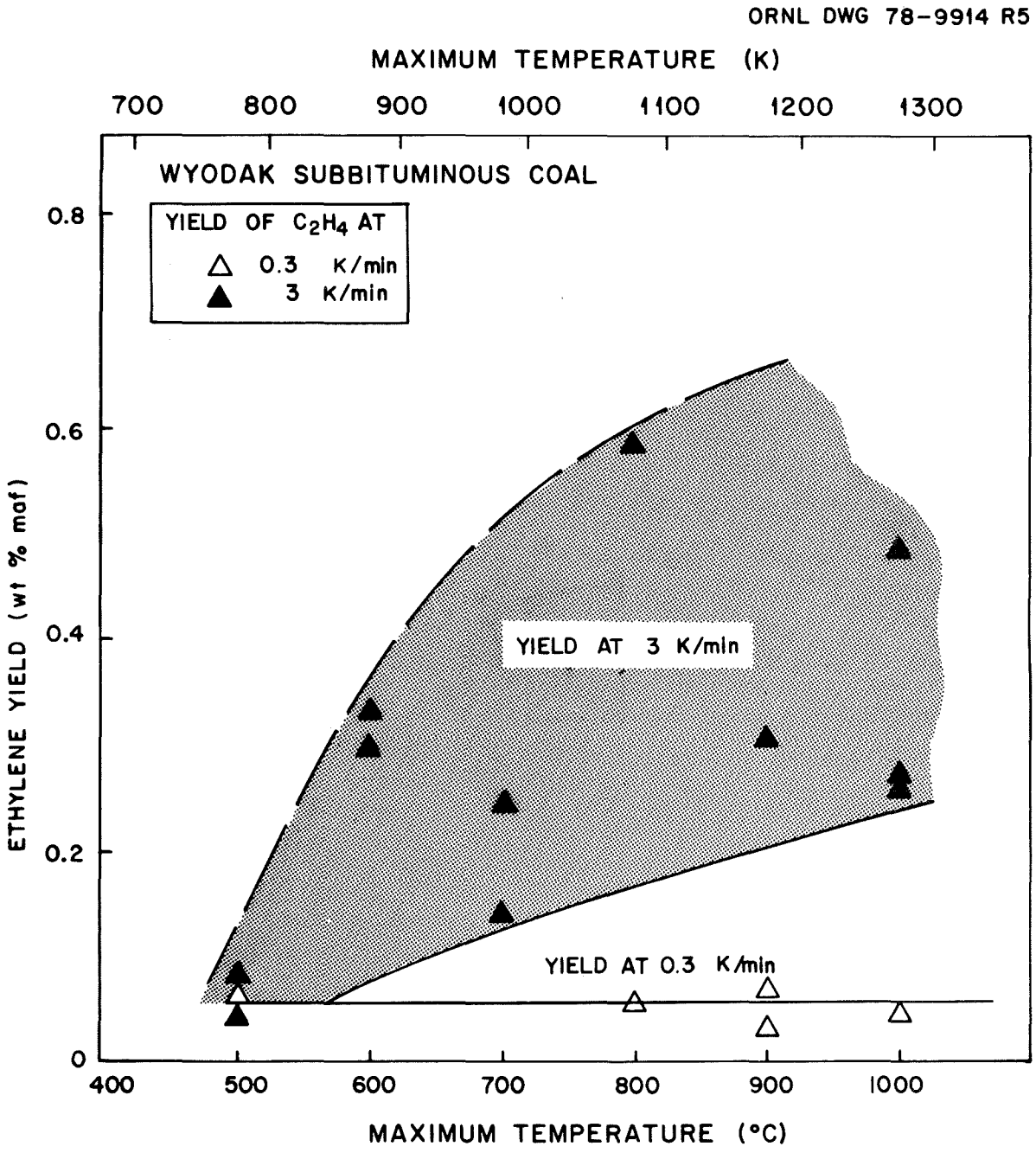

Fig. 3.20. Changes in ethylene yields with conditions of block heating — Wyodak subbituminous coal.

examine trends in cracking, although a change in heating rate was also observed to change the extent of swelling (to be discussed in Sect. 3.7).

Yields of oil and tar (Fig. 3.17) were lower as higher heating rates were used (steeper internal temperature gradients). To reiterate, (1) only experiments using inert purge gas (Ar) were considered in this subsection and (2) purge gas had no effect on oil and tar yields. Slight increases occurred in yields of gas (Fig. 3.16) and water (Fig. 3.18) at 3 K/min compared to 0.3 K/min. Ethylene yields were also indicative of increased cracking at higher heating rates. Ethane yield from Pittsburgh coal was constant at 1.19 $\pm$ 0.24 wt % maf. In contrast, ethylene yields increased dramatically when higher heating rates were applied (Fig. 3.21). Yields of methane, another product of cracking, also were higher at 3 K/min (Table 3.2).

Trends in char yields (Fig. 3.19) stood in sharp contrast to the hypothesis that cracking was more extensive at higher heating rates. In inert gas at 3 K/min, char yields were lower by 5 to 10 wt % maf than at 0.3 K/min; one would expect higher, rather than lower char yields if cracking and carbon deposition were more extensive at 3 K/min. Two possible explanations were (1) data error or (2) increased coking at 0.3 K/min as a result of decreased convection of products from the block, thereby increasing residence times of escaping vapors. This inconsistency was recognized but remains unexplained.

3.3.4 Cracking of methane

Methane cracking apparently occurred in the blocks of low-rank coal, based on comparisons of yields from dry blocks and dry powders. Production of methane by cracking of oils obscured this mechanism in other experiments on low-rank coals and on bituminous coal.

Complete decomposition of methane may be written as

$$CH_4 \rightarrow C + 2H_2 \ , \qquad (3.2)$$

the reverse of the hydrogasification reaction. Hydrogen-carbon bonds in methane are quite strong (bond energy of 416 kJ/mole),[9] therefore,

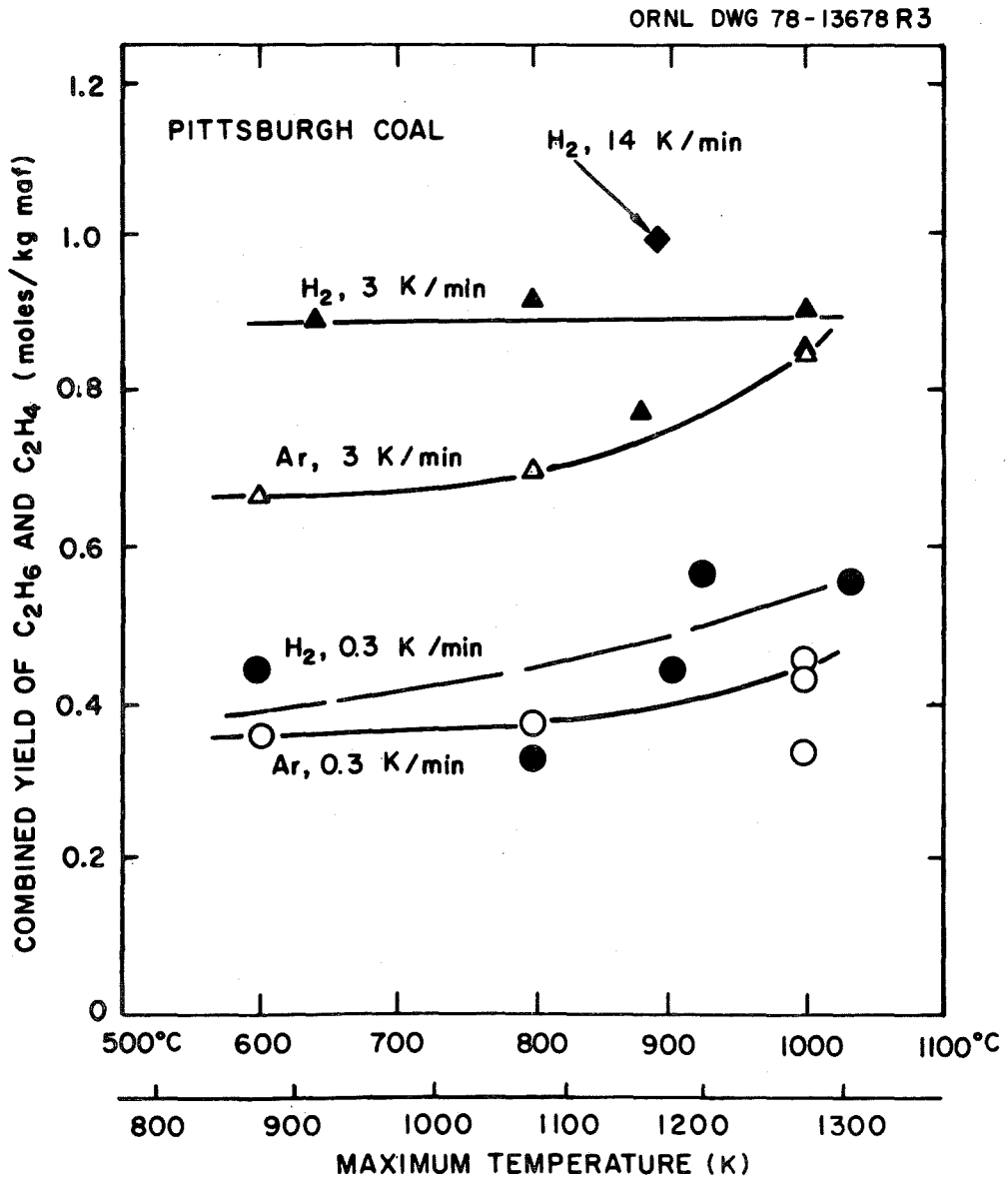

Fig. 3.21. Changes in ethylene (C_2H_4) yields with conditions of block heating — Pittsburgh bituminous coal. Total of C_2H_4 and ethane (C_2H_6) is shown here, but C_2H_6 yield was constant (in available data) at 0.4 mole/kg maf coal.

Table 3.2. Changes in methane yields from blocks of Pittsburgh bituminous coal heated in an inert purge gas

Maximum temperature (K)	Yields of methane (wt % maf)	
	0.3 K/min	3 K/min
870	2.08	2.85
1070	2.61	3.45
1270	3.07, 2.96, 2.95	3.78, 4.50

methylation of other organics would be a more plausible reaction for consuming methane. Nevertheless, at higher temperatures, the decomposition may proceed rapidly in the presence of catalytic ash. Methane decomposition has been used in other research as a method of depositing carbon onto coal chars at 1088 to 1128 K (815 to 855°C). Kinetics for homogeneous cracking is poor, but carbon surfaces are known to catalyze several cracking reactions.[10] Furthermore, naturally occurring mineral matter in the coal (notably siderite and calcite) also are known to catalyze cracking and carbon deposition.[11]

Methane decomposition was most apparent in Wilcox lignite. From pyrolysis of dry powder, methane yield was 4.36 wt % maf,[5] whereas yield from a dry block heated at 3 K/min (3.16 wt % maf) was 28% less. Comparison of Wyodak data from dry powder[6] and a dry block showed a much smaller difference, with methane yields of 4.85 and 4.49 wt % maf, respectively. Cracking of the methane was a reasonable explanation for these differences, and the dissimilarity of the mineral composition of the two coals may account for the larger difference in the lignite.

3.3.5 Implications of secondary cracking for UCG

Tars and methane may be cracked by the mechanisms discussed in Sect. 3.3.4, as forward gasification proceeds in UCG. As in the blocks, the pyrolysis products must escape through cavity walls and chunks of fallen coal. More of the same cracking can occur as these organic products are swept through the hot roof rubble toward the production well. Because heavy tars may condense as they are swept from the reaction cavity, they can be revaporized and cracked further as the hot reaction zone expands.

These implications were borne out by the comparison of oils from laboratory and field tests (Table 3.3).[12] The simulated distillation curve for oil from laboratory pyrolysis of powdered Hanna coal was skewed toward the high-boiling end of the range, with 24% boiling above 811 K (1000°F). At the other extreme, heavy ends were absent in oils produced by reverse combustion linkage in the field; they had been destroyed as the pyrolysis products were fed back into the flame front.

Table 3.3. Comparison of boiling-point distributions for oils from laboratory pyrolysis and UCG field tests

Boiling range	Percentage of sample boiling within the range.			
		Hanna I field test[a]		
	Powder carbonization[a]	From reverse combustion	Forward gasification	Block pyrolysis[b]
311-478 K (100-400°F)	0	30.0	6.2	5.5
478-533 K (400-500°F)	11.3	46.7	16.9	19.7
533-589 K (500-600°F)	16.3	22.0	25.6	24.2
589-644 K (600-700°F)	13.1	1.3	28.2	22.2
644-700 K (700-800°F)	15.2	0	16.0	18.5
700-755 K (800-900°F)	12.4	0	5.3	9.9
755-811 K (900-1000°F)	7.5	0	1.8	0
Residue	24.2	0	0	0

[a]Source of data: S. B. King, C. F. Brandenburg, and W. J. Lanum, "Characterization of Nitrogen Compounds in Tar Produced from Underground Coal Gasification," presented at the 169th National Meeting of the American Chemical Society, Philadelphia, Pennsylvania, April 6-11, 1975, Hanna No. 1 coal; oil samples from the field test were collected at the production well.

[b]Experiment BP2-19; 3 K/min to 1273 K (1000°C), predried block of Wyodak coal in inert purge gas.

Oils from field UCG (forward gasification) and block pyrolysis fell between the extremes because of the mechanistic similarities between cracking in UCG and in block pyrolysis.

Most importantly, the cracking of these compounds can deposit carbon onto the char. The high reactivity of this deposited carbon makes it susceptible to gasification reactions (Sect. 3.4) and can affect the overall reactivity of the char (Sect. 3.6).

3.4 Self-Gasification of Coal Blocks

Self-gasification of coal was observed when naturally moist blocks of Wilcox lignite and Wyodak subbituminous coal were heated. Stated simply, if steam generated by drying escaped through hot char [hotter than about 490 K (670°C)], then steam gasification occurred by the reaction of steam with carbon deposits from cracking, with oil and tar vapors, and possibly with char. Clearly, this is a major mechanism by which coal moisture participates in UCG, primarily in the high-moisture coals. Data showing the occurrence and extent, along with implications of this gasification mechanism, are presented here.

3.4.1 Mechanisms and reactions

Self-gasification of coal occurred as steam generated by drying escaped through char along a path of increasing temperature. The gasification of carbon deposits or char was lumped with the steam reforming of tar vapors as self-gasification. This approach was taken partly because the products of different carbon sources were difficult to separate, but also because all the carbon sources, after all, had originated from the coal. Thus, from external measurements, the effects of different reactions all gave the appearance of the block gasifying itself.

A primary reaction was the gasification of carbon as carbon deposits or char. The heat of reaction for steam gasification of carbon,

$$C + H_2O \rightarrow H_2 + CO \ , \qquad (3.3)$$

is endothermic, so that the reaction equilibrium becomes more favorable

with increased temperature. The equilibrium constant, K_p, for gasification of amorphous graphite reaches 1.0 at 940 K (670°C). If steam is present, gasification would become thermodynamically favorable at temperatures around 920 K (650°C).

Steam reforming of organic vapors occurs by the general reaction

$$a\ (\text{vapor}) + b\ H_2O \rightarrow c\ H_2 + d\ CO\ , \tag{3.4}$$

where a, b, c, and d are stoichiometric coefficients. Reaction equilibria for this gasification of vapors follow the same trend as for gasification of carbon; if the vapor is a hydrocarbon, greater amounts of H_2 than CO will be produced.

Carbon monoxide produced by these reactions may be converted to carbon dioxide by the water-gas shift reaction:

$$CO + H_2O \rightleftharpoons CO_2 + H_2. \tag{3.5}$$

Equilibrium for this reaction is rather insensitive to temperature. The equilibrium constant is 1.0 at approximately 1070 K (800°C), but it varies only within an order of magnitude (5 to 0.5) over the range 800 to 1500 K. If no other reactions involving CO or CO_2 occur, such as

$$CO_2 + C \rightarrow 2CO \tag{3.6}$$

(the Boudouard reaction), the amount of carbon contained in CO and CO_2 will be the amount of carbon gasified. Changes in this amount were used as indicators of self-gasification.

3.4.2 Conditions for self-gasification

The three conditions for self-gasification were

1. a region of wet, drying coal, releasing steam;
2. steam escaping through a region of temperatures around 920 K or above; and
3. presence of a carbon source.

These conditions were met experimentally when blocks of wet coal were heated at 2 K/min or faster to temperatures of 920 K or above. Consumption of water and generation of H_2, CO, and CO_2 will be discussed

here to illustrate the occurrence of self-gasification; carbon sources will be discussed in Sect. 3.4.3.

Effects of temperature. By comparing yields at different temperatures from wet blocks heated at 3 K/min to yields from dry powder, the occurrence of self-gasification and the effects of temperature were shown. In dry, powdered coal, no water was available for gasification, and, at these heating rates, temperatures throughout each particle were essentially uniform. In the wet blocks, temperature measurements (Fig. 3.3 and Fig. 3.5) showed that steam was formed and escaped through hot char, thus providing the elements for gasification.

Yields from blocks vs powders of Wilcox lignite diverged at about 870 K (600°C), indicating the onset of gasification. At or above 870 K, net yields of water (Fig. 3.10) from blocks began to be less than the yields from powders. In experiments run to 1070 and 1270 K, net yields of water from blocks were negative because of the way net yield was calculated — actual yield of water minus the calculated original moisture in the coal block. The negative yield may be interpreted as being a lower yield of water than if the block had simply been dried, that is, water actually was consumed. (Water consumption from the lignite experiments is tabulated in Appendix A-1, Table A-1.10.) At the same temperatures that water was consumed, gas yields (Fig. 3.8) from the wet blocks were higher than for powder, indicating the evolution of gas. Divergence in gas yields again occurred at or about 870 K. The gases evolved in wet block experiments in which temperatures were run to 1070 and 1270 K were predominantly H_2, CO, and CO_2. All these changes were indicative of self-gasification.

Such a direct comparison was not possible for yields from Wyodak blocks and powders because (1) secondary cracking was appreciable, increasing gas yield at the expense of oil and tar, and (2) water yield was not separated from yields of organic liquids. Nevertheless, yields could be compared between wet blocks heated at 3 K/min and blocks that were dried at gasification temperatures

(i.e., predried blocks and wet blocks heated at 0.3 K/min.) Net yields of combined liquids (Fig. 3.14) from wet and "dry" blocks diverged around 800 K (530°C) and were negative for wet blocks at high temperatures. Gas yields (Fig. 3.13) also diverged near 800 K. Water consumption and generation of H_2, CO, and CO_2 again indicated the occurrence of self-gasification.

An interesting feature of gas yields from wet Wyodak blocks (Fig. 3.13) was that yield leveled off in experiments run to 1170 K (900°C) and above. At a heating rate of 3 K/min, the center of the Wyodak coal block, of the size used and 33.6% moisture content, dried out when the block surface reached approximately 1170 K (see Fig. 3.2). Because the steam supply for gasification was gone, self-gasification stopped.

Effects of heating rate. Heating wet blocks of coal at 2 K/min or above caused self-gasification to occur, and the amount of gasification increased with heating rate. These effects were further confirmation of the mechanism involved.

To re-emphasize, various heating rates were used to experimentally manipulate temperature gradients in the coal blocks. The magnitude of heating rates was similar to those in UCG, but the results of heating rates in blocks must be interpreted from a mechanistic point of view before being applied to UCG (Sect. 3.4.4). Different heating rates caused the extent of drying — and, conversely, the size of the wet core — to be different at any given surface temperature.

Temperature and yield measurements in Wilcox lignite confirmed that the extent of drying is the cause of increased self-gasification at higher heating rates (Table 3.4). Heating a wet block at 3 K/min left a wet core comprising 25% of the block that was still drying when block surface temperature reached 920 K (640°C). This temperature approximated the lowest temperature at which gasification reactions would occur. Heating a wet block at 10 K/min left 50% of the block as wet core at 920 K. Powders and predried blocks have already been dried before heating, and wet blocks heated at 0.3 K/min had dried out when the

Table 3.4. Increases in self-gasification of lignite with the amount of steam contacting hot char[a]

Experiment	Conditions of pyrolysis	Vol % of block still wet at 920 K surface temperature[b]	H_2O consumption[c] (mol/kg maf)	Gas yields (mol/kg maf)			Carbon in CO and CO_2 (g-atom/kg maf)
				H_2	CO	CO_2	
BP2-52	Predried block, 3 K/min	0	*d*	8.57[e]	3.44	2.61	2.19
BP2-51	Wet block,[f] 0.3 K/min	0	1.8	6.02	3.62	2.49	2.23
BP2-54	Wet block, 3 K/min	~25	9.9	10.94	4.42	3.37	2.82
BP2-53	Wet block, 10 K/min	~50	12.7	13.20	4.86	4.29	3.25

[a] In each experiment a block of Wilcox lignite was heated to a maximum temperature of 1073 K (800°C) in inert gas; see also Fig. 3.11.

[b] Calculated from temperature profiles.

[c] From Table A-1.10.

[d] Poor collection of H_2 for measurement.

[e] H_2 yield was increased by cracking of oils.

[f] Because of slow heating, the block had completely dried when surface temperature reached 680 K (410°C).

surface reached 680 K (410°C), precluding self-gasification. Occurrence of more self-gasification in the wet blocks heated at 3 and 10 K/min was indicated by increased consumption of water and generation of H_2, CO, and CO_2. The explanation for this effect is that more of the block remained wet, producing more steam at gasification (higher) temperatures.

For the same reason, increased heating rates in wet blocks of Wyodak subbituminous coal (Table 3.5) and of Wilcox lignite (Table 3.6) also produced more self-gasification. Within the scatter of the data, yields of condensibles declined with higher heating rates (Table 3.6).

3.4.3 Carbon sources for self-gasification

Three carbon sources may be gasified by escaping steam: carbon deposited by secondary cracking, organic vapors, and pyrolysis char. Gasification of carbon deposits was identified primarily from changes in char reactivity and secondarily from char yields. Large yields of H_2 relative to CO and CO_2 pointed to steam reforming. Pyrolysis char, the solid residue of coal pyrolysis, may have been gasified but confirmation of it was not possible. Char yields reported here were the total amounts of solid residue from block heating, including pyrolysis char and carbon deposits not consumed by gasification.

Carbon or high-carbon-content deposits were left on the pyrolysis char by secondary cracking reactions analogous to the coking of catalyst by hydrocarbons. Solano, Mahajan, and Walker[11] reported that this type of deposit seemed to be very reactive. Changes in reactivity of the char blocks from Wilcox lignite indicated that reactive constituents, such as the carbon deposits, had been gasified by steam and hydrogen (discussed further in Sect. 3.6). Also indicative of this mechanism of gasification, heating of "dry" blocks of Wyodak coal (predried blocks or wet blocks heated at 0.3 K/min) produced more char than heating of Wyodak powder, apparently because of secondary cracking. However, heating blocks that were self-gasified (wet blocks at 3 K/min) produced nearly the same amount of char as that from powdered coal. In

Table 3.5. Increases in self-gasification of subbituminous coal[a] with increased heating rates

Surface heating rate (K/min)	Yields (wt % maf)				Experiment	Material balance (wt % maf)
	Char	Net condensibles	H_2	Carbon in CO and CO_2		
0.3	57.0	9.3	1.568	5.68	BP2-16	91.2
2	55.4	9.2[b]	3.020	10.16	BP1-13	110.2
3	52.6	-12.9[c]	3.733	14.56	BP2-17	88.8
4	45.7	- 4.6	4.320	15.08	BP1-7	101.3

[a]In each experiment, a wet block of Wyodak coal was heated to 1273 K (1000°C) in inert purge gas.

[b]Possible water leak into condenser.

[c]Probably major source of error in material balance.

Table 3.6. Comparison of product yields from powders and wet blocks of Wilcox lignite

	Maximum temperature			
	943 K (670°C)		1073 K (800°C)	
	Powder 6-7 K/min[a]	BP2-48, 3 K/min in H_2	Powder 6-7 K/min[a]	BP2-49 0.3 K/min in H_2
Char yield, wt % maf	55.1	53.7	52.1	50.0
Yield of oil and tar, wt % maf	12.4	5.6	12.3	4.7
Net water yield, mol/kg maf lignite	5.66	4.72	5.72	10.6
Gas yield, mol/kg maf lignite				
H_2	2.98	4.24[b]	4.81	-1.85[c]
CH_4	2.55	3.85	2.72	6.14
CO	1.53	2.48	2.11	1.901
CO_2	2.66	3.19	2.77	1.849
Material balance, %	100.0	97.8	99.9	98.6

[a]Source of data: J. B. Goodman, M. Gomez, and V. F. Parry, Laboratory Carbonization Assay of Low-rank Coals at Low, Medium, and High Temperatures, RI-5383, U.S. Bureau of Mines, January 1958.

[b] Increased slightly by self-gasification.

[c] Negative, indicating H_2 from purge gas was consumed.

self-gasification, either deposits had been removed by gasification, leaving only pyrolysis char, or carbon had not been deposited at all in the presence of steam.

Steam reforming of organic vapors would cause self-gasification of the block. As discussed in Sect. 3.4.1, steam reforming of hydrocarbons would produce more H_2 than CO. Yield data from Wilcox lignite (Table 3.4) and from Wyodak subbituminous coal (Table 3.5) showed this effect. On a molar basis, consumption of H_2O and yield of H_2 were greater than the amount of gasified carbon (carbon in CO and CO_2) produced.

Gasification of pyrolysis char could conceivably explain these char yields, but reactivity data indicate, instead, that carbon deposition caused the changes. Char yields from blocks of Wilcox lignite at 1000°C (Fig. 3.11) were less than pyrolysis char yields from powder. This decrease in char below pyrolysis yields could result from gasification.

3.4.4 Implications of self-gasification for UCG

Self-gasification such as that observed in coal block pyrolysis must also occur during UCG. In UCG, self-gasification would occur in chunks of collapsed roof coal and in the cavity wall as the gasification cavity expands. Steam from water influx and from elsewhere in the UCG cavity upstream of the drying coal can also penetrate the char and gasify it, but in very wet coals, little steam would be able to diffuse in against the fluxes of escaping steam and reaction products.

Higher heating rates in UCG, caused by faster air injection rates or the injection of oxygen instead of air, could reduce the amount of self-gasification. Superficially, this hypothesis would seem to contradict block data, but it followed directly from extrapolation of results from the finite block size to the semi-infinite geometry of a coal seam. As discussed at the end of Sect. 3.1, increases in UCG heat flux or in the moisture content of the coal would result in a narrow reaction zone (char zone) in the wall of the underground

reaction cavity; this fact is supported by estimates of char zone thickness from field UCG tests.[7] The extent of self-gasification would decrease because residence time of steam in the char zone would be less. In the extremes of high heat flux and high moisture content, the char zone would become so narrow (have such a steep temperature gradient) that no UCG could take place.

Lower heating rates (slower oxygen or air injection) or less coal moisture would cause broader char zones and more self-gasification. In a thick char zone, the longer residence time of escaping steam would cause more complete gasification. This increased efficiency in the use of coal moisture would be counterbalanced by lower gas production rates as steam generation and pyrolysis became slower. Based on these observations, an optimum in air injection rate exists for a given coal moisture content because the extent of gasification and the gas production rate are both influenced by these variables.

Char permeability also would affect the extent of self-gasification. When gas yields from Wilcox lignite and Wyodak subbituminous coal were compared (Figs. 3.8 and 3.13), self-gasification was observed to be more extensive in Wyodak coal despite its lower moisture content (30% vs 37%). The Wyodak char structure was less open than was Wilcox char,[3] so that the difference probably was caused by greater mass-transfer resistance in Wyodak char.

In summary, self-gasification of coal by escaping steam is surely an important mechanism in UCG cavity growth and in the gasification of collapsed-roof coal. As will be discussed in Sect. 3.6, this steam outflux also affected subsequent reactivity of the char. The results here also suggest how air injection rate, coal moisture content, and char permeability would affect the extent of self-gasification in UCG.

3.5 Effects of Reactive Purge Gases

During UCG, a mixture including H_2, CH_4, other hydrocarbon gases, organic vapors, CO, CO_2, H_2S, steam, and N_2 sweeps past the reacting coal face. Purge gases of H_2 or a simulated UCG product gas were used

instead of inert gas in order to investigate the effects of reactive gases. Use of H_2 caused hydrogasification and water generation reactions, and use of the mixed gas caused hydrogasification, steam gasification, and water-gas shift.

3.5.1 Reactions of blocks heated in hydrogen

Hydrogasification was the dominant reaction caused by using H_2 as the purge gas. Hydrogasification was observed except when both (1) steam convection from the block was low and (2) temperatures were favorable for reaction. Low permeability of bituminous coal during its plastic state may have limited the penetration of H_2 and, subsequently, this reaction. Temperature profiles were not significantly affected by the H_2 purge gas, although measurements showed a slightly higher thermal diffusivity of wet Wilcox lignite in H_2 (Sect. 4.1.1).

Mechanisms. Hydrogasification is thermodynamically favored at lower temperatures, and CH_4 cracking (the reverse reaction) is favored at higher temperatures. The equilibrium constant, K_p, is greater than 1 for the hydrogasification of carbon,

$$C + 2H_2 = CH_4 \ , \qquad (3.7)$$

only at temperatures less than 820 K (550°C), whereas reaction kinetics are more favorable as temperatures increase. Thus, optimal conditions of the reaction would be in a range of between 770 to 920 K (550 to 650°C).

Hydrogasification of carbon would be unlikely without the presence of a catalyst. Bond dissociation energy for the H-H bond is high (436 kJ/mole),[9] so that direct attack of carbon by hydrogen atoms would require catalytic dissociation of H_2. An alternative hydrogasification route would also be demethylation of the escaping organic vapors, or of compounds inside the coal, by H_2.

Water may have been generated by reactions between H_2 and the coal blocks. Reactions could not be identified, but yields indicated that oxygenated groups in the coal were the oxygen source.

Observations from Wilcox lignite. Hydrogasification occurred in all hydrogen-purged experiments on Wilcox lignite. The reaction occurred in experiments BP2-48 and BP2-49 to a significant extent (Table 3.6).

In BP2-48, a wet block was heated at 3 K/min to 940 K (670°C). Hydrogasification occurred while the char block, dried out at the end of the experiment, remained at 940 K in H_2. Flow rates at that time showed that (1) all gas evolution had stopped except for a small but steady evolution of CH_4 and (2) that H_2 was being consumed. Hydrogasification was quenched by switching to inert purge gas. Water, H_2, CO, and CO_2 yields indicated that some self-gasification had also occurred. If water had been generated by reactions of hydrogen, it also could have participated in steam gasification, accounting for the higher yields of water (Fig. 3.12) and gas (Fig. 3.8) in H_2 relative to inert gas.

More hydrogasification occurred during BP2-49 because the block dried out at about 680 K (410°C) as a result of slow heating. As a result, H_2 had easy access to the char as the block was heated through the range of optimal hydrogasification temperatures (770 to 870 K). In that experiment, yield of H_2 dropped by 6.66 mol and CH_4 yield increased by 3.42 mol, a stoichiometric ratio of nearly 2:1.

In all other lignite experiments, steam flux was high and less hydrogasification was observed (Figs. 3.8, 3.11, and 3.12). Overall gas yields and methane yields were slightly higher when H_2 rather than inert gas was used, and char yields were not detectably changed.

Experiment BP2-49 provided the principal evidence that water was being generated by reactions of the coal block with H_2 purge gas. As shown in Table 3.6, more moles of H_2O per kg maf were generated from lignite blocks than from powders. Although the oxygen source for water generation cannot be determined with certainty because of the other reactions that occur simultaneously, possible sources are:

1. char, which was also thought to be increased by carbon deposits from secondary cracking and decreased by hydrogasification;
2. oil and tar, which also were being cracked; and
3. CO and CO_2, possibly in a sequence of reactions to produce part of the increased methane yield.

Yield of each of these products was less in the hydrogen-purged block experiment than it was for powder.

Observations from Pittsburgh coal. Hydrogasification was observed when Pittsburgh seam bituminous coal was heated in H_2. The bituminous coal contained little moisture (0.8% vs 37.5% in lignite), so that steam flux was much less than the product flux of pyrolysis gas. Methane evolution from these blocks was about 20% higher in H_2 than in inert gas, apparently because of hydrogasification. However, the extent of H_2 penetration and reaction may be limited by the low permeability of bituminous coal or coke. Although nonswelling, low-rank coals have an accessible porosity, Pittsburgh coal became fluid when heated, making penetration and escape of gases more difficult.

Data from rapid pyrolysis and hydrogasification of powders showed interesting parallels to these block phenomena. In experiments by Anthony and Howard,[8] powdered Pittsburgh bituminous coal was heated at 650 to 750 K/min to 1273 K (1000°C) in H_2 and in He. For particles of less than 600-μm diameter, use of hydrogen produced a higher yield of volatiles than did helium, as measured by coal weight loss. However, with larger particles and the same heating conditions, the weight loss was unaffected by cover gas, indicating that either product flux or coal fluidity had prevented access of H_2 to the interior of the particles at temperatures suitable for hydrogasification (820 to 970 K).

Hydrodealkylation was observed to occur in the blocks heated in H_2, based on changes in yields and in oil composition. As shown in Table 3.7, variation of heating rate from 0.3 to 14 K/min caused yields of oil to decrease as yields of light hydrocarbon gases increased. Atomic H/C ratios of the oils decreased from 1.26 to 0.89, characteristic of an oil with a very aromatic structure (low H/C) as allyl groups (high H/C) are stripped off. This hydrodealkylation was one mode by which hydrogasification reactions occurred.

Finally, oil quality data from block indicated that heavier compounds were cracked during heating in H_2. Boiling points of the heaviest compounds in the oil (distillation endpoint of Table 3.8)

Table 3.7. Changes in yield and composition of organic liquids during heating of blocks of Pittsburgh bituminous coal in hydrogen to approximately 1170 K (900°C)

Experiment	BP2-39	BP2-37	BP2-38
Surface heating rate, K/min	0.3	3	14
Yield of condensible organics, wt % maf	14.91	8.59	7.01
Atomic H/C ratio of condensible organics	1.26	0.92	0.89
Methane yield, wt % maf	6.56	6.94	7.97

Table 3.8. Distillation endpoints of oils from block heating of Pittsburgh bituminous coal in H_2

Surface heating rate (K/min)	Maximum block temperature (K)	Distillation endpoint (K)
3	913 (640°C)	860
3	1073 (800°C)	760
3	1273 (1000°C)	710

decreased in experiments run to progressively higher temperatures. Apparently, if vapors were forced to escape through hot char, the heavy ends were eliminated selectively by cracking or hydrocracking.

3.5.2 Effects of a simulated UCG product gas

A purge gas that simulated the product gas of UCG was used in two block heating experiments, one on bituminous coal (experiment BP2-57) and one on lignite (BP2-58). Hydrogasification, steam gasification, and water-gas shift were identified by comparison with the results of previous experiments in inert gas and in H_2. Some detailed discussion of the experiments and control experiments is first necessary to interpret the experimental results.

Compositions of the purge gases in these two experiments were reported in Table 2.2. Purge gas was made up by injecting H_2O into a premixed gas, the composition of which approximated the product gas from Hanna and Hoe Creek UCG field tests.

In each experiment, a wet block was heated in the mixed gas at 3 K/min to 1073 K (800°C), generating internal temperature gradients. For experimental convenience, purge gas was switched to inert gas when the surface temperature reached 1073 K. By this technique, yields were made to reflect only changes in the pyrolysis and associated side-reactions. If the flow of reactive gas had been continued, gasification reactions would have continued until the block was consumed.

Control experiments: Purge gas decomposition. Shakedown tests were conducted to measure reactions of the mixed gas in the absence of coal. First, mixed gas without steam was purged through the reactor as it was heated at 3 K/min to 1273 K (1000°C). Generation of CH_2, CO, and H_2O was observed, and H_2 and CO_2 were consumed.

In a second test, 18 mole% steam was added to the dry mixed gas when reactor temperature reached 398 K (125°C), to prevent condensation. The same heating conditions were applied as in the first test. In contrast, however, little self-reaction of the mixed gas was observed

below 1073 K (800°C). Some carbon was produced, either by cracking of methane or by the reverse Boudouard reaction (CO decomposition). Because the block tests with this purge gas were limited to 1073 K, only a slight correction to gas yields for self-reaction was necessary.

Bituminous coal experiment. A block of Pittsburgh coal was heated in experiment BP2-57 at 3 K/min to 1073 K. Small amounts of carbon powder were observed in the reactor system (less than 100 g).

By comparison to previous experiments in inert gas and H_2, the effects in the mixed gas were additional gasification and water-gas shift, both because of the added steam. Increased yields of H_2, CO, and CO_2 relative to previous experiments (Table 3.9) indicated that some additional gasification by the external steam had occurred (CO_2 was probably produced by the water-gas shift reaction). The carbon source for this gasification may have been oil vapors; oil yields were lower, and overall char yield actually increased. Based on stoichiometric comparison of gas yields from BP2-57 and the inert-gas-purged experiments, 60% of the steam fed to the reactor was consumed by gasification, and carbon consumption was 0.7 wt % maf coal. Some hydrogasification also occurred in BP2-57, as it had in the hydrogen-purged experiments, apparently producing more CH_4 in BP2-57 despite a lower H_2 partial pressure.

Lignite experiment. In experiment BP2-58 , a block of Wilcox lignite was heated at 3 K/min to 1073 K in the mixed purge gas. Data analysis was incomplete because material balance data was poor.

Yields were compared (Table 3.10) to previous experiments conducted in inert gas and in H_2 to show the results of using the mixed purge gas to be hydrogasification and some adjustment in the water-gas shift equilibrium. The extent of hydrogasification, as indicated by CH_4 yield, was about the same as during a hydrogen-purged experiment. Water-gas shift reactions, in which CO is consumed and CO_2 is produced, occurred because of the steam in the purge gas.

Table 3.9. Comparison of yields from block pyrolysis of Pittsburgh bituminous coal in Ar, H_2, and mixed purge gas

	Net yield[a] (wt % maf)		
	In Ar	In mixed gas	In H_2
Oil and tar	9.4	7.1	6.9
Water[b]	6.6	4.7	5.4
Subtotal	16.0	11.8	12.3
Char	62.6	66.5	65.5
Gas			
H_2	1.187	1.298	0.84
CH_4	5.53	8.53	7.01
C_2	2.05	1.91	2.66
C_3	0.635	0.30	0.41
CO	1.650	2.89	1.41
CO_2	0.933	1.159	0.86
H_2S	0.86	1.31	0.90
Subtotal	12.85	16.68	13.59
Total	91.5	95.0	91.4
Carbon in CO and CO_2	1.108	1.736	0.973

[a]All experiments 3 K/min to 1073 K (800°C). Yields in Ar and H_2 based on previous correlations (Figs. 3.15 to 3.18).

[b]Net yield of water was gross yield of water, minus calculated coal moisture and injected steam.

Table 3.10. Comparison of yields from block pyrolysis of Wilcox lignite in Ar, H_2, and mixed purge gas

	Net yield[a] (wt % maf)		
	In Ar	In mixed gas	In H_2
Oil and tar	5.1	5.9	4.4
Water (net)[b]	-7.6[c]	0.8	-0.9
Subtotal	-2.5	6.7	3.5
Char	56.3	48.8[d]	56.0
Gas			
H_2	2.20	2.29	1.982
CH_4	3.10	6.21	5.78
C_2	1.02	1.36	1.07
C_3	0.30	1.12	0.37
CO	12.38	11.18	14.99
CO_2	14.83	15.54	12.64
H_2S	0.52	0.40	0.40
Subtotal	34.36	38.10	37.22
Total	88.2	93.7	96.7
Carbon in CO and CO_2	15.10	9.03	9.88

[a] All experiments 3 K/min to 1073 K (800°C).

[b] Net yield of water was gross yield of water, minus calculated coal moisture and injected steam.

[c] Probably the primary source of error in the low material balance.

[d] Low; char may have been lost by pyrophoric combustion.

Significantly, no gasification by added steam seemed to occur. Yield of carbon in CO and CO_2 would include gasified carbon; carbon yield was lower in the order: inert gas >> H_2 > mixed gas. The steam gasification reaction was probably inhibited by the presence of H_2 and CO. As the coal was heated through the temperature range where K_p is approximately 1, H_2 and CO would decrease the conversion by steam. Such inhibition by H_2 has been studied experimentally with powders.[13]

3.5.3 Implications for UCG

These experiments provided data on the effects of the UCG product gas on the reactions in coal blocks. Hydrogasification, the water-gas shift, and some additional steam gasification (in the bituminous coal only) were observed.

The results emphasized the value of coal block research in correlating data from research on powdered coal and in modeling of UCG. Many of the individual reactions that occur in UCG may be studied with success using coal powders, but only after the reactions have been identified in block pyrolysis studies. Combustion in UCG was not included in the original research presented in this report.

3.6 Pyrophoricity of Char

Chars from blocks of Wilcox lignite, Wyodak subbituminous coal, and Hanna bituminous coal were all pyrophoric; that is, at room temperature the fresh chars would begin to heat up and even to burn when exposed to air. Others have observed that this measurement of char reactivity decreased with increasing rank, as was our observation. Additionally, it appeared that a competition between the deposition of reactive carbon (Sect. 3.3) and gasification reactions (Sects. 3.4 and 3.5) affected pyrophoricity. Trends in pyrophoricity as a measure of reactivity provided insights into reactions and surface area changes that can affect UCG.

3.6.1 Observations of pyrophoricity

Char blocks produced by the experiments described in the preceding sections were cooled to room temperature in inert gas and were exposed suddenly to room air (see Sect. 2.3). As a relative measure of pyrophoricity, the initial rate of self-heating (K/min) was recorded. For Wyodak coal samples, the oxidation was not quenched but the blocks were allowed to reach maximum temperature. This maximum temperature could also be used to compare relative pyrophoricity, although less accurately because (1) blocks can burn extensively, and (2) the maximum temperature also depends on other parameters, such as integrity of the char block after the experiment.

Most of the data are from blocks of char produced from heating Wilcox lignite. In Fig. 3.22, the initial rates of self-heating were compared for blocks prepared at different heating rates in both inert and H_2 purge gas, and from both wet and predried coal blocks. The predried block was most pyrophoric, whereas use of H_2 or of higher pyrolysis heating rates significantly decreased pyrophoricity. The effect of maximum temperature is not shown in Fig. 3.22, but pyrophoricity was observed to be higher in chars prepared at 1073 K (800°C) than at 873 or 1273 K.

Pyrophoricity data from Wyodak and Hanna chars were more limited. At comparable conditions, pyrophoricity was about 40% less for the Wyodak char than for char from Wilcox lignite. Wyodak pyrophoricity was highest in chars prepared at about 970-1070 K (700-800°C), and pyrophoricity of small blocks (60-mm-diam) was about four to six times higher than that of large blocks (160-mm-diam). Hanna char was less pyrophoric than Wyodak char by at least a factor of three.

3.6.2 Causes of changes in pyrophoricity

The decrease in pyrophoricity observed with increasing heating rate was consistent with powder data on char reactivity. The reasons for decreases associated with block heating conditions were not immediately obvious,

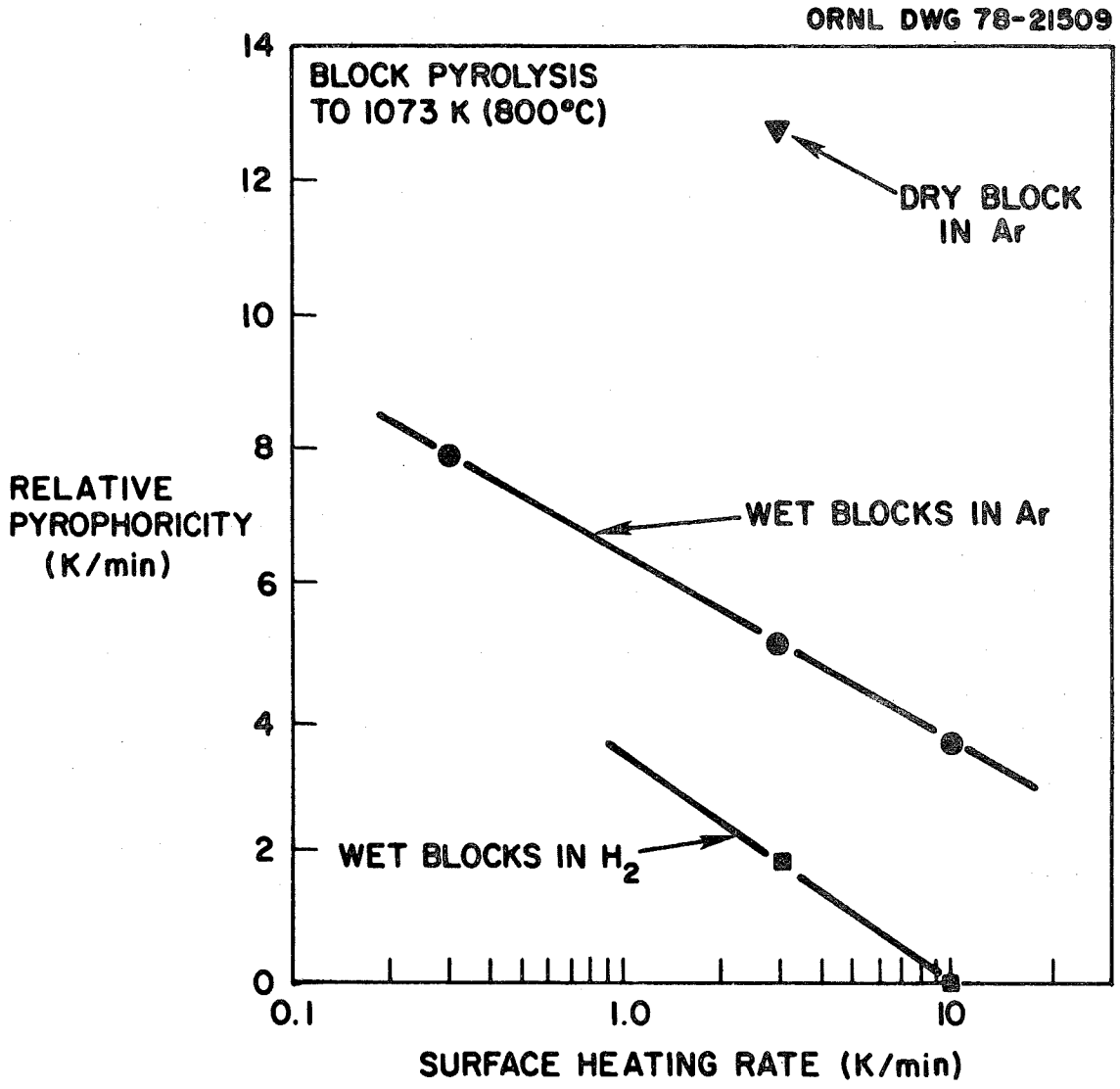

Fig. 3.22. Relative pyrophoricity of lignite chars as affected by conditions of block heating.

but they were necessarily linked to decreases in the number of available reactive sites. Two possible causes of such a reduction, based on observations of reactivity in powdered coal, are (1) carbon deposition at the bottle-necked openings of pores, thereby decreasing site accessibility, and (2) scavenging of freshly deposited carbon, decreasing the number of active sites.

Theory. The rank effect observed in these coal block experiments was also apparent from measurements on powdered coal char. Hippo and Walker[14] measured decreasing reactivity of chars (to air and CO_2 at high temperatures) as a function of increasing rank. They attributed the decrease to poorer mass transport of O_2 to reactive sites because of smaller macropore volume and smaller amounts of catalytic mineral matter (primarily compounds of Ca and Mg).

Carbon deposition was linked to decreases in char reactivity in work by Kamashita, Mahajan, and Walker,[10] and was explained using the concept that coal and char are molecular sieves. Experimentally, powdered North Dakota lignite was pyrolyzed at 1128 or 1273 K (855 or 1000°C). Carbon was deposited by the thermal cracking of CH_4, and reactivity with air was measured subsequently at 648 K (375°C). Compared to control samples (no carbon deposition), reactivities of these samples were lower. In addition, surface areas measured by N_2 adsorption (at 77 K) and CO_2 adsorption (at 298 K) were lower when carbon deposits were present. Surface areas measured by N_2 absorption in the presence of deposited carbon were lower than the CO_2-measured values. The CO_2-measured surface areas included surface areas of the micropores, which the N_2 adsorption did not. This difference is caused primarily by the higher kinetic energy of CO_2 molecules at 298 K compared to N_2 molecules at 77 K, which allows CO_2 to penetrate smaller holes. Apparently, small amounts of deposited carbon obstructed the diffusion of air to reactive sites within small pores.

In later work, Solano, Mahajan, and Walker[11] presented data on interactions between carbon deposition and gasification. Based on the data, they suspected a very high reactivity of the carbon deposited by cracking and a very high catalytic cracking activity of the carbon exposed by gasification.

However, the net effect of gasifying this reactive carbon cannot be predicted. Steam gasification could result in decreased char reactivity through scavenging of the reactive carbon deposits, or it could result in increased char reactivity through opening of previously blocked pores.

Evaluation of block effects. Gasification of deposited carbon by steam or hydrogen apparently reduced pyrophoricity of the blocks by scavenging the reactive carbon, which otherwise would have increased the reactivity of the char. Pore blockage did not account for the decreased pyrophoricity in Ar-purged experiments, although pores may have been obstructed in experiments purged with H_2.

Surface areas of three lignite chars were measured[15] to establish whether pore blockage accounted for the lowered pyrophoricity of chars. Each char was sampled from the surface of a block that had been subjected to heating at 3 K/min to a maximum of 1073 K (800°C); purge gas and moisture content were variables. The variable conditions in order of decreasing pyrophoricity of char were: (1) predried block pyrolyzed in inert gas (Ar), (2) naturally wet block (27.5% H_2O) pyrolyzed in Ar, and (3) wet block pyrolyzed in H_2. Braunauer-Emmett-Teller (BET) surface areas were calculated from adsorption isotherms of N_2 (at 77 K) and CO_2 (at 193 K), measured on a Cahn RG Electrobalance. The results for dry, unreacted lignite[3] and the three chars[13] are presented in Table 3.11.

Comparison of surface areas from dried lignite and from the char of a predried block showed that greater pore volume had been opened by pyrolysis. Earlier (Sect. 3.2.2), secondary cracking and carbon deposition were identified from yields as having occurred in heating this predried block. However, surface area measured with CO_2, which approximated the overall pore area, was hardly affected by charring the lignite. As noted previously, CO_2 can penetrate micropore-sized openings (0.4 to 0.5 nm or 4 to 5 Å) but N_2 cannot. The large increase observed in N_2-measured surface area of char was interpreted to mean that many pores in the lignite had been connected to open macropores through openings smaller than 0.5 nm. Thus, the char would be more reactive than raw lignite because more reactive sites were present (by deposited carbon from cracking and by creation of reactive sites through pyrolysis) and

Table 3.11. Surface areas of lignite chars from surface region of blocks heated at 3 K/min to 1073 K (800°C)

Sample	Surface area (m^2/g) By N_2	By CO_2
Dry, unreacted lignite [a]	2.3	238 [b]
Char from predried block heated in Ar [c]	279	288
Char from wet block heated in Ar [c]	240	272
Char from wet block heated in H_2 [c]	145	147

[a] Darco mine, Texas, average of two samples. Source of data: H. Gan, S. Nandi, and P. L. Walker, Jr., "Nature of the Porosity in American Coals," Fuel 51 (4), 272-277 (October 1972).

[b] Measured by CO_2 adsorption isotherm at 298 K using Dubinin-Polanyi equation.

[c] Source of data: G. L. Alexander, B. V. Hu, and A. H. Kwai, Coal Block Pyrolysis: Effects of Changing Surface Characteristics, ORNL/MIT-294, Oak Ridge National Laboratory, Oak Ridge, Tenn., (in publication).

because more sites are accessible (by the opening of pore bottle-necks).

As seen in Fig. 3.22, char prepared from a wet block in inert gas was less pyrophoric than char from a dry block; however, surface areas were not significantly reduced (Table 3.11). Apparently, accessibility of reactive sites was unchanged by self-gasification, but the number of reactive sites was reduced, probably the result of gasification (Sect. 3.4) of reactive carbon deposited by secondary cracking. Thus, the decrease in pyrophoricity with increased heating rates (Fig. 3.22) was accounted for by the associated increase in self-gasification. The scavenging of reactive sites would also imply that char produced from bulk coal may be less reactive than char from coal powder (where cracking and self-gasification are minimized). This possibility is also consistent with the observation that small blocks of Wyodak char (less self-gasification) were more pyrophoric than larger blocks.

As discussed in Sect. 3.5, both H_2 and steam may gasify reactive carbon. Therefore, because hydrogasification and steam gasification were both occurring, pyrophoricity of char prepared from wet blocks in H_2 (vs Ar) was even lower. Surface areas of this char were lower than surface areas of the other chars and may have been associated with the lower pyrophoricity. However, surface areas measured both with N_2 and CO_2 were the same, so that the decrease in surface area was not caused by blockage of micropores but, possibly, by gasification of the pyrolysis char.

3.6.3 Implications for UCG

Changes in char reactivity provided insight into the possible forms of carbon that would be gasified easily in UCG. In addition, reactive deposits of carbon could also affect the velocity and maximum temperature of the UCG combustion front.

An insight into the application of gasification kinetics to UCG modeling was that rates measured on freshly charred powders may be high. Interpretations of pyrophoricity data imply that charred powders would be more reactive than charred bulk coal. To test this hypothesis,

kinetic experiments should be run using powders ground from the char blocks of these experiments.

3.7 Swelling in Coal Blocks

In block tests on Pittsburgh bituminous coal, swelling was observed to decrease with higher heating rates. The opposite behavior is observed in pyrolysis of powders, but analysis showed that the block behavior was a reasonable consequence of UCG-like temperature gradients and swelling behavior. The reduced swelling observed in coal blocks suggested that swelling problems in UCG of bituminous coal may be less severe than anticipated.

3.7.1 Observations of swelling phenomena

Powdered coal swells more if higher heating rates are applied; however, heating of blocks at 0.3, 3, and 14 K/min produced progressively less swelling. Other potentially important variables, maximum temperature and the purge gas, caused no changes in swelling. No effect of maximum block temperature was observed for 873 to 1273 K (600-1000°C). Although the swelling can be greater in the presence of hydrogen,[16] no difference was observed between charred blocks produced in H_2 or in inert gas.

In experiments at 0.3 K/min, the 0.15-m-diameter blocks swelled outward to fill the cross section of the reactor completely (33+% expansion) and swelled axially (vertically) as much as 45%. The chars were hard, brittle, and bubbled. Bubbling was uniform throughout the block except for large cavities frequently found at the center. Figure 3.23 shows the char block from experiment BP2-39, produced at 0.3 K/min. The block had swelled against the reactor wall, giving a porous, glossy appearance to its surface. Around the sides of the cylinder, a thick rim had swelled upward 100 mm; at the center, the top of the block had sagged 50 mm. The combined effects produced a 200-mm-diameter, 330-mm-high char block with a crater in the top.

ORNL Photo 0318-78

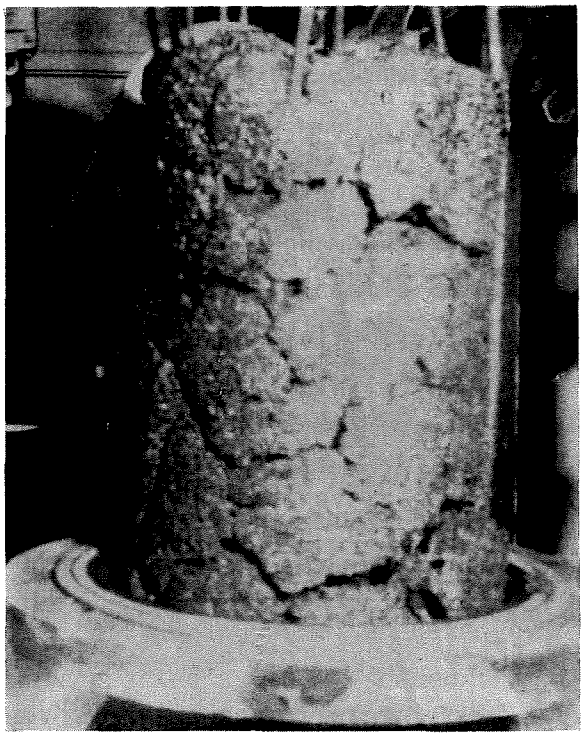

Fig. 3.23. Char block after heating at 0.3 K/min to 1198 K (925°C; experiment BP2-39).

Less swelling was observed in experiments at 3 K/min, and the surface of each of these blocks melted in layers resembling lava. Figure 3.24 shows this lava-like surface on the block from experiment BP2-37. Because of swelling, the height increased by 20% and the diameter increased by 28%. In addition, internal textures in these blocks varied with radial position. The lava-like char at the surface was porous and brittle, but nearer the center of the block a harder, cohesive coke was found. At the center, the char was crumbly around a hollow core. Comparing the inert-gas-purged experiments having a maximum temperature of 1273 K (1000°C), the cylindrical hollows were smaller (about 9 cm^3) in blocks prepared at 3 K/min than in those at 0.3 K/min (about 30 cm^3).

In a single experiment at 14 K/min, a glazed, slightly enlarged block of char was produced (Fig. 3.25). Block height increased by only 11% and diameter by 13%. Bubbles were found only within a 16-mm radius of the center, and a grainy char extended from the bubble-filled area to the surface.

3.7.2 Interpretation of block swelling behavior

The differences observed in swelling behavior at different heating rates can be correlated to the steepness of temperature profiles. Ignoring other effects, plasticity or fluidity is commonly described as a simple function of temperature.[16, 17] When temperature is increased to some temperature θ_s (softening temperature), the solid structure of caking coals will begin to soften and can be plasticly deformed. Fluidity increases to a maximum as temperature continues to rise, and, at temperature θ_r (resolidification temperature), the coal (as char or semi-coke) will resolidify. Because gas is formed by pyrolysis reactions at fluidity temperatures, bubbles can cause formation of a foam in the plastic coal as the convection of gas is restricted, resulting in swelling of the coal. Data in the literature[17,18] (Table 3.12) describe these temperatures of fluidity for Pittsburgh seam coal.

ORNL Photo 0319-78

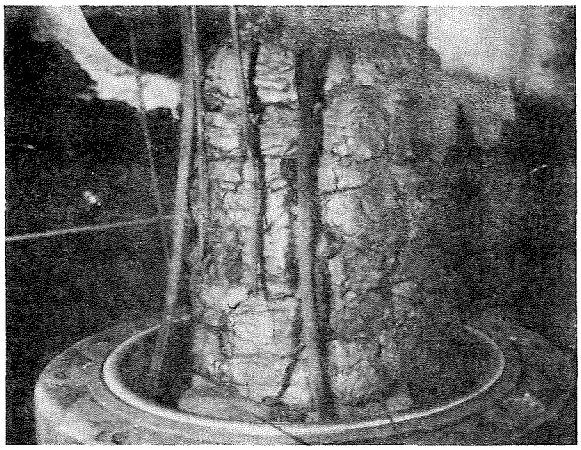

Fig. 3.24. Char block after heating at 3 K/min to 1153 K (880°C; experiment BP2-37).

ORNL Photo 0320-78

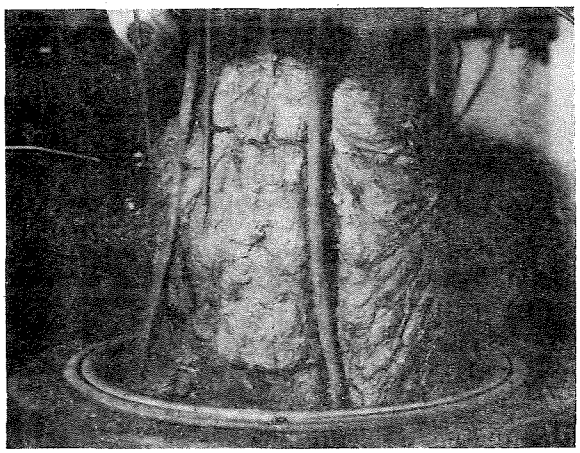

Fig. 3.25. Char block after heating at 14 K/min to 1163 K (890°C; experiment BP2-38).

Table 3.12. Experimental measurements of fluidity in Pittsburgh seam bituminous coal at overall heating rate of 4.8 K/min

Coal source	% volatile matter (dry, mineral-matter-free)	Temperatures (K)		
		Range of fluidity	Range of high fluidity[a]	Maximum fluidity[b]
Warden Mine[c]	38.1	614–722[d] (314–449°C)	685–719 (412–446°C)	701 (428°C)
Bruceton Mine[c]	40.1	609–708[d] (336–435°C)	688–711 (415–438°C)	699 (426°C)
Monongalia County, W. Va.[e]	41.5			
Wetzel County, W. Va.[f]	45.2	616–(673+) (343–>400°C)		

[a]Average from Gieseler and Davis plastometers.

[b]Average from Agde-Damm dilatometer, Gieseler plastometer, and Davis plastometer.

[c]Source of data: R. E. Brewer and J. E. Griff, Ind. Eng. Chem. (Analytical Edition), 11, No. 5, p. 242, May 1939.

[d]By Gieseler plastometer.

[e]Coal used in ORNL block pyrolysis experiments.

[f]Coal used in Pricetown I UCG field test. Source of data: H. D. Shoemaker et al., Directional Viscoelastic Properties of the Pittsburgh Coal at Elevated Temperatures in Compression and Shear, Morgantown Energy Research Center, MERC RI-76/5, August 1976.

Because the internal temperatures at 0.3 K/min were nearly uniform and the entire block was within the temperature range of plasticity for a long time, extensive melting and swelling occurred. An extreme example of fluidity was in experiment BP2-43 (pyrolysis in H_2 at 0.3 K/min to 1300 K), in which nearly all of the block melted and flowed into the bottom of the reactor.

However, at higher heating rates (steeper temperature profiles), only a narrow band of coal was within the plasticity range at a given time. For a surface heating rate of 3 K/min (Fig. 3.6), this band was about 8 mm wide when surface temperature had reached 973 K (700°C) and 11 mm wide at 1098 K (825°C). Thus, the surface melted first and flowed as a layer on the solid coal core. As the experiment progressed, the surface resolidified, but the narrow band of plastic coal continued to advance toward the block center with the moving temperature gradient. The mechanical constraint of a hard, semi-coke surface thus accounted for the overall reduction in swelling. (The hollow cavities in these blocks apparently were formed by collection of gas in the center of the block when the center region became plastic.)

At 14 K/min, the band of coal within the plasticity range was even narrower because the surface glazed before it resolidified. As a result, the overall amount of swelling was less than at 3 K/min.

Actually, the range of fluidity changes slightly with heating rate but not enough to affect the results just discussed. Studies of plasticity with an Audibert-Arnu dilatometer[19] showed that θ_s changed little with heating rate, but that some change occurred in θ_r. For example, θ_r approached θ_s at very low heating rate, but θ_r was 710 K (437°C) at 1 K/min, 735 K (462°C) at 4 K/min, and 755 K (482°C) at 20 K/min. Thus, although the temperature range of plasticity (θ_s to θ_r) was affected by the different heating rates, no effect of heating rate on the swelling of blocks was detectable. The stronger effect of steep temperature gradients caused positions at θ_s and at θ_r either to be very close together or far apart.

3.7.3 Implications for UCG

Restrictions of swelling to a plastic zone can be expected during UCG field tests in bituminous coal. Su et al.[20] reported reverse combustion linkage in a large block at METC. They observed a narrow fluid zone similar to those observed in the blocks described here. Sectioning of the METC coal block revealed a 6-mm-wide "phase change zone" of glossy, bubbly char and a 50-mm-wide band of semi-coke at the leading edge of the reacted area of coal. In x-ray studies of pyrolysis in coke ovens, these zones have also been observed within the thermal waves moving from the walls toward the center of the oven.[19] Similar thermal behavior and swelling may be expected in UCG, decreasing the amount of swelling during forward gasification.

In swelling coal, UCG is not expected to propagate by progressive collapsing of the roof above a horizontal reaction path. Such propagation is thought to occur in the LVW process (Sect. 1) in shrinking coals, but swelling coals would not break off when heated. Propagation would be most likely to occur instead by movement of a thermal wave, as simulated by Su et al.[20] Swelling in this mode of propagation would follow the trends observed in our coal block research.

3.8 Summary of Results

Experimental results from the heating of coal blocks are summarized in Fig. 3.26. For a wet block heated at 3 K/min or for heated coal walls during UCG, this sketch shows temperature regimes, reactions, heat transfer mechanisms, and directions of mass flux. Pyrolysis of the coal is shown to occur at 520 K (250°C) and above, although the pyrolysis reactions that produce condensible vapors (water, oil, and tar) occur primarily between 520 and 870 K (250 and 600°C). Secondary cracking of tars, self-gasification, and water-gas shift were the principal classes of reactions that occurred in blocks but not in powders. By understanding when these additional reactions occur, experimental data from pyrolysis of powders may be incorporated into models of UCG.

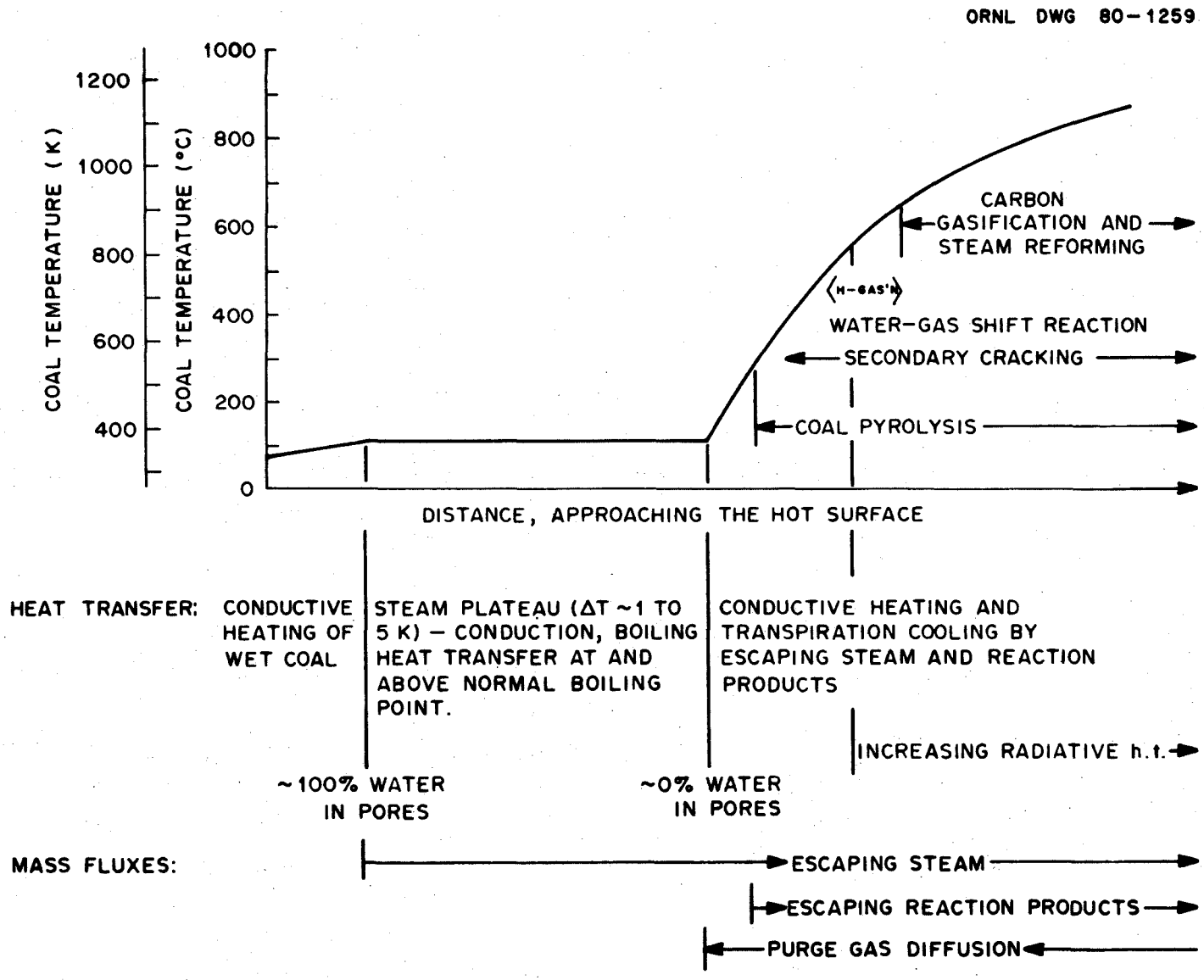

Fig. 3.26. Summary of mechanisms observed in block pyrolysis research.

3.9 References for Section 3

1. R. D. Gunn, D. L. Whitman, and D. D. Fischer, "A Permeation Theory for In Situ Coal Gasification," SPE J. (5), 300-314 (October 1978).

2. R. W. Lyczkowski, A Mechanistic Theory for Drying of Porous Media, UCRL-52456, Lawrence Livermore National Laboratory, April 1978.

3. H. Gan, S. Nandi, and P. L. Walker, Jr., "Nature of the Porosity in American Coals," Fuel 51 (4), 262-277 (October 1972).

4. C. B. Thorsness and R. J. Cena, "In Situ Coal Gasification Modeling," presented at the 86th National Meeting of AIChE, Houston, Texas, April 1-5, 1979.

5. J. B. Goodman, M. Gomez, and V. F. Parry, Laboratory Carbonization Assay of Low-rank Coals at Low, Medium, and High Temperatures, RI-5383 U.S. Bureau of Mines, January 1958.

6. J. H. Campbell, Pyrolysis of Subbituminous Coal as It Relates to In Situ Gasification (Part 1: Gas Evolution), UCRL-52035, Lawrence Livermore National Laboratory, March 1976; (Part 2: Characterization of Liquid and Solid Products), UCRL-52035 Part 2, Lawrence Livermore National Laboratory, June 1976.

7. J. H. Campbell, "Pyrolysis of Subbituminous Coal in Relation to In-Situ Coal Gasification," Fuel 57 (4), 217-224 (April 1978).

8. D. B. Anthony and J. B. Howard, "Coal Devolatilization and Hydrogasification," AIChE J. 22 (4), 625-656 (July 1976).

9. G. M. Barrow, Physical Chemistry, 3rd Ed., McGraw-Hill New York, 1973.

10. M. Kamashita, O. P. Mahajan, and P. L. Walker, Jr., "Effect of Carbon Deposition on Porosity and Reactivity of a Lignite Char," Fuel 56 (4), 444 (October 1977).

11. A. L. Solano, O. P. Mahajan, and P. L. Walker, Jr., "Carbon Deposition from Methane over Minerals," Fuel 56, 452-3 (October 1977).

12. S. B. King, C. F. Brandenburg, and W. J. Lanum, "Characterization of Nitrogen Compounds in Tar Produced from Underground Coal Gasification," presented at the 169th National Meeting of the Americal Chemical Society, Philadelphia, Pa., April 6-11, 1975.

13. J. Fischer et al., Laboratory Support for In Situ Gasification Reaction Kinetics, Quarterly Report for the Period April-June 1977, ANL/CEN/FE-77-6, Argonne National Laboratory, Argonne, Ill.

14. E. Hippo and P. L. Walker, Jr., "Reactivity of Heat-Treated Coals in Carbon Dioxide at 900°C, Fuel 54, 245-248 (October 1975).

15. G. L. Alexander, B. V. Hu, and A. H. Kwai, Coal Block Pyrolysis: Effects of Changing Surface Characteristics, ORNL/MIT-294, Oak Ridge National Laboratory, Oak Ridge, Tn. (in publication).

16. D. W. van Krevelen, Coal, Elsevier Publishing Co., Amsterdam, 1961.

17. H. D. Shoemaker et al., Directional Viscoelastic Properties of the Pittsburgh Coal at Elevated Temperatures in Compression and Shear, Morgantown Energy Research Center, MERC RI-76/5, August 1976.

18. R. E. Brewer and J. E. Triff, Ind. Eng. Chem. (Analytical Edition) 11 (5), 242 (May 1939).

19. H. H. Lowry, Ed., Chemistry of Coal Utilization, Supplementary Volume, Wiley, New York, 1963.

20. F. Y. Su et al., Analysis and Interpretation of Laboratory Coal Gasification Simulation Data, MERC/CR-78/2, Morgantown Energy Research Center, February 1978.

4. THERMAL AND PHYSICAL PROPERTIES OF COAL

Accurate measurements of coal properties are important to the accurate modeling of UCG. However, few or no data exist for most properties of the low-rank, wet coals that are of particular interest in UCG.

Traditionally, coals used have been bituminous and anthracite, which typically have low moisture contents. As a result, the effects of low rank and moisture content on bulk properties — thermal diffusivity, thermal conductivity, and density — have received little attention. The high moisture contents of lignite and subbituminous coal in situ have especially important effects on these bulk properties as do drying effects on shrinking. Unfortunately, data on both wet and dry low-rank coals are scarce.

Various coal properties have been studied as part of this project, with most of the effort focused on measurement, literature review, and correlation of thermal diffusivity and thermal conductivity (Sect. 4.1). Data on bulk and ultimate density of wet and dry coals, shrinking properties, and porosity are also reported (Sect. 4.2). Finally, a study in which enthalpy and specific heat are correlated is reviewed and applied to coals of interest (Sect. 4.2). (Swelling data were reported in Sect. 3.5 and data on internal surface areas of chars in Sect. 3.7.2).

4.1 Thermal Diffusivity and Thermal Conductivity

Conduction is an important mechanism in the heating and drying of coal during UCG. For example, in the development and movement of steam plateaus,[1] at low temperatures, conduction is the sole means of heat transfer to the plateau from the hotter surface (Sect. 3.1). Also, as discussed in Sect. 1.1, the thermal models currently used for locating and describing the reaction fronts during field tests rely on accurate values of thermal conductivity. These data are reported here, compared to the literature, and included in correlations. Only temperature data from blocks of Wilcox lignite (wet and dry) were analyzed by the methods

of Sect. 4.1.1, but the methods could be applied to existing temperature data from the other coals studied and from overburden tests.

Data on thermal properties of char are also needed. Gunn et al., in their sensitivity analysis of a permeation model, showed how char conductivity can affect the maximum UCG temperature, front movement rates, and other parameters.[2] Because char data[3-5] are even more scarce than coal data, the dynamic methods of Sect. 4.1.1 could be usefully applied by stepwise heating of coal blocks — pyrolyzing coal to some temperature, cooling slightly, and then reheating without interference from heats of reaction.

4.1.1 Measurements

Using internal temperatures from block heating tests, thermal diffusivity was measured for wet and dry unreacted Wilcox lignite. Thermal conductivity was calculated from thermal diffusivity using other measured properties of the same coal.

Dry lignite. Thermal diffusivity of dry, unreacted lignite was measured by evaluating the terms in the cylindrical conduction equation

$$\alpha \left[\frac{1}{r} \cdot \frac{\partial}{\partial r} \left(r \frac{\partial T}{\partial r} \right) + \frac{\partial^2 T}{\partial z^2} \right] = \frac{\partial T}{\partial t} \qquad (4.1)$$

where

α = thermal diffusivity = $k/\rho \cdot C_p$, m^2/s,
k = thermal conductivity, W/m·K,
ρ = density, kg/m^3,
C_p = specific heat, J/kg·K,
r = radical coordinate, m,
T = temperature, K,
z = axial coordinate, m,
t = time, s.

Experimentally, convection of steam would have caused this model to break down above 100°C, so the lignite was predried to 400 K (127°C) for measurement of diffusivity in dry coal. Also, pyrolysis reactions would have introduced a term for heat of reaction in Eq. (4.1), so measurements in dry coal were restricted to temperatures of less than 573 K (300°C), at which pyrolysis is negligible.

In the particular experiment analyzed (BP2-52), the derivatives in Eq. (4.1) were evaluated directly from the temperature data, treating the block as an infinite cylinder. Experimental boundary conditions on initial temperature distribution and surface heating rate precluded exact solution of the unsteady condition equation. Nevertheless, graphical evaluation of the derivatives and substitution into Eq. (4.1) yielded a reasonable value with reasonable precision for thermal conductivity.

A set of temperature-position-time data was analyzed approximately 44 min into the experiment, when the block center was 405 K and the surface was 573 K (300°C); surface heating rate was approximately 3 K/min. By substitution into Eq. (4.1), the value of α was 0.094 $\pm$ 0.017 mm^2/s (or $\pm$ 18%, based on evaluations at eight positions within the block). From literature data on specific heat (C_p) (Ref. 6) and measured bulk density (Sect. 4.3), k was determined to be 0.14 $\pm$ 0.03 W/m·K. By comparison, for a dry, German brown coal,[7] k was reported to be 0.151 W/m·K.

Wet lignite. For evaluating thermal properties of wet lignite, experimental boundary conditions were suitable for exact solution of Eq. (4.1).

Three models were applied: In model 1, conduction was modeled neglecting end effects, as if the coal cylinders were infinite. In addition, the blocks were modeled as finite cylinders in which either all faces were heated (model 2) or one end was insulated (model 3). In the experiment, the block was mounted on three small cubes of firebrick, covering only 30% of the bottom face of the block. For this reason, model 2 would be expected to be the most realistic.

For the infinite cylinder (model 1), a solution was presented by Carslaw and Jaeger.[8] Assuming uniform initial temperature and a linear rise in surface temperature, the boundary conditions may be stated as

$$\begin{aligned} T &= T_o && \text{for } t = 0 \text{ and all } r, \\ \partial T/\partial r &= 0 && \text{for all } t, \text{ and } r = 0, \\ T &= T_o + bt && \text{for all } t, \text{ and } r = r_o, \end{aligned} \tag{4.2}$$

where

T_o = initial temperature, K,

b = rate of surface temperature increase, K/s,

r_o = overall radius, m.

The full solution was expressed in terms of Bessel functions:

$$T = T_o + bt - \frac{b}{4\alpha}(r_o^2 - r^2) + \frac{2b}{r_o\alpha} \sum_{m=1}^{\infty} \frac{J_o(\lambda_m r)}{\lambda_m^3 J_1(\lambda_m r_o)} e^{-\alpha t \lambda_m^2} \tag{4.3}$$

where λ_m are the roots of the equation $J_o(\lambda_m r_o) = 0$. For longer times (t) as those used in these experiments, the last term disappears to give a quasi-steady-state solution,

$$T = \left(\frac{b}{4\alpha}\right) \cdot r^2 + \left(T_o + bt - \frac{br_o^2}{4\alpha}\right) , \tag{4.4}$$

which describes a parabolic shape for the radial temperature profile.

Model 2 assumed a linear rise in surface temperature on sides, top, and bottom of a finite cylinder. Boundary conditions were then:

$$T = T_o \quad \text{for } t = 0 \text{ and all } r \text{ and } a; \tag{4.5}$$

$$\partial T/\partial r = 0 \quad \text{for all } t, r = 0, \text{ and all } z \text{ (axis of symmetry)}; \tag{4.6}$$

$$T = T_o + bt \quad \text{for all } t, r = r_o, \text{ and all } z \text{ (cylinder sides)}; \tag{4.7}$$

$$T = T_o + bt \quad \text{for all } t \text{ and } r \text{ and } z = +L/2 \text{ (top)}; \tag{4.8}$$

$$T = T_o + bt \quad \text{for all } t \text{ and } r \text{ and } z = -L/2 \text{ (bottom)}, \tag{4.9}$$

where L is the overall length in m. Equation (4.1) was then integrated, using these boundary conditions and Duhamel's superposition principle, giving the solution

$$T = T_o + bt - \frac{8b}{\pi\alpha} \sum_{m=1}^{\infty} \sum_{n=0}^{\infty} (-1)^n \cdot \frac{\cos(k_n z)}{2n+1} \cdot \frac{J_0(\lambda_m r)}{\lambda_m r_o \cdot J_1(\lambda_m r_o)} \cdot \frac{1 - e^{-\alpha t(\lambda_m^2 + k_n^2)}}{\lambda_m^2 + k_n^2}, \qquad (4.10)$$

where the eigenvalues λ_m and k_n were defined as

$$J_0(\lambda_m r_o) = 0 , \qquad (4.11)$$

$$k_n = (2n + 1)\pi/2L . \qquad (4.12)$$

When L becomes very large, this solution reduces to the infinite cylinder model [Eq. (4.3)].

For model 3, a finite cylinder in which one end is insulated, four boundary conditions were described by Eqs. (4.5, 4.6, 4.7, and 4.8), but Eq. (4.9) was replaced by

$$\partial T/\partial z = 0 \qquad \text{for all t, all r, and } z = -L/2 . \qquad (4.13)$$

Again by integrating using Duhamel's superposition principle, an equation similar to Eq. (4.10) resulted as the solution to model 3:

$$T = T_o + bt - \frac{8b}{\pi\alpha} \sum_{m=1}^{\infty} \sum_{n=0}^{\infty} \frac{\cos k_n(z - L/2)}{2n+1} \cdot \frac{J_0(\lambda_m r)}{\lambda_m r_o \cdot J_1(\lambda_m r_o)} \cdot \frac{1 - e^{-\alpha t(\lambda_m^2 + k_n^2)}}{\lambda_m^2 + k_n^2} . \qquad (4.14)$$

The three models [Eqs. (4.3, 4.10, and 4.14)] were evaluated on a PDP-11/40 minicomputer by testing different temperature profiles from different block heating experiments. Model 2, the finite cylinder with all surfaces heated, yielded results that best fit the data.

Thermal diffusivities calculated from model 2 are presented in Table 4.1. Based on the finite cylinder model, α of the wet (37.5%) Wilcox lignite was measured to be 0.14 mm^2/s, and k, 0.33 W/m·K. By way of comparison, an Australian brown coal (41% moisture) was reported to have α = 0.1315 mm^2/s and k = 0.32 W/m·K (Ref. 9).

Table 4.1. Thermal diffusivity of wet Wilcox lignite from model 2

Experiment	Surface temperature (K)	Thermal diffusivity (mm^2/s)	Correlation coefficient
BP2-49, 0.3 K/min, in H_2	80	0.1554	0.967
	90	0.1492	0.597
	100	0.1706	0.969
BP2-41, 0.3 K/min, in Ar	80	0.1197	0.902
	90	0.1241	0.922
	100	0.1263	0.887
Mean		0.1409	
Standard deviation		0.0205	

Thermal diffusivities measured when H_2 was used as the purge gas were somewhat higher than those measured when Ar was used (averages of 0.158 $\pm$ 0.011 vs 0.123 $\pm$ 0.003 mm^2/s). The difference may have been linked to the higher thermal conductivity of hydrogen, even though all pores were assumed to be filled with water.

4.1.2 Literature review

The literature was reviewed for data on thermal diffusivity and thermal conductivity of wet and dry coals of different rank. The limited data[7,9-12] for dry low-rank coals are listed in Table 4.2, but only the first three measurements should be regarded as valid. Questionable experimental techniques were used for the last three measurements. Mineral matter content was calculated by the Parr formula from measured ash content because in the unpyrolyzed, uncombusted coal, it represents more accurately the inorganic content. Data for dry bituminous coals[3,5,13-17] are summarized in Table 4.3, and, for completeness, data for cannel coals and anthracites[14-17] are reviewed in Table 4.4. Although they are discussed in greater detail in Sect. 4.1.3, the available data[3,5,9,18,19] on the effect of moisture on conductivity are presented in Table 4.5.

Of particular interest for UCG modeling was that such models for low-rank coals previously have used conductivity data from bituminous coal. By so doing, data may overestimate thermal conductivity of dry, low-rank coal by 50% and underestimate that property for wet, low-rank coal by 50%.

Trends in thermal diffusivity were plotted in Fig. 4.1. Volatile content was used as a rough measure of rank: decreasing rank (toward subbituminous coal and lignite) was indicated by increasing volatile content. Thermal diffusivity increased slightly with increasing rank (possibly a porosity effect) and tended to increase with mineral content. (The conductivity of minerals is generally higher than that of coal.) For ten samples of whole bituminous coal, α averaged 0.151 $\pm$ 0.007 mm^2/s.

Table 4.2. Thermal diffusivity and thermal conductivity of dry, low-rank coals

Rank	Seam	Reference	Thermal diffusivity (mm^2/s)	Thermal conductivity, k(W/m·K)	Temperature (K)	Comments
Lignite	Wilcox, Texas	This work	0.09	0.14	405-573	
Brown coal	Ilse mine, Germany	7	0.12-0.13	0.151	293	
Subbituminous	Hanna No. 1, Wyoming	10		0.16	298-363	Brittle, crumbly, cracked sample
Subbituminous	San Juan Mine, New Mexico	11		0.038	366	Questionable data; from "drying" coal, so heat of vaporization may have interfered
Subbituminous	Various mines, New Zealand	12		0.21-0.24	310-367	Questionable data; from model of conduction in powdered coal
Brown coal	Morwell No. 5 cut, Australia	9		0.225	293	Questionable data; from thermal conductivity of wet coal, assuming volumetric average of gas, H_2O, and coal thermal conductivity

Table 4.3. Thermal diffusivity and thermal conductivity of dry bituminous coals. Ranked in order of volatile content [wt %, dry, mineral-matter-free (dmmf)]; excludes cannel coal

Coal source (mine, seam, country)	Reference	Mineral matter (wt % dry)	Volatile matter (wt % dmmf)	Thermal diffusivity (mm^2/s)	Thermal conductivity (W/m·K)	Temperature (K)
Cannel-like bituminous						
Sample 3, U.K.	14	9.1[a]	48.4		0.163[b]	288-373
Sample 2, U.K.	14	8.7[a]	47.5		0.167[c]	288-373
Sample 4, U.K.	14	7.7[a]	43.4		0.159[b]	288-373
High-volatile bituminous						
Binley, 9-ft., U.K.	3	6.4	42.2		0.184	423-673
Barnsley Thick durain, U.K.	14	9.1[a]	41.9	0.158[d]	0.218[d]	288-373
Polysaevskaya, U.S.S.R.	15	6.5[a]	41.0	0.163	0.157	473-573
Pittsburgh seam, U.S.A.	5	9.3	40.6	0.155[e]	0.213[e]	423
				0.143[f]	0.196[f]	423
Woolaton, Tupton, U.K.	3	22.1	40.3		0.268	423-673
Woodside, U.K.	3	4.2	39.3		0.243	423-673
Hedwigswunsch, Germany	16,17	2.7[a]	39.0	0.147[g]	0.230[g]	303
Radford, Tupton, U.K.	3	20.2	38.8		0.222	423-673
Hucknall, Main Bright, U.K.	3	6.1	38.4		0.227	423-673
Dearne Valley, Shafton, U.K.	3	5.6	37.6		0.205	423-673
Trencherbone clarain, U.K.	14	3.1[a]	37.4	0.144[h]	0.188[h]	288-373
Hedwigswunsch, Germany	16	4.7[a]	36.9		0.241[g]	303
Clipstone, Low Main, U.K.	3	4.5	36.4		0.194	423-673
Vane Tempest Maudlin, U.K.	3	1.7	35.6		0.241	423-673
Barnsley Thick clarain, U.K.	14	1.7[a]	35.1	0.120[i]	0.155[i]	288-373
Trencherbone durain, U.K.	14	7.6[a]	34.1	0.152[j]	0.230[j]	288-373
Arley durain, U.K.	14	1.4[a]	33.8	0.157[k]	0.209[k]	288-373
Arley clarain, U.K.	14	1.6[a]	32.9	0.135[l]	0.180[l]	288-373
Dorstfeld, Germany	16,17	2.6[a]	32.2	0.147[j]	0.217[j]	303
					0.280[j]	303
Bilsthorpe, U.K.	3	15.8	31.9		0.266	423-673

Table 4.3 (continued)

Coal source (mine, seam, country)	Reference	Mineral matter (wt % dry)	Volatile matter (wt % dmmf)	Thermal diffusivity (mm^2/s)	Thermal conductivity (W/m·K)	Temperature (K)
Medium-volatile bituminous						
Monopol, Otto, Germany	16	3.5[a]	29.1		0.205[m]	303
Monopol, Rottgersbank, Germany	16,17	6.0[a]	28.6	0.156[n]	0.229[n]	303
Monopol, Ida, Germany	16	2.9[a]	27.4		0.205[k]	303
Monopol, Emil, Germany	16,17	2.4[a]	26.8	0.150[n]	0.215[n]	303
Gleiwitzer, Germany	16	3.1[a]	26.2		0.207[o]	303
Gleiwitzer, Germany	16,17	3.7[a]	25.9	0.158[o]	0.212[o]	303
Monopol, Rudolf, Germany	16	2.1[a]	25.9		0.205[o]	303
Cwmtillery Garw, U.K.	3	4.3	25.5		0.27	423-623
Monopol, Wilhelm, Germany	16	1.3[a]	24.9		0.194[o]	303
Dorstfeld, Germany	16,17	1.7[a]	24.2	0.153[p]	0.210[p]	303
Low-volatile bituminous						
Amalie, Dickebank I, Germany	17	3.7[a]	20.3	0.142[q]	0.195[p]	303

[a]Estimated using measured ash and 1% sulfur in Parr formula.
[b]Possibly contains 2.9% H_2O.
[c]Possibly contains 2.2% H_2O.
[d]Possibly contains 6.6% H_2O.
[e]Parallel to bedding planes.
[f]Perpendicular to bedding planes.
[g]Possibly contains 2.8% H_2O.
[h]Possibly contains 4.1% H_2O.
[i]Possibly contains 9.9% H_2O.
[j]Possibly contains 1.3% H_2O.
[k]Possibly contains 1.4% H_2O.
[l]Possibly contains 1.5% H_2O.
[m]Possibly contains 1.0% H_2O.
[n]Possibly contains 0.8% H_2O.
[o]Possibly contains 1.1% H_2O.
[p]Possibly contains 0.7% H_2O.
[q]Possibly contains 1.2% H_2O.

Table 4.4. Thermal diffusivity and thermal conductivity of cannel coals and anthracites

Coal source (mine, seam, origin)	Reference	Moisture (wt %)	Mineral matter[a] (wt % dry)	Volatile matter (wt % dmmf)	Thermal diffusivity (mm^2/s)	Thermal conductivity (W/m K)	Temperature (K)
Cannel coals							
Notts, U.K.	14	2.5	34.9	62.4	0.156	0.26	288-373
Lohberg, Germany	16,17	1.2	11.3	57.6	0.167	0.268	303
Shale cannel, U.K.	14	1.5	37.0	41.9	0.278	0.42	288-373
Cannel coal, U.K.	14	1.9	27.4	39.4	0.190	0.29	288-373
Semianthracite							
Katherine, Mausegatt, Germany	16,17	0.8	2.4	14.0	0.158	0.213	303
Gewerkschaft, Kreftenscheer I, Germany	16,17	0.7	7.7	12.4	0.200	0.256	303
Carl Funke, ZKF 5, Germany	16,17	1.1	9.8	12.1	0.186	0.275	303
Anthracite							
Heinrich, Geitling, Germany	16	0.8	13.9	12.0		0.316	303
Carl Funke, ZKF 4, Germany	16,17	1.2	5.9	11.2	0.234	0.362	303
Carl Funke, ZKF 4, Germany	16,17	1.2	5.9	11.2	0.164	0.231	303
Finefrau seam, Germany	16,17	0.8	2.5	10.3	0.178	0.249	303
Carl Funke, ZKF 2, Germany	16,17	1.0	3.2	10.3	0.170	0.218	303
Carl Funke, ZKF 1, Germany	16,17	1.0	3.2	9.8	0.175	0.236	303
Carl Funke, ZKF 3, Germany	16	0.9	2.3	9.7		0.209	303
Carl Funke, ZKF 3, Germany	16	1.7	2.4	8.9		0.267	303
Carl Funke, ZKF 2, Germany	16,17	1.3	2.3	8.4	0.170	0.224	303
Shukovugol 26, K6 seam, U.S.S.R.	15	0.0	12.4	2.3	0.26	0.233	423

[a]Estimated using 1% sulfur, dry basis, and the Parr formula.

Table 4.5. Correlation of thermal conductivity with coal moisture content

Coal source (mine, seam, country)	Reference	Temperature (°C)	Moisture (wt %)	Thermal conductivity (W/m·K)			
				Dry coal	Water	Wet coal	
						Measured	Predicted from Eq. (4.8)
Bituminous							
Pittsburgh seam, U.S.A.	5	50	2.4	0.213[a]	0.639	0.214[a]	0.223
		50	2.4	0.192[b]	0.639	0.196[b]	0.203
Clipstone, Low Main, U.K.	3	20	4.5	0.194	0.598	0.218	0.212
Dearne Valley, Shafton, U.K.	3	20	4.7	0.205	0.598	0.241	0.223
Baddesley brights, U.K.	3	20	9.4	0.226	0.598	0.263	0.261
Hucknall, Main Bright, U.K.	3	20	9.8	0.227	0.598	0.292	0.263
Woolaton, Tupton, U.K.	3	20	10.1	0.268	0.598	0.310	0.301
Binley, 9-ft., U.K.	3	20	13.0	0.184	0.598	0.334	0.238
Lignite and brown coals							
Sandow, Wilcox, U.S.A.	This work	60-100	37.5	0.14	0.660	0.33	0.34
Ilse mine, Germany	18	20	3.4	0.151	0.598	0.155	0.166
		20	12.1	0.151	0.598	0.165	0.205
		20	41.4	0.151	0.598	0.299	0.336
		20	41.4	0.151	0.598	0.301	0.336
		20	44.5	0.151	0.598	0.322	0.350
		20	44.5	0.151	0.598	0.323	0.350
		20	44.5	0.151	0.598	0.311	0.350
		20	47.6	0.151	0.598	0.336	0.364
		20	47.6	0.151	0.598	0.332	0.364
No. 5 cut, Morwell, Australia	9	20-60	41	0.151[c]	0.627	0.32	0.35
		20-60	63	0.151[c]	0.627	0.52	0.45

[a] Parallel to bedding plane.
[b] Perpendicular to bedding plane.
[c] Estimated by using value from H. Gan, S. Nandi, and P. L. Walker, Fuel 51 (4):272-277 (October 1972).

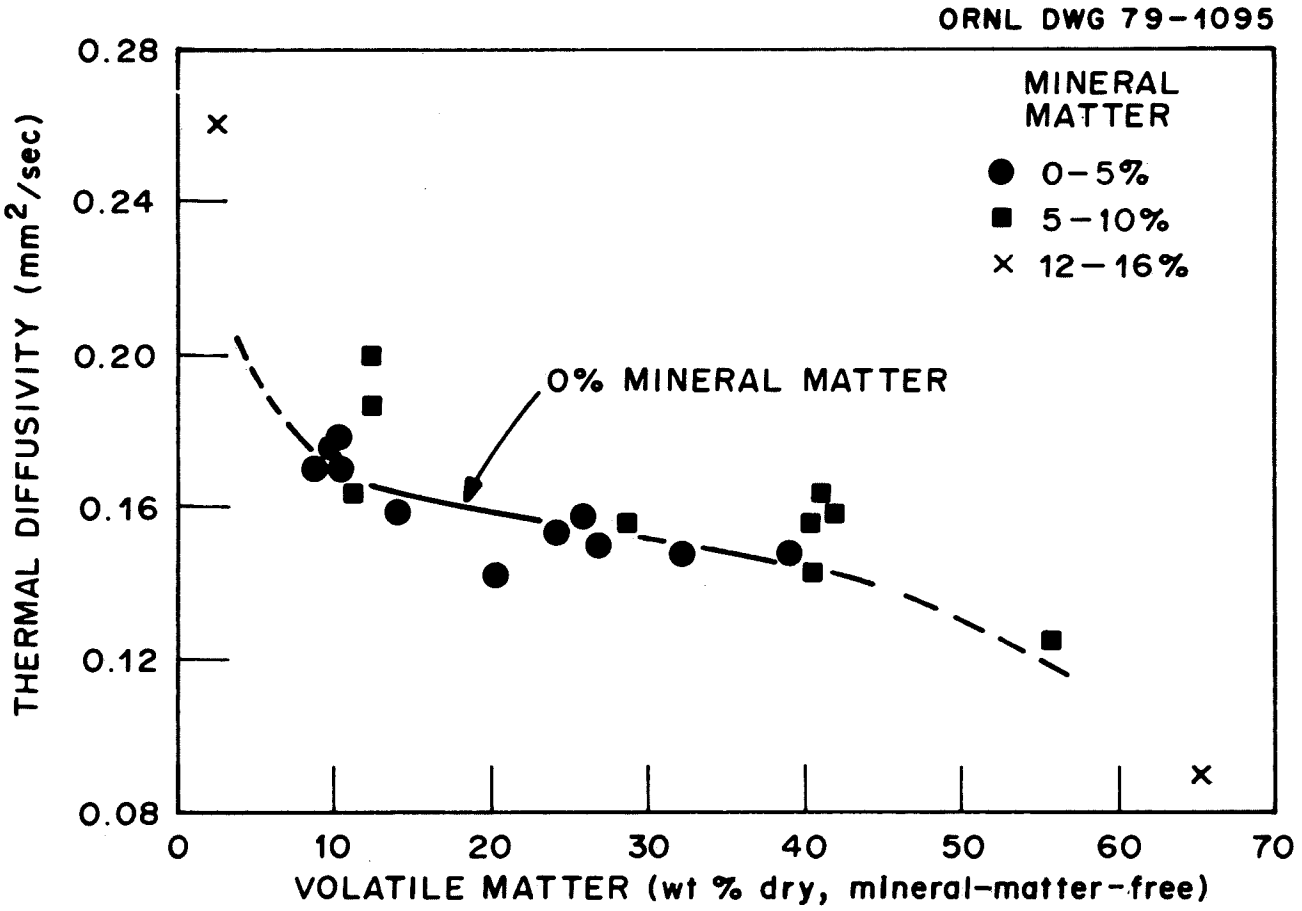

Fig. 4.1. Thermal diffusivity of coals as a function of approximate rank (volatile content was used as the rank parameter).

More data on thermal conductivity were available than data on diffusivity, but much more scatter was apparent. Although a correlation with volatile content (as an indicator of rank) and mineral content can be calculated, the data are too scattered for an accurate correlation (Fig. 4.2). Multiple linear regression resulted in an equation that showed reasonable qualitative trends with mineral and volatile content,

$$k_{\text{dry coal}} = 0.249 + 0.001251(\%\ \text{mineral matter}) - 0.001616(\%\ \text{volatile matter}) \qquad (4.15)$$

but which had an extremely poor correlation coefficient (0.43).

One reason for the wide scatter in the data available was the difficulty of reproducing a measure of thermal conductivity, even for samples of the same coal. Sample handling procedures that cause cracks can cause variations of 20% in the measured results, and differences within the seam at a given location can cause another 10% variation.[20] The types of minerals present will affect conductivity, as will the extent of mineral dispersion (e.g., lenses of pyrite). For correlation, volatile content in low-rank coals was not an ideal measure of rank (although it is the only available measure for most of the data) nor was rank a precise predictor of porosity and density.

Another heterogeneity that can cause scatter in thermal conductivity data is petrographic makeup. Table 4.6 compares thermal diffusivity and k for various durains, clarains, and cannel coals.[14,16,17] Durain is a dull black lithotype containing significant amounts of exinite and inertinite, evenly mixed; whereas claraine is a striated blend of durain and bitrain, a glossy lithotype containing more vitrinite. Thermal conductivity of durain was consistently higher, but whether the maceral groups (vitrinite, exinite, inertinite) or the physical striations of clarain caused its conductivity to be lower is unclear. Cannel coal is made up predominantly of sporinite (an exinite maceral derived from plant spores) and micrinite (an inertinite maceral that is generally granular); its conductivities were higher than conductivities of the other lithotypes.

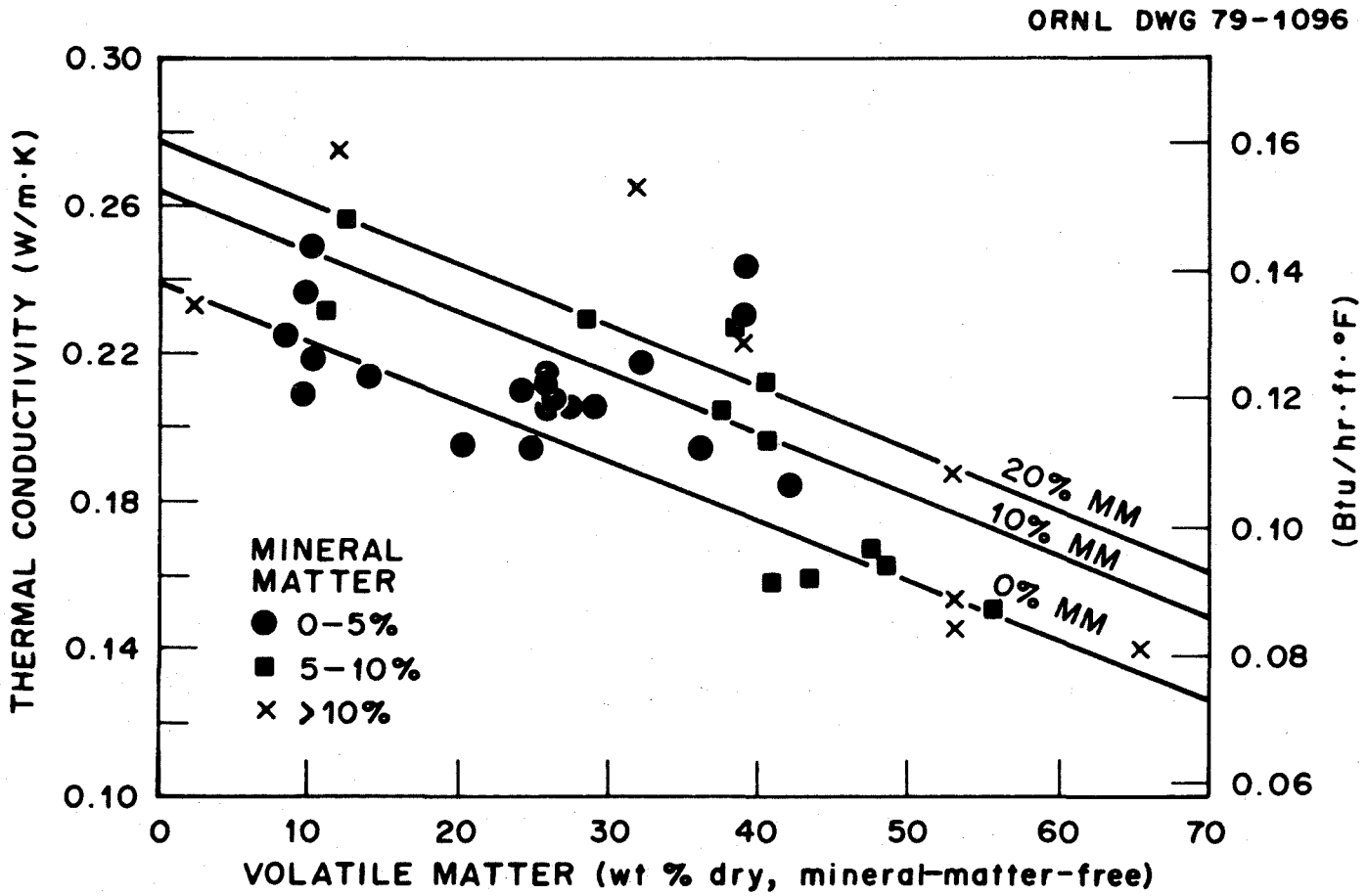

Fig. 4.2. Trends in the variation of coal thermal conductivity with volatile content and mineral content.

Table 4.6. Lithotype effect on thermal diffusivity and conductivity

Coal source	Reference	Lithotype	Thermal diffusivity (mm^2/s)	Thermal conductivity[a] (W/m·K, dmmf)
Barnsley Thick, U.K.	14	Durain, bituminous	0.158	0.207
		Clarain, bituminous	0.120	0.153
Trencherbone, U.K.	14	Durain, bituminous	0.152	0.221
		Clarain, bituminous	0.144	0.184
Arley, U.K.	14	Durain, bituminous	0.157	0.207
		Clarain, bituminous	0.135	0.178
Notts, U.K.	14	Cannel coal[b]	0.156	0.22
Lohberg, Germany	16,17	Cannel coal[b]	0.167	0.254
Unspecified, U.K.	14	Cannel coal[b]	0.190	0.256

[a]Corrected to mineral-matter-free basis by Eq. (4.14).

[b]Predominantly sporinite (spore-derived material with high hydrogen-to-carbon ratio) and micrinite (probably derived from decayed plant matter).

Anisotropy also can cause scatter of the data because conductivity would be affected by the direction of heat conduction with respect to the bedding planes. Most data[5,16,21] indicated that conductivity was higher in a direction parallel to the bedding plane (Table 4.7), perhaps because discontinuities between coal layers would tend to cause increased heat transfer resistance in the direction normal to these discontinuities. However, cleat structures (fracture structures) can exist normal to the bedding plane, possibly explaining the opposite relationship observed in Yubari coal.

4.1.3 Correlations

Wet coal. The simplest correlation for moisture effect was to assume that k depended linearly on moisture content:

$$k_{\text{wet coal}} = k_{\text{dry coal}} + \frac{\%\ \text{moisture}}{100} \times (k_{\text{water}} - k_{\text{dry coal}}) \quad . \quad (4.16)$$

This correlation was tested on the wet bituminous coals and lignites listed in Table 4.5, and its suitability as a first approximation is shown in Fig. 4.3. The correlation coefficient was 0.85 when one data point (for Binley 9-ft coal) was omitted. Fritz and Kneese[18] presented the most detailed data, which indicated that a linear relationship was valid above about 12% moisture for the brown coal used in their work.

Dry coal. Its porous nature is a primary reason for the poor thermal conductivity of dry coal. Accordingly, attempts to correlate $k_{\text{dry coal}}$ have used porosity either as an explicit parameter or implicitly through some rank parameter. Also, because of the influence of porosity, temperature has little or no effect on $k_{\text{dry coal}}$ at less than 673 K (400°C).[3,13]

Changes in k_s, the intrinsic thermal conductivity of the "homogeneous" solid, also affect $k_{\text{dry coal}}$. Fritz[7] used ultimate density (density on a pore-free basis) to correlate changes in k_s, as measured for low porosity coals and shown in Fig. 4.4. These data were extrapolated to the values for nonporous graphite, 163 W/m·K at 2250 kg/m^3. Use of this correlation

Table 4.7. Anisotropic effects on thermal conductivity of bituminous coals

Coal	Reference	Thermal conductivity (W/m·K), oriented in direction: Perpendicular to bedding planes	Thermal conductivity (W/m·K), oriented in direction: Parallel to bedding planes	Percentage difference
Pittsburgh, U.S.A.	5	0.196	0.213	+8.7
Gleiwitzer, Germany	16	0.207	0.215	+3.9
Monopol, Rudolf, Germany	16	0.204	0.213	+4.4
Monopol, Emil, Germany	16	0.215	0.222	+3.3
Yubari, Japan	21	0.258	0.241	-6.8

Source: J. D. Clendenin et al., Thermal and Electrical Properties of Anthracite and Bituminous Coals, Pennsylvania State College, Mineral Industries Experiment Station, Technical Paper 160, 1949, pp. 11-67.

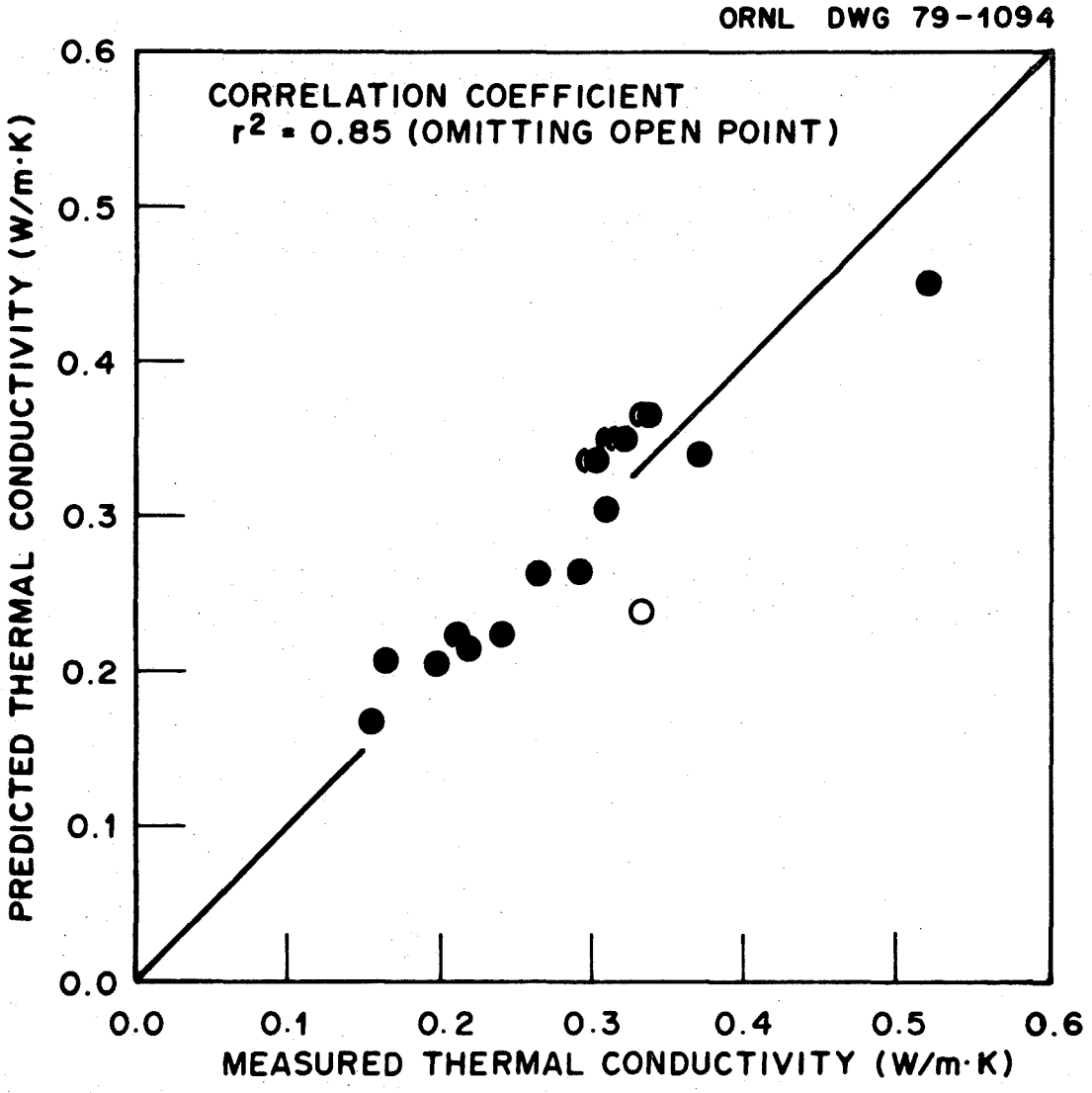

Fig. 4.3. Comparison of measured and predicted thermal conductivities for wet bituminous coals and lignites [using Eq. (4.16)].

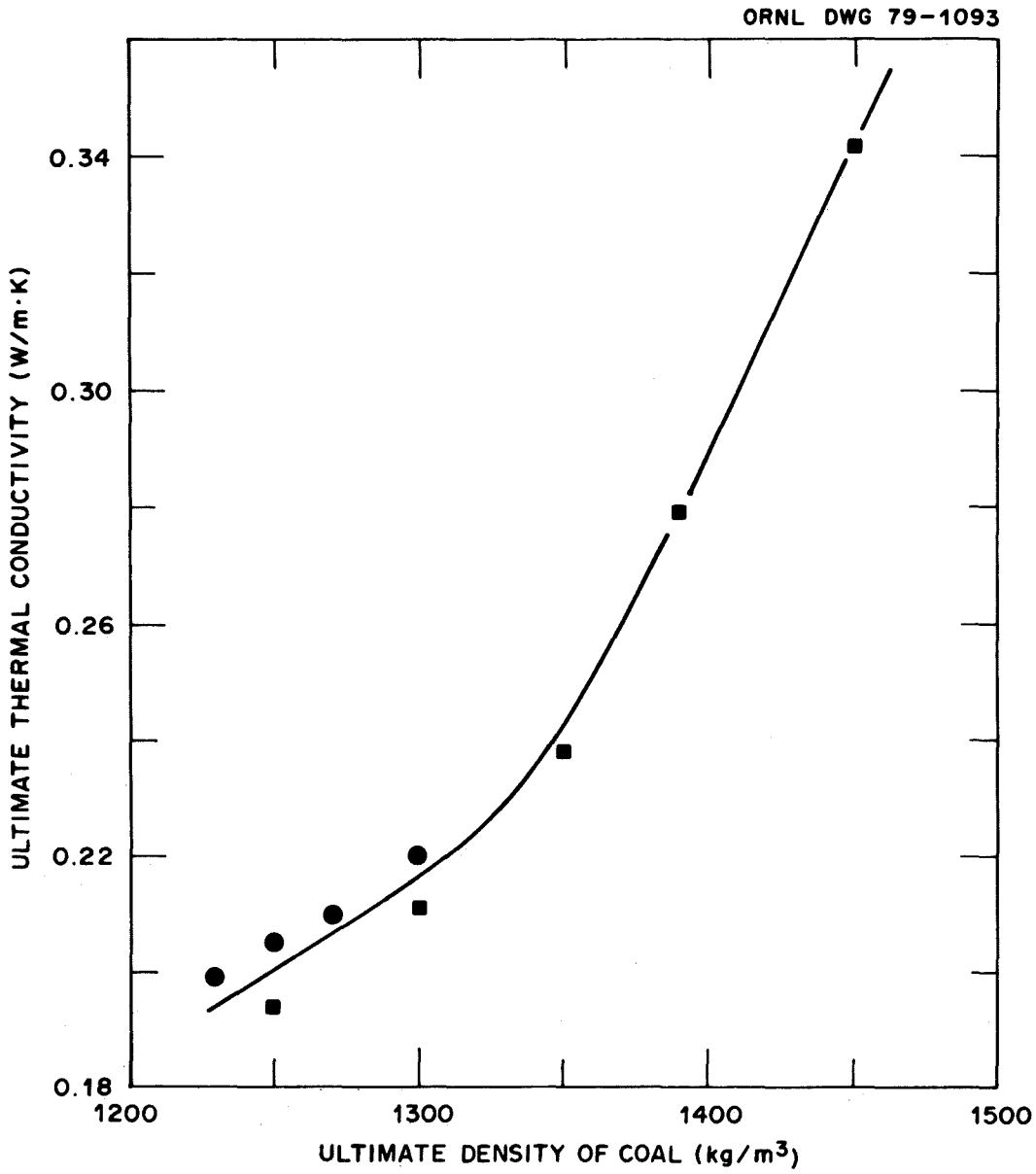

Fig. 4.4. Correlation of thermal conductivity (k_S) with density (ρ_S) of pore-free coal.

is best restricted to low-ash coals because variations in types of mineral matter were not provided for. Gan et al.[19] correlated k_s with ultimate density, using percent carbon (maf) as the rank parameter; he observed a minimum of 1270 kg/m^3 (mineral-matter-free) at about 80% carbon. However, because mineral matter has higher density and conductivity than the organic portion of the coal, it would tend to increase the density and thermal conductivity from the mineral-matter-free value.

Several models for $k_{dry\ coal}$ have been proposed, each based on k_s and the fractional porosity, p. Fritz[7] tested the equations of Maxwell,

$$k_{dry\ coal} = k_s \left(\frac{1 - p}{1 + 0.5\ p} \right) , \tag{4.17}$$

and of Burger,

$$k_{dry\ coal} = k_s \left(\frac{1 - p}{1 + 0.67\ p} \right) , \tag{4.18}$$

using his own correlation of k_s with ultimate density of the solid (Fig. 4.4). A third equation has been cited[22,23] as a good approximation for thermal conductivity of a porous medium:

$$k_{dry\ coal} = k_s^{\ p} \left(\frac{k_f}{k_s} \right)^{1-p} , \tag{4.19}$$

where k_f is the thermal conductivity of the fluid filling the pores. These equations were tested for three coals in Table 4.8 using measured porosities and predicted k_s from Fig. 4.4. Equations (4.16 and 4.17), which predicted about the same values, agreed best with the data but predicted values that were 40% high for Wilcox lignite.

In summary, for first approximation of thermal conductivity in unreacted, dry coals, the best correlations were Eqs. (4.16 and 4.17), using the Fritz correlation of k_s with ultimate density.

Table 4.8. Tests of thermal conductivity correlations with density and porosity

Rank source	Coal		
	Lignite Wilcox Tex.	Brown coal Ilse mine, Germany	Bituminous Pittsburgh seam
Ultimate density, kg/m^3	1440	1410	1315[a]
Thermal conductivity of solid, k_s (Fig. 4.4) W/m·K	0.331	0.300	0.221
Overall porosity, %	30	32	3.0
Thermal conductivity of interstitial gas, mW/m·K	25.6[b]	25.6[c]	27.6[d]
Predicted thermal conductivity, W/m·K			
By Eq. (4.16), Maxwell's	0.202	0.176	0.211
By Eq. (4.17), Burger's	0.193	0.168	0.210
By Eq. (4.18)	0.120	0.128	0.127
Measured thermal conductivity, W/m·K	0.14	0.151	0.205

[a]Estimated from carbon content by correlations in H. Gan, S. Nandi, and P. L. Walker, "Nature of the Porosity in American Coals," Fuel 51, (4), 272-277 (October 1972).

[b]Argon, 490 K.

[c]Air, 293 K.

[d]Nitrogen, 323 K.

4.2 Density, Shrinkage, and Porosity

Density, shrinkage, and porosity were measured for three coals of interest: lignite from the Wilcox (Texas) formation, Wyodak subbituminous coal from the Roland-Smith (Wyoming) seams, and bituminous coal from the Pittsburgh (West Virginia) seam. These measurements are described here and compared.

Part of the utility of such data may be understood by comparing them to the analysis of porosity and density of coal powders by Gan et al.[19] Their data, although extensive, did not include density of wet coals, shrinkage from drying, or porosity and density of large pieces of dried coal, which may contain cracks. Because modeling of UCG depends on accurate bulk properties, measurements of these other parameters is important.

Density of water-saturated chunks of coal was determined in a large water pycnometer. After chunks were dried in a vacuum at 106°C for 16 h, shrinkage was measured in each of three orthogonal dimensions; wet density and shrinkage measurements are listed in Table 4.9. Comparison of shrinkage was particularly interesting because the lignite shrank 8.4% in each dimension (sample standard deviation 3.0%), the subbituminous coal shrank $9.3 \pm 3.3\%$, and no shrinkage of the bituminous coal was observed.

Densities of the powders (ground from the chunks used for shrinkage tests) were measured in a mercury porosimeter and in a helium densitometer to characterize pore volume in the dried coal (Table 4.10). Helium was able to penetrate pores easily, thus the densitometer measures an intrinsic density (ultimate density) for the solid itself, excluding pores.

In contrast, mercury penetration depended on applied pressure: at 15 psi a measure of bulk particle density could be read and at 14,000 psi an approximation of intrinsic density was the result. Pore size distributions may be determined by applying gradual increases to the applied mercury pressure; because low-rank coals are easily crushed, distributions estimated in these coals by this method are subject to error.

Table 4.9. Wet density and shrinkage measurements

Coal	Density of wet coal (kg/m^3)	Shrinkage from drying (linear %)		
		Length	Width	Thickness
Wilcox lignite A	1217	[a]	9.53	[a]
	1234	[a]	7.08	[a]
		12.78	8.98	[a]
		5.7	7.11	6.11
		4.42	13.42	4.23
		10.19	8.83	10.84
Wyodak subbituminous C coal	1263	7.39	4.00	13.28
	1283	8.80	11.46	10.61
Pittsburgh bituminous coal, hvAb	1302	[b]	[b]	[b]
	1306	[b]	[b]	[b]

[a] Chips fell off during drying.

[b] Not detected.

Table 4.10. Density and porosity of coal powders

Coal sample	Wilcox lignite 1	Wilcox lignite 2	Wyodak subbituminous 3	Wyodak subbituminous 4
Density by mercury porosimeter, kg/m^3				
15 psig	1240	1250	1099[a]	1099[a]
75 psig	1257	1264		
250 psig	1274	1275		
15000 psig	1462	1369	1363[a]	1435[a]
Density by helium densitometer, kg/m^3	1449	1423	1372[b]	
Particle porosity, %	14.4[c]	12.2[c]	19.9	

[a]Source of data: K. M. Gupta, Porous Material Div., Lindeman Labs., Inc., Ithaca, New York; personal communication, August 16, 1979.

[b]Using helium density as intrinsic density.

[c]Source of data: H. Gan, S. Nandi, and P. L. Walker, "Nature of the Porosity in American Coals," Fuel 51, (4), 272-277 (October 1972), adjusted to mineral-matter-containing basis.

Data are summarized in Table 4.11. An important bulk effect was that much higher porosities were measured for the lignite chunks than for the lignite powder. These data may be understood by considering that the particle density (as measured in mercury at 15 psi) included only the solid volume and the volume of pores 3 μm or less in diameter. Larger pores in lignite would be easily filled by mercury, and the void volume of large cracks, which open up when the low-rank coals are dried, was eliminated by crushing the chunks into powder for porosimetry.

4.3 Enthalpy and Specific Heat Correlation

Gomez et al.[6] reported enthalpy data and correlations for several coals, cokes, and shales. They found that (1) a mass-weighted combination of coal (or char) enthalpy with ash enthalpy produced suitable correlations, (2) the correlation of ash enthalpy was the same for ashes of all the materials studied, and (3) the correlation of ash-free coal enthalpy was the same for the lignite and subbituminous coal samples.

Using correlations from the Gomez data, enthalpy and specific heat functions were determined for Wilcox lignite, Wyodak subbituminous coal, and Hanna No. 1 coal (Table 4.12). These properties had been measured by Gomez for Wilcox lignite,[6] and agreement between the correlation and the actual data was satisfactory. A correlation is tabulated for a Wilcox lignite char prepared at 500°C, which was also tested by Gomez. Similarly, properties of wet coal may be calculated as a mass average with the enthalpy and specific heat of H_2O.

4.4 References for Section 4

1. R. W. Lyczkowski, A Mechanistic Theory for Drying of Porous Media, Report UCRL-52456, Lawrence Livermore National Laboratory, Livermore, Calif., April 1978.

2. R. D. Gunn, D. L. Whitman, and D. D. Fischer, "A Permeation Theory for In-Situ Coal Gasification," Soc. Pet. Eng. J. 18 300-314 (October 1978).

Table 4.11. Summary of shrinkage, density, and porosity measurements

Coal properties	Coal type		
	Lignite A Wilcox, Tex.	Subbituminous C Roland-Smith, Wyo.	High-volatile A bituminous Pittsburgh, W.Va.
Moisture content, wt %	37.48	33.42	1.77
Shrinkage from drying, %[a]	8.4 ± 3.0	9.3 ± 3.3	None
Density, kg/m^3			
Wet coal	1230	1270	1304
Bulk dry coal[b]	1000	1130	1280
Dry coal powder	1245		
Intrinsic density	1440	1372[c]	1315[c]
Porosity, vol %			
Powder particles	13.5	20	
Bulk dry coal	30	18	3.0

[a]Average linear shrinkage.

[b]Calculated by: (wet density) x (1 - moisture/100)/(1 - shrinkage/100)^3.

[c]Source of data: H. Gan, S. Nandi, and P. L. Walker, "Nature of the Porosity in American Coals," Fuel, 51 (4), 272-277 (October 1972), adjusted to mineral-matter-containing basis.

Table 4.12. Correlations of enthalpy and specific heat for coals and chars as functions of temperature (K)

Coal properties	Correlation
Ash, 376-1031 K[a]	$-181.9 + 0.633 \times T + 0.297 \times 10^{-3} \times T^2$
Low-rank coal, maf, 305-450 K[a]	$-203.1 + 0.378 \times T + 1.212 \times 10^{-3} \times T^2$
Wilcox lignite, dry	$-200.1 + 0.414 \times T + 1.084 \times 10^{-3} \times T^2$
Wyodak subbituminous coal, dry	$-202.0 + 0.392 \times T + 1.163 \times 10^{-3} \times T^2$
Hanna No. 1 hvCb coal, dry	$-196.4 + 0.459 \times T + 0.922 \times 10^{-3} \times T^2$
Char from Wilcox lignite pyrolyzed at 500°C, dry, 368-724 K[a]	$-169.8 + 0.190 \times T + 1.101 \times 10^{-3} \times T^2$
Specific heat, kJ/kg·K	
Wilcox lignite, dry	$0.414 + 2.168 \times 10^{-3} \times T$
Wyodak subbituminous coal, dry	$0.392 + 2.326 \times 10^{-3} \times T$
Hanna No. 1 hvCb coal, dry	$0.459 + 1.845 \times 10^{-3} \times T$
500°C Wilcox char, dry	$0.190 + 2.202 \times 10^{-3} \times T$

[a]Source of data for correlation: M. Gomez, J. B. Gayle, and A. R. Taylor, Jr., Heat Content and Specific Heat of Coals and Related Products, BM/RI-6607, U.S. Bureau of Mines, 1965.

3. S. Badzioch, D. R. Gregory, and M. A. Field, "Investigation of Temperature Variation of the Thermoconductivity and Thermaldiffusivity of Coal," Fuel, 43, 267-280 (1964).

4. Y. S. Touloukian et al., Thermal Conductivity — Nonmetallic Solids, pp. 808-810, IFI/Plenum, New York, 1970.

5. J. M. Singer and R. P. Tye, Thermal, Mechanical, and Physical Properties of Selected Bituminous Coals and Cokes, BM/RI-8364, U.S. Bureau of Mines, 1979.

6. M. Gomez, J. B. Gayle, and A. R. Taylor, Jr., Heat Content and Specific Heat of Coals and Related Products, BM/RI-6607, U.S. Bureau of Mines. 1965.

7. W. Fritz, Forsch. Geb. Ingenieurwes. 14 (1), 1-10 (1943).

8. H. S. Carslaw and J. C. Jaeger, Conduction of Heat in Solids, p. 201 Oxford University Press, Oxford, 1959.

9. B. R. Stanmore and A. R. Boyd, "Heat Transfer and Thermal Effects in Heated Cylinders of Victorian Brown Coal," pp. 115-120 in 2nd Australasian Conference on Heat and Mass Transfer, University of Sydney, Sydney, 1977.

10. R. Acton, Sandia National Laboratories, Albuquerque, N. Mex., personal communication, July 25, 1978.

11. N. E. Vanderborgh, G. R. B. Elliott, and G. E. Cort, "Concurrent Heat and Mass Transfer during Drying of Blocks at Subbituminous Coals," Proceedings of the Fourth Underground Coal Conversion Symposium, Steamboat Springs, Colorado, July 17-20, 1978, SAND 78-0941, Sandia National Laboratories, Albuquerque, N. Mex., 1978.

12. I. K. Walker and K. J. D. MacKenzie, N. Z. J. Sci. 17 (1), 77-92 (1974).

13. J. D. Clendenin et al., Thermal and Electrical Properties of Anthracite and Bituminous Coals, Pennsylvania State College, Mineral Industries Experiment Station, Technical Paper 160, 1949, pp. 11-67.

14. F. S. Sinnatt and H. MacPherson, Fuel, 3, 12 (January 1934); cited in ref. 13.

15. A. A. Agroskin, E. I. Goncharov, and L. V. Lovetskii, Khim. Tverd. Topl., 4, 3-12 (1968); translated as "Combined Determination of the Thermal Characteristics of Coal During High-Temperature Pyrolysis," SLA-74-6007, Sandia National Laboratories, Albuquerque, N. Mex., 1974.

16. W. Fritz and H. Diemke, Feuerungstechnik 27, (5), 129-136 (1939); cited in ref. 13.

17. W. Fritz and H. Moser, Feuerungstechnik 28, (5), 97-107 (1940); cited in ref. 13.

18. W. Fritz and H. Kneese, "Thermal Conductivity, Specific Heat, and Thermal Diffusivity of Coke and Brown Coal," Feuerungstechnik, 30 (12), 273-280 (1942).

19. H. Gan, S. Nandi, and P. L. Walker, "Nature of the Porosity in American Coals," Fuel 51 (4), 272-277 (October 1972).

20. A. M. Godridge, "Thermal Conductivity of Solid Coal Samples," Fuel 35, 279-281, 1956.

21. S. Nukiyama, Trans. Soc. Mech. Eng. (Japan) 2, 8-96 (1936); cited in ref. 13.

22. J. M. Smith, Chemical Engineering Kinetics, 2nd Ed., p. 426, McGraw-Hill, New York, 1970.

23. W. Woodside and J. H. Messmer, "Thermal Conductivity of Porous Media. I. Unconsolidated Sands," J. Appl. Phys. 32 (9), 1688-1706 (1961).

5. CHARACTERIZATION OF OVERBURDEN

5.1 Purpose of Testing

Characteristics of overburden (the strata overlying a coal seam) were measured using the block pyrolysis system. Some of these properties were:

1. physical properties (e.g., density and shrinkage);
2. chemical composition (i.e., moisture, carbon, hydrogen);
3. friability or collapse when dried or heated; and
4. products and yields from thermal decomposition.

Initial tests have used six cored samples from the Hoe Creek 2 site of Lawrence Livermore National Laboratory.

The importance of understanding the behavior of overburden is illustrated in Fig. 5.1, an example of overburden collapse into the UCG cavity. Sampling well SS-2 was cored to obtain samples of strata before the Hoe Creek 2 UCG field test in the Felix No. 2 seam. Coring subsequent to the test revealed the collapse of strata from as high as 15 m above the seam. Heating, weakening, and geological stresses had caused the overburden rock to fall into the hot gasification cavity, where any organic matter in the rock was heated and pyrolyzed. Cores from strata that had collapsed at the field site were tested in the laboratory. Decomposition and spalling data are presented here.

5.2 Characterization

Cores were inspected at the drilling site and visually characterized by Livermore personnel. Several bands of unconsolidated sand were observed, but the samples tested in these experiments were of siltstone and claystone (Fig. 5.1). After gross descriptions were logged (Table 5.1), the 60-mm-diam (2-3/8-in.) cores were cut into approximately 140-mm (5-1/2-in.) lengths, wrapped in plastic and aluminum foil, and sealed in a layer of wax. At ORNL, holes for thermocouples were drilled in the cores and the cores were x-rayed, as described in Sect. 2.3.

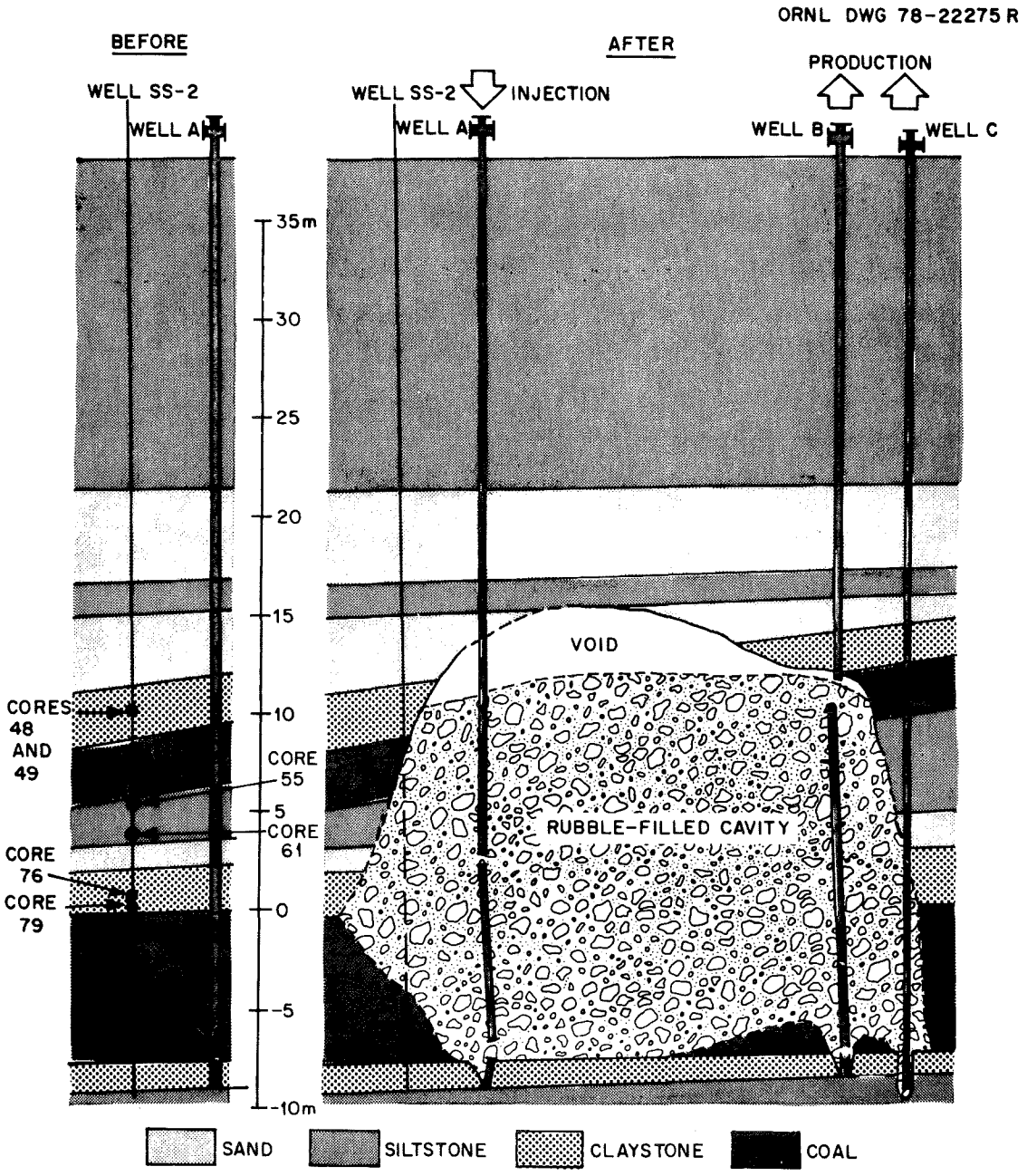

Fig. 5.1. Location of overburden cores from the Hoe Creek 2 UCG field test site, Gillette, Wyoming; (left) before field test at time of coring, and (right) after field test. (Source: LLL In Situ Gasification Program Quarterly Progress Report, April through June 1978, UCRL-50026-78-2, Lawrence Livermore National Laboratory, October 1978.)

Table 5.1. Description and properties of overburden samples from the site of the Hoe Creek 2 UCG field test

Core number experiment	79 OB-4	76 OB-5	61 OB-6	55 OB-7	49 OB-3	48 OB-1 & OB-2
Location in well SS-2[a]						
Depth from surface, m	38.9	38.4	35.1	33.8	28.4	28.1
Height above Felix No. 2, m	0.2	0.7	4.0	5.3	10.7	11.0
Distance from Felix No. 1, m	5.7 beneath	5.3 beneath	2.0 beneath	0.6 beneath	1.7 above	2.0 above
Description[a]	Dark black, carbonaceous, slightly silty claystone. Carbonaceous material increases with depth and color darkens.	Thinly bedded clayey siltstone and claystone; medium black with brownish cast; tends to disk with stress relief.	Very silty claystone or very clayey siltsone; medium brown; very thinly bedded; slightly calcareous.	Medium brown to buff with black carbonaceous speckles; thinly interbedded, very fine-grained silty sand and claystone; dries quickly with formation of shrinkage cracks;[a] broke into pieces, so placed in a mesh basket for experiment.	Slightly silty claystone; light brown to light black slightly carbonaceous, thin-bedded.	
Analyses						
Moisture, wt %	15.6	13.4	13.0	14.3	13.3	[c]
Carbon, % dry[b]	5.02	2.04	1.26	1.75	3.63	[c]
Hydrogen, % dry	1.03	0.42	0.42	0.65	0.58	[c]
Density, kg/m^3, and shrinkage						
Bulk density of wet solid	2000	2190	2200	2190	2200	[c]
Shrinkage from drying, %	1.5[d]	0.6	0.8-2.0		None	[c]
Bulk density of dry solid[e]	1800	1930	2000		1900	[c]

[a] Source: H. C. Ganow, Lawrence Livermore National Laboratory, personal communication, Oct. 11, 1978.
[b] Includes carbon in carbonates.
[c] Not measured, but should be same as for core 49.
[d] Average linear shrinkage, three dimensions; sample of core dried in vacuum at 107°C for 16 h.
[e] Calculated from moisture content, wet bulk density, and shrinkage.

Before heat treatment, a segment was sliced from the bottom of each core for other tests. Analytical results (Table 5.1) showed that moisture content was fairly constant (13 to 16%), but carbon and hydrogen content varied, apparently reflecting differences in amount of organic matter. Density of the wet solid was 2190 to 2200 kg/m^3 except for core 79, a more carbonaceous sample that had a density of 2000 kg/m^3. Shrinkage after drying varied from none to 2.0%; thus, the calculated densities of dry solid were 1800 to 2000 kg/m^3.

As each core was heated to 1273 K in an inert purge gas, internal temperatures and gas evolution were measured. Although no organic liquid products were detected, significant amounts of H_2, CO, and CO_2 were produced, along with small amounts of CH_4, C_2, and C_3 gases (Table 5.2). Overall gas yields (wt % of dry sample) were as high as one-third of those measured from Wyodak coal blocks.

After heat treatment, the solid residues were photographed and described so that decrepitation could be compared. The different strata were composed of different-sized particles in various states of consolidation; therefore, this decrepitation varied in amount and type, as Figs. 5.2 through 5.7 illustrate. Cores 55 and 79 flaked apart at closely spaced bedding planes, but large cracks formed in cores 48, 49, and 61. The material in cores 48, 49, and 76 hardened, forming a brick-like residue. The vertical bands shown in Figs. 5.3 and 5.6 were small amounts of drilling mud ($BaSO_4$) from the coring operation and were not part of the overburden.

Some trends in the type of spalling in different components of the overburden were apparent. The principal influence was varying particle size in sedimentary rocks: sand larger than silt, which is larger than clay. The most fragile samples before heat treatment were the unconsolidated sands; none were tested in this series because they were too fragile even to withstand drying. Core 55, which had high sand content and was quite fragile, spalled upon drying. In contrast, samples having a high clay content (cores 48, 49, and 76) hardened like clay brick. Organic content in cores 55 and 79 may have

Table 5.2. Results of heating tests for overburden from Hoe Creek 2 site

Core experiment	79 OB-4	76 OB-5	61 OB-6	55 OB-7	49 OB-3	48 OB-1 & OB-2[a]
Sample weight, (kg, dry)	0.6577 0.555	0.8183 0.709	0.7561 0.658	0.7830 0.671	0.7287 0.632	0.9323 0.808[b]
Product yields, (kg)						
Solid residue	0.4679	0.6437	0.6161	0.6051	0.597	0.7332
Oil and tars	0[c]	0[d]	0[c]	0[c]	0[c]	0[c]
Gases	0.0322	0.059	0.0297	0.0366	0.0352	0.082
Yields, wt %-dry						
Solid residue	84.3	90.8	93.6	90.2	94.5	90.7
Oils and tars	0[c]	0[d]	0[c]	0[c]	0[c]	0[c]
H_2	0.357	0.219	0.143	0.243	0.205	0.105
CH_4	0.104	0.075	0.056	0.105	[e]	[e]
C_2's	0.052	0.045	0.030	0.094	0[c]	0.040
C_3's	0.040	0.035	0.024	0.013	0[c]	0[c]
CO	2.61	3.50	1.610	1.469	[e]	[e]
CO_2	2.61	4.44	2.63	3.26	4.73	3.61
H_2S	0.018	0[c]	0.022	0.003	0[c]	0[c]
Total gases	5.79	8.31	4.52	5.19	5.7	10.1
Total balance	90.1	99.1	98.1	95.4	100.2	100.8
Characteristics of solid residue	Spalled at bedding planes; 3.6% shrinkage in each dimension	Solid with no signs of flaking or shrinkage. Hard, breaking smoothly when struck by a hammer	Several large cracks, vertical and horizontal, splitting the block into hard segments. Complete break-off of top two-thirds. Broke into powder when struck	Layered spalling along bedding planes; very easily crumbled into dust	Hardened into a strong, brick-like material with no detectable shrinkage	

[a]Core was heated in OB-1 at 0.3°C/min to 800°C, then cooled and reheated at 3°C/min to 1000°C in OB-2.
[b]Assumes 13.3% moisture, same as for core 49.
[c]Not detected.
[d]Condensed water was dark and contained small black particles, possibly carbon from CO decomposition.
[e]Errors in analysis by gas chromatograph.

ORNL Photo 1281-79

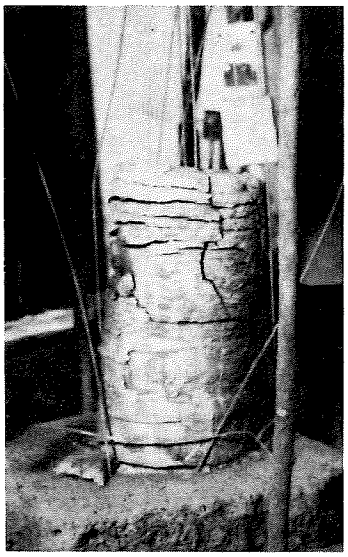

Fig. 5.2. Core 79 after experiment OB-4.

ORNL Photo 1282-79

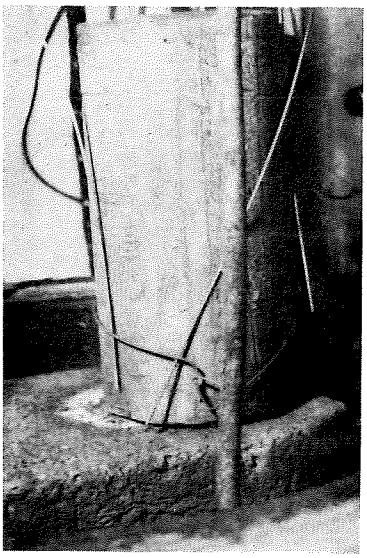

Fig. 5.3. Core 76 after experiment OB-5.

ORNL Photo 1283-79

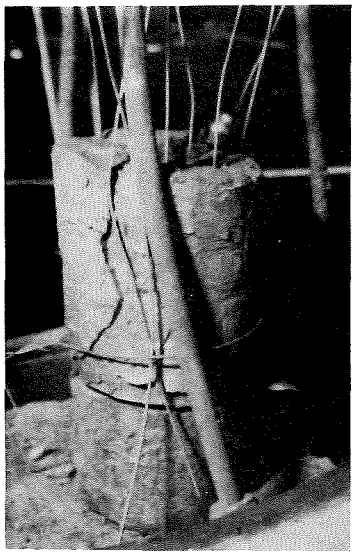

Fig. 5.4. Core 61 after experiment OB-6.

ORNL PHOTO 1284-79

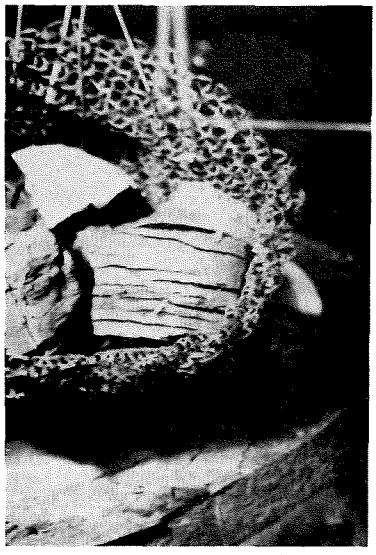

Fig. 5.5. Core 55 after experiment OB-7.

ORNL Photo 1280-79

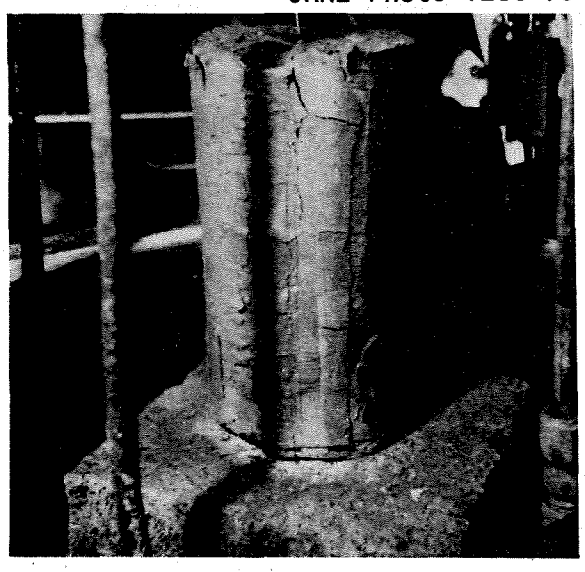

Fig. 5.6. Core 49 after experiment OB-3.

ORNL Photo 1279-79

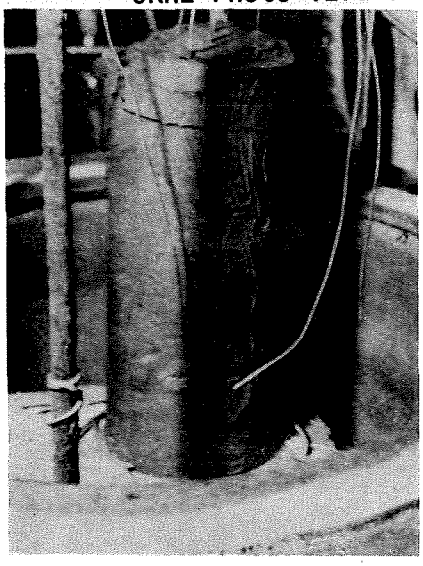

Fig. 5.7. Core 48 after experiments OB-1 and OB-2.

influenced the bedded spalling, but the wide variations in spalling existed in spite of moisture contents that were nearly constant.

Geological descriptions have been published for Department of Energy UCG sites at Hanna, Wyoming[1]; Princetown, West Virginia[2]; Hoe Creek, Wyoming[3]; and Rawlins, Wyoming.[4] Each was bounded by shales containing organic matter in varying proportions. Our study has shown that this organic component can be degraded.

5.3 References for Section 5

1. L. A. Schrider and J. Pasini III, "Preliminary Results Released for Wyoming In Situ Gasification Tests," Coal Age, 78 (12), 58-61 (December 1973).

2. W. J. O'Brien, A Summary of the Geology of the Underground Gasification Site, METC/RI-78/11, Morgantown Energy Technology Center, Pricetown, W. Va., September 1978.

3. R. Stone and D. F. Snoeberger, Evaluation of the Native Hydraulic Characteristics of the Felix Coal (Eocene, Wasatch Formation) and Associated Strata. Hoe Creek Site, Campbell County, Wyoming, UCRL-51992, Lawrence Livermore National Laboratory, January 1976.

4. J. H. Daniel and P. Alexander, "Underground Gasification for Steeply Dipping Coal Beds," Proc. 4th UCC Symp., SAND 78-0841, Sandia National Laboratories, Albuquerque, N. Mex., June 1978, pp. 65-75.

6. CONCLUSIONS

Blocks of coal, when heated, were shown to behave differently compared to the powders that are used in conventional pyrolysis experiments. These differences resulted from the coupling of pyrolysis with other phenomena, such as drying, heat transfer, mass flux of escaping products, and coal plasticity. Specifically our experiments showed that:

1. Low thermal conductivities of all the coals studied contributed to the occurrence of significant internal temperature gradients within the blocks. These gradients were steepened when wet coal was dried slowly, causing the formation of steam plateaus and by transpiration cooling of the dry coal and char by escaping steam.
2. Yields from blocks were different than yields from powders because of secondary cracking and self-gasification reactions. In secondary cracking, oil and tar produced by pyrolysis were pyrolyzed further as they escaped through the block. In self-gasification, steam produced by drying and pyrolysis gasified the coal as it escaped through the hot surface. Some char may have been gasified as well, but gasification of carbon deposits from cracking and steam reforming of organic vapors were the more significant reactions.
3. When blocks were heated in a hydrogen atmosphere, additional methane was produced and hydrogen was consumed. When a purge gas simulating UCG product gas was used, increases in methane yield, gasification, and water-gas shift occurred.
4. Reactivity of char from Wilcox lignite (as indicated by pyrophoricity) was affected by scavenging of reactive, cracking-deposited carbon by gasification reactions.
5. The rate at which bituminous blocks were heated affected swelling. In contrast to the opposite behavior of powders, swelling was less at higher heating rates. The cause was a coupling of internal temperature gradients and plasticity phenomena.

Data and correlations of coal properties were also studied. Thermal diffusivity and thermal conductivity of wet Wilcox lignite (37.5% moisture)

were measured at 0.14 $\pm$ 0.02 mm^2/s and 0.14 $\pm$ 0.03 W/m·K, respectively. Literature data on these thermal properties were reviewed, and recommendations of predictive correlations were made. Density, shrinkage, and porosity data were also measured. Application of a literature correlation for specific heat and enthalpy of coal and char was studied.

Finally, overburden samples from the UCG field test site of the Hoe Creek 2 experiment were analyzed. Properties and behavior of the samples when heated were used to better understand subsidence of strata in UCG.

Application of these data and observations can be used to improve models of UCG. A thorough understanding of the phenomena that occur during UCG will contribute to design and control of the UCG process.

Appendixes

APPENDIXES

These appendixes complete the summary of our research conducted on block-coal pyrolysis.

In Sect. A-1, data from the block heating tests are tabulated, including data on the experiments, yields, gas properties, and pyrophoricity. Note that the data in Tables A-1.4 through A-1.7 are effluent flows rather than gas evolution rates because the experimental system did not exhibit plus flow. Instead, dynamic response of the cold system was that of a first-order system (V = 47 L) with dead time (240 x 2.23 mmol/s, or 12 L of equivalent-plus flow volume).

Section A-2 lists the other documentation for this research: publications, presentations, and data notebooks.

Appendix A-1

Tabulated Data from Block Heating Tests

Table A-1.1 Experimental conditions for heat testing of coal blocks ("block pyrolysis")

Run number	Date of run	Heating rate (K/min)	Maximum temperature, (K)	(°C)	Cover gas: Gas used	Cover gas: Flow rate (mole/min)	Coal block: Coal used	Coal block: Dimensions (mm) Height	Coal block: Dimensions (mm) Diameter	Coal block: Weight (kg)	Coal block: Weight (kg maf)
BP1-1	1/27/75	1.7[a]	760	(490)	N_2	0.20	Ky. bit.		150	4.156	
BP1-2	3/20/75	1.6[a]		[b]	N_2	0.29	Wyodak	168	155.6	3.728	2.343
BP1-3	4/03/75	2.6[a]	1220	(950)	N_2	0.26	Wyodak		150	3.973	2.497
BP1-4	4/17/75	2.9	1220	(950)	Ar	0.170	Wyodak		157	4.610	2.897
BP1-5	5/12/75	2.8[a]	1070	(800)	Ar	0.170	Wyodak		151	3.303	2.076
BP1-6	5/21/75	3.6	910	(640)	Ar	0.170	Wyodak	Irregular		4.583	2.880
BP1-7	5/30/75	3.7	1270	(1000)	Ar	0.170	Wyodak	Irregular		5.055	3.177
BP1-8	6/13/75	3.1		[b]	Ar	0.170	Wyodak	152	162	4.813	3.025
BP1-9	6/20/75	3.2		[b]	N_2	0.20	Wyodak		157	4.553	2.861
BP1-10	6/27/75	2.8	1180	(910)	Ar	0.170	Wyodak		159	5.554	3.490
BP1-11	7/07/75	3.4	770	(500)[c]	Ar	0.170	Wyodak		152	5.059	3.179
BP1-12	7/15/75	3		[c]	Ar	0.170	Wyodak		156	5.345	3.359
BP1-13	7/21/75	2.0	1270	(1000)	Ar	0.170	Wyodak		154	4.324	2.717
BP2-1	12/22/75	0.5	1190	(920)	Ar	0.170[d]	Wyodak	152	159	3.859	2.425
BP2-2	1/22/76	2.8	1310	(1040)	Ar	0.170[d]	Wyodak	126	159	3.209	2.017
BP2-3	2/05/76	1.1[a]	770	(500)	Ar	0.170[d]	Wyodak	165	152	3.699	2.325
BP2-4	2/18/76	0.33	770	(500)	Ar	0.170[d]	Wyodak	178	152	4.496	2.825
BP2-5	2/25/76	3.0	770	(500)	Ar	0.1361	Hanna	57	64	0.227	0.197
BP2-6	3/03/76	0.30	770	(500)	Ar	0.1339	Hanna	59	64	0.232	0.202
BP2-7	3/11/76	0.35	870	(600)	Ar	0.1357	Wyodak	172	149	3.866	2.430
BP2-8	3/18/76	3.0	870	(600)	Ar	0.1365	Wyodak	64	64	0.253	0.1590
BP2-9	4/01/76	3.0	970	(700)	Ar	0.1365	Wyodak	64	64	0.254	0.1596
BP2-10	4/23/76	0.31	970	(700)	Ar	0.1365	Wyodak	141	162	3.734	2.346
BP2-11	5/04/76	5[a]	1070	(800)	Ar	0.1365	Wyodak	302	159	6.976	4.384
BP2-12	5/14/76	2.5	1070	(800)	Ar	0.1374	Wyodak	262	159	6.147	3.863
BP2-13	6/09/76	0.32	1070	(800)	Ar	0.1432	Wyodak	178	152	5.553	3.490

Table A-1.1 (continued)

Run number	Date of run	Heating rate (K/min)	Maximum temperature, (K)	(°C)	Cover gas: Gas used	Cover gas: Flow rate (mole/min)	Coal block: Coal used	Coal block: Dimensions (mm): Height	Coal block: Dimensions (mm): Diameter	Coal block: Weight (kg)	Coal block: Weight (kg maf)
BP2-14	7/07/76	0.28	1170	(900)	Ar	0.1383	Wyodak	184	156	4.258	2.676
BP2-15	7/27/76	3.3	1170	(900)	Ar	0.1383	Wyodak	216	152	5.041	3.168
BP2-16	8/24/76	0.28	1270	(1000)	Ar	0.1406	Wyodak	207	152	4.903	3.081
BP2-17	9/09/76	3.0	1270	(1000)	Ar	0.1499	Wyodak	184	152	4.380	2.752
BP2-18	9/27/76	0.31	1170	(900)[e]	Ar	0.1388	Wyodak	257	159	6.277	3.944
BP2-19	10/18/76	3.1	1270	(1000)[e]	Ar	0.1383	Wyodak	184	149	4.074	2.560
BP2-20	11/12/76	3.0	870	(600)	Ar	0.1343	Wyodak	172	151	3.901	2.451
BP2-21	11/22/76	3.1	770	(500)	Ar	0.1459	Wyodak	178	152	3.959	2.488
BP2-22	12/09/76	0.30	870	(600)	Ar	0.1365	Wyodak	178	152	4.014	2.522
PB2-23	1/26/77	0.3	1270	(1000)[e]	Ar	0.1334	Pittsburgh	152	152	3.550	3.29
BP2-24	2/11/77	3	1270	(1000)	Ar	0.1348	Pittsburgh	165	160	4.086	3.78
BP2-25	2/25/77	3	1070	(800)	Ar	0.1343	Pittsburgh	222	152	5.087	4.71
BP2-26	3/15/77	0.3	1270	(1000)	Ar	0.1339	Pittsburgh	194	157	4.591	4.25
BP2-27	3/31/77	3	870	(600)	Ar	0.1352	Pittsburgh	152	149	3.518	3.26
BP2-28	4/21/77	0.3	870	(600)	Ar	0.1352	Pittsburgh	184	152	4.421	4.09
BP2-29	5/31/77	1.9-6.1[a]	870	(600)	Ar	0.1312	Pittsburgh	207	152	4.814	4.45
BP2-30	6/27/77	0.3	1270	(1000)	Ar	0.1307	Pittsburgh	222	152	4.857	4.49
BP2-31	7/13/77	0.3	1070	(800)	Ar	0.1285	Pittsburgh	159	160	4.127	3.82
BP2-32	7/25/77	3	1270	(1000)	Ar	0.1299	Pittsburgh	162	156	4.043	3.74
BP2-33	8/13/77	3	910	(640)	H_2	0.1294	Pittsburgh	240	157	6.133	5.24
BP2-34	8/31/77	3	1270	(1000)	H_2	0.1316	Pittsburgh	178	152	4.564	3.64
BP2-35[f]	9/21/77	3	870	(800)	H_2	0.1316	Pittsburgh	219	152	5.384	4.98
BP2-36[f]	10/04/77				H_2		Pittsburgh				
BP2-37	10/17/77	3	1150	(880)	H_2	0.1374	Pittsburgh	184	151	4.217	3.90
BP2-38	10/31/77	14	1160	(890)	H_2	0.1294	Pittsburgh	197	154	4.658	4.31
BP2-39	11/14/77	0.3	1200	(925)	H_2	0.1339	Pittsburgh	225	149	5.000	4.63

Table A-1.1 (continued)

Run number	Date of run	Heating rate (K/min)	Maximum temperature (K)	(°C)	Cover gas: Gas used	Cover gas: Flow rate (mole/min)	Coal block: Coal used	Coal block: Dimensions (mm) Height	Coal block: Dimensions (mm) Diameter	Coal block: Weight (kg)	Coal block: Weight (kg maf)
BP2-40	11/30/77	3.0	1100	(825)	H_2	0.1401	Wyodak	219	152	4.993	3.138
BP2-41	12/15/77	0.3	870	(600)	H_2	0.1339	Pittsburgh	213	135	4.820	4.46
BP2-42	1/10/78	0.3	1170	(900)	H_2	0.1200	Pittsburgh	151	135	3.676	3.40
BP2-43	1/31/78	0.3	1305	(1032)	H_2	0.1370[g]	Pittsburgh	171	151	3.492	3.23
BP2-44	2/13/78	5[h]	920	(650)	H_2	0.1312	Pittsburgh	191	147	4.513	4.18
BP2-45	3/07/78	0.3	1070	(800)	H_2	0.1214	Pittsburgh	198	146	4.513	4.18
BP2-46	3/31/78	3	1070	(800)	H_2	0.1281	Wilcox	159	135	3.609	1.940
BP2-47	4/21/78	3	1270	(1000)	H_2	0.1295	Wilcox	175	151	3.921	2.108
BP2-48	5/04/78	3	870	(600)	H_2	0.1262	Wilcox	168	149	3.743	2.012
BP2-49	5/15/78	0.3	1070	(800)	H_2	0.1336	Wilcox	194	151	4.319	2.321
BP2-50	5/26/78	9	1070	(800)	H_2	0.1238	Wilcox	184	146	3.927	2.111
BP2-51	6/12/78	0.3	1070	(800)	Ar	0.1364	Wilcox	179	146	4.085	2.196
BP2-52	6/26/78	3	1070	(800)[i]	Ar	0.1530	Wilcox	202	149	4.555	2.448
BP2-53	7/12/78	10	1070	(800)	Ar	0.1346	Wilcox	203	149	4.558	2.450
BP2-54	8/04/78	3	1070	(800)	Ar	0.1349	Wilcox	189	151	4.342	2.334
BP2-55	8/30/78	3	1270	(1000)	Ar	0.1303	Wilcox	198	149	4.497	2.417
BP2-56	10/18/78	3	870	(600)	Ar	0.1249	Wilcox	187	152	3.939	2.117
BP2-57	4/20/79	3	1070	(800)	Mix[j]	0.1396	Pittsburgh	175	146	4.040	3.74
PB2-58	5/07/79	3	1070	(800)	Mix[j]	0.1206	Wilcox	194	149	4.353	2.34

[a] Irregular rate.
[b] Aborted at 1070 K (800°C) surface temperature.
[c] Incomplete.
[d] Estimated base flow rate of purge gas.
[e] Coal block dried in vacuum before heating.
[f] Aborted early in heat-up.
[g] Base flow of 0.0247 mol/min during first 5.5 h.
[h] Dried block; heated at 5 K/min to 770 K; held until center reached 670 K; then 5 K/min to 920 K.
[i] Block predried by heating to 405 K (132°C) before 3 K/min heating began.
[j] See Table 2.2 for composition.

Table A-1.2. Cumulative yields of major products from block heating ("block pyrolysis") experiments

Experiment	Coal	Gross yields (kg)				Overall balance (%)	Yields (wt % of maf coal)				
		Char	H_2O	Oils	Gas		Char[a]	H_2O[b]	Oils	Gas	Total
BP 1-4	Wyodak	1.814			1.417		53.4[c]			48.9[a]	
BP 1-7	Wyodak	1.630		1.552[d]	1.913	100.8	45.7		-4.6	60.2	101.3
BP 1-10	Wyodak	2.105		1.825	1.728	101.3	54.7		-1.2	49.5	102.0
BP 1-13	Wyodak	1.659		1.703	1.239	106.4	55.4		9.2	45.6	110.2
BP 2-1	Wyodak	1.508		>1.411[e]			56.5		>4.7[b]		
BP 2-2	Wyodak	1.209		1.136	0.816	98.5	54.3		2.9	40.5	97.7
BP 2-3	Wyodak	1.782		1.478	0.312	96.6	71.0		10.1	13.4	94.5
BP 2-4	Wyodak	2.379		1.843	0.215	99.1	79.2		11.7	7.62	98.6
BP 2-5	Hanna	0.144			0.0363		69.5			18.4	
BP 2-6	Hanna	0.145		0.020	0.0471	91.4	68.2		-1.5	23.3	90.0
BP 2-7	Wyodak	1.569			0.526		58.9			21.6	
BP 2-8	Wyodak	0.1119		>0.054[e]	0.0358		65.2		[b]	22.5	
BP 2-9	Wyodak	0.1039		>0.059[e]	0.0314		59.9		[b]	19.7	
BP 2-10	Wyodak	1.635		1.607	0.500	100.5	64.5		15.0	21.3	100.8
BP 2-11	Wyodak	2.612		2.339	2.131	101.5	54.1		-0.1	48.6	102.6
BP 2-12	Wyodak	2.359		1.912	1.719	97.7	55.9		-4.0	44.5	96.3
BP 2-13	Wyodak	2.320		2.381	0.757	98.5	61.1		14.7	21.7	97.5
BP 2-14	Wyodak	1.710		1.714	0.677	96.4	58.4		10.6	25.3	94.3
BP 2-15	Wyodak	1.877		1.503	1.575	98.5	53.9		-6.1	49.7	97.6
BP 2-16	Wyodak	1.925		1.934	0.771	94.5	57.0		9.3	25.0	91.2
BP 2-17	Wyodak	1.599		1.117	1.354	93.0	52.6		12.9	49.2	88.8
BP 2-18	Wyodak	2.587		2.643	0.970	98.8	60.1		13.5	24.6	98.1
BP 2-19	Wyodak	1.659		1.699	0.689	99.5	59.4		12.9	26.9	99.1
BP 2-20	Wyodak	1.644		1.338	0.490	90.9	62.4		1.1	22.0	85.5
BP 2-21	Wyodak	1.794		1.731	0.371	98.4	67.0		16.1	14.9	98.0
BP 2-22	Wyodak	1.765		1.738			64.9		15.4		
BP 2-23	Pitts.	2.372	0.1710	0.427	0.542	98.9	66.1	3.29	13.00	16.50	98.9

Table A-1.2 (continued)

Experiment	Coal	Gross yields (kg)				Overall balance (%)	Yields (wt % of maf coal)				
		Char	H_2O	Oils	Gas		Char[a]	H_2O[b]	Oils	Gas	Total
BP 2-24	Pitts.	2.346	0.2324	0.311	0.594	100.8[f]	65.4[f]	6.25[f]	9.50[f]	18.14[f]	99.3[f]
BP 2-25	Pitts.	3.335	0.3180	0.434	0.696	94.0	64.7	4.84	9.22	14.79	93.6
BP 2-26	Pitts.	3.235	0.213	0.544	0.696	102.1	70.0	3.10	12.81	16.38	102.3
BP 2-27	Pitts.	2.410	0.1771	0.3579	0.426	95.8	67.9	3.53	10.99	13.09	95.5
BP 2-28	Pitts.	3.183	0.110	0.616	0.418	97.9	71.7	0.78	15.06	10.22	97.7
BP 2-29	Pitts.	3.375	0.686		0.570	96.2	69.6	13.49		12.80	95.9
BP 2-30	Pitts.	3.237	0.1558	0.667	0.973	103.6	65.9	1.55	14.84	21.65	103.9
BP 2-31	Pitts.	2.770	0.1321	0.4948	0.509	100.5	66.4	1.55	12.96	13.33	94.2
BP 2-32	Pitts.	2.624	0.272	0.357	0.769	99.5	64.0	5.36	9.54	20.55	99.5
BP 2-33	Pitts.	4.483	0.4387	0.4454	0.818	100.9	70.3[g]	6.36[g]	8.59[g]	15.78[g]	101.3[g]
BP 2-34	Pitts.	3.213	0.253	0.384	0.663	98.9	65.1[g]	4.73[g]	10.55[g]	18.21[g]	98.6[g]
BP 2-35	Pitts.	3.812	0.321	0.353	0.770	97.6	70.4	4.53	7.09	15.46	97.5
BP 2-37	Pitts.	2.820	0.2134	0.3512	0.668	96.1	66.1	3.56	9.00	17.12	95.8
BP 2-38	Pitts.	3.104	0.2750	0.3020	0.920	98.8	65.9	4.47	7.01	21.36	98.7
BP 2-39	Pitts.	3.149	0.129	0.690	0.657	92.5	61.9	0.88	14.91	14.20	91.9
BP 2-40	Wyodak				1.372					43.71	
BP 2-41	Pitts.	3.357	0.1272	0.5778	0.315	90.8	69.1	0.94	12.96	7.25	90.3
BP 2-42	Pitts.	2.330	0.1218	0.4958	0.635	97.5	62.3	1.67	14.58	18.67	97.2
BP 2-43	Pitts.	2.277	0.1670	0.4071	0.514	96.4	64.3	3.26	12.60	15.91	96.1
BP 2-44	Pitts.	2.846	0.1967	0.5234	0.251	84.6	60.8	4.63	12.31	5.90	83.6
BP 2-45	Pitts.	3.092	0.228	0.518	0.330	92.4	67.9	3.55	12.40	7.90	91.8
BP 2-46	Wilcox	1.402	1.336	0.085	0.722	98.2	56.0	-0.90	4.38	37.22	96.7
BP 2-47	Wilcox	1.380	1.474	0.064	0.925	98.0	49.2	0.17	3.04	43.87	96.3
BP 2-48	Wilcox	1.407	1.574	0.113	0.605	98.8	53.7	8.47	5.62	30.09	97.8
BP 2-49	Wilcox	1.539	2.063	0.109	0.576	99.3	50.0	19.10	4.70	24.81	98.6
BP 2-50	Wilcox	1.620	1.249	0.128	0.843	97.8	60.5	-10.59	6.06	39.96	95.9
BP 2-51	Wilcox	1.619	1.685	0.156	0.577	98.8	57.5	6.97	7.10	26.28	97.8
BP 2-52	Wilcox	1.825	1.713	0.194	0.703	97.4	58.3	0.20	7.92	28.70	95.1

Table A-1.2 (continued)

Experiment	Coal	Gross yields (kg)				Overall balance (%)	Yields (wt % of maf coal)				
		Char	H_2O	Oils	Gas		Char[a]	H_2O[b]	Oils	Gas	Total
BP 2-53	Wilcox	1.427[h]	1.402	0.178	0.995	87.8[h]	42.0[h]	-12.54	7.27	40.61	77.3[h]
BP 2-54	Wilcox	1.694	1.450	0.129	0.802	93.6	56.3	-7.64	5.14	34.36	88.1
BP 2-55	Wilcox	1.576	1.607		1.051	94.2	48.9	-3.28		43.49	89.1
BP 2-56	Wilcox	1.686	1.691	0.090	0.354	97.0	63.4	10.10	4.25	16.71	94.4
BP 2-57	Pitts.	2.745	0.243	0.268	0.630	96.2	66.5	4.7	7.1	16.68	95.0
BP 2-58	Wilcox	1.523	1.651	0.139	0.891	96.6	48.8	0.8	5.9	38.1	93.7

[a]Calculated by subtracting weight of ash in the starting coal from gross weight of char, then dividing by maf coal weight.

[b]Net yield by subtracting coal moisture content.

[c]Maf weight not accurately known because of air-drying of the coal block.

[d]All values in this column represent combined yields of H_2O and oils.

[e]Poor recovery of condensibles.

[f]Based on corrected coal weight (error in weighing is estimated).

[g]Adjusted for ash-rich strata based on char analyses and photographs.

[h]Pyrophoric char; burned extensively.

Table A-1.3. Cumulative yields of gas components from block heating experiments

Experiment	Gas yield (mole/kg maf)									
	H_2	CH_4	C_2H_6	C_2H_4	C_3	C_4	CO	CO_2	H_2S	Total
BP 1-4	19.743	3.085	0.622[a]		0.328	0.060	7.851	3.847	0.015	35.55
BP 1-7	21.430	3.347	0.791		0.335	0.106	8.304	4.251	0.045	38.61
BP 1-10	13.493	5.323	1.586		0.606	0.108	4.216	3.767	0.057	29.16
BP 1-13	14.981	3.609	0.798		0.461	0.080	4.763	3.695	0.129	28.51
BP 2-2	14.247	3.049	0.226	0.256	0.054	0.000	6.226	2.910	0.000	26.97
BP 2-3	1.062	0.985	0.183	0.018	0.142	0.075	0.683	1.631	0.001	4.78
BP 2-4	0.937	1.329	0.193	0.025	0.288	0.176	0.975	2.376	0.019	6.32
BP 2-7	2.912	3.626	0.077	0.000	0.178	0.043	3.002	1.822	0.000	11.66
BP 2-8	2.629	2.468	0.216	0.121	0.257	0.168	1.296	2.631	0.000	9.79
BP 2-9	4.564	1.022	0.213	0.093	0.206	0.072	2.763	1.697	0.003	10.63
BP 2-10	4.737	2.760	0.196	0.054	0.117	0.109	1.572	2.233	0.053	11.83
BP 2-11	8.757	3.539	0.239	0.313	0.114	0.070	7.990	3.856	0.016	24.89
BP 2-12	14.852	3.833	0.213	0.230	0.098	0.063	6.380	3.641	0.016	29.32
BP 2-13	5.526	2.905	0.226	0.020	0.184	0.062	2.478	1.708	0.003	13.11
BP 2-14	6.493	2.862	0.240	0.011	0.235	0.069	3.234	1.949	0.003	15.10
BP 2-15	16.400	3.097	0.185	0.138	0.109	0.042	8.697	3.494	0.006	32.17
BP 2-16	7.778	2.993	0.218	0.015	0.208	0.065	2.593	2.136	0.000	16.01
BP 2-17	18.518	2.778	0.172	0.114	0.088	0.032	8.708	3.413	0.010	33.83
BP 2-18	7.679	2.684	0.191	0.028	0.106	0.042	2.598	2.329	0.000	15.66
BP 2-19	8.433	2.798	0.175	0.104	0.111	0.049	3.396	2.180	0.004	17.25
BP 2-20	3.120	2.225	0.285	0.129	0.286	0.129	1.171	2.578	0.001	9.92
BP 2-21	0.699	1.432	0.229	0.032	0.224	0.086	0.848	1.789	0.000	5.34
BP 2-23	8.817	3.066	0.546	0.025	0.240	0.094	0.758	0.288	0.029[b]	13.863
BP 2-24	7.08	3.78	0.305	0.413	0.205	0.079	0.696	0.719	0.020[b]	12.80
BP 2-25	5.886	3.449	0.299	0.395	0.146	0.062	0.589	0.212	0.251	11.289
BP 2-26	7.541	2.959	0.330	0.008	0.725	0.106	0.892	0.170	0.170	12.543
BP 2-27	2.200	2.851	0.468	0.198	0.415	0.155	0.301	0.201	0.096	6.885

Table A-1.3 (continued)

Experiment	Gas yield (mole/kg maf)									
	H_2	CH_4	C_2H_6 [a]	C_2H_4	C_3	C_4	CO	CO_2	H_2S	Total
BP 2-28	2.062	2.084	0.346	0.016	0.192	0.098	0.301	0.153	0.113	5.365
BP 2-29	3.208	3.208	0.361	0.171	0.253	0.095	0.563	0.196	0.000[b]	8.056
BP 2-30	7.131	2.945	0.450	0.010	0.275	0.157	1.026[c]	1.049[c]	0.263	13.306
BP 2-31	5.965	2.613	0.366	0.009	0.164	0.089	0.775	0.188	0.133	10.301
BP 2-32	7.577	4.498	0.335	0.520	0.166	0.062	1.084	0.260	0.134	14.636
BP 2-33	0.867	4.003	0.575	0.413	0.383	0.112	0.470	0.255	0.154	7.232
BP 2-34	9.592	4.261	0.497	0.412	0.230	0.079	1.456	0.247	0.129	16.902
BP 2-35	4.186	4.369	0.339	0.583	0.093	0.031	0.503	0.195	0.118	10.416
BP 2-37	5.596	4.324	0.356	0.421	0.158	0.054	0.889	0.216	0.096	12.110
BP 2-38	5.489	4.971	0.321	0.676	0.068	0.042	1.914	0.243	0.024[b]	13.748
BP 2-39	1.486	4.092	0.311	0.007	0.114	*d*	0.651	0.149	0.899[e]	7.709
BP 2-40	6.994	4.731	1.779[a]		0.420	*d*	3.224	2.995	*f*	20.14
BP 2-41	-4.275	2.468	0.443		0.165	*d*	0.149	0.124	0.236	-0.691
BP 2-42	0.400	5.493	0.399		0.124	*d*	0.982	0.188	1.154[e]	8.740
BP 2-43	2.173	4.632	0.555		0.170	*d*	1.093	0.267	0.303	9.193
BP 2-44	3.699	1.160	0.487		0.111	*d*	0.287	0.152	0.099	5.995
BP 2-45	1.754	2.927	0.328		*f*	*d*	0.416	0.114	0.012[b]	5.551
BP 2-46	9.83	3.602	0.363		0.085	*d*	5.35	2.871	0.117	22.22
BP 2-47	12.51	4.428	0.27		0.053	*d*	6.53	3.32	0.092	27.20
BP 2-48	4.239	3.849	0.465		0.1138	*d*	2.482	3.189	0.060	14.40
BP 2-49	-1.8478	6.140	0.408		0.1111	*d*	1.9009	1.849	0.052	8.61
BP 2-50	9.338	3.597	0.537		0.099	*d*	4.79	3.78	0.068	22.21
BP 2-51	6.02	1.399	0.274		0.085	*d*	3.62	2.49	0.160	14.05
BP 2-52	8.57	1.966	0.554		0.1583	*d*	3.44	2.609	0.109	17.41
BP 2-53	13.202	2.105	0.468		0.1003	*d*	4.86	4.29	0.075	25.10

Table A-1.3 (continued)

Experiment	Gas yield (mole/kg maf)									
	H_2	CH_4	C_2H_6	C_2H_4	C_3	C_4	CO	CO_2	H_2S	Total
BP 2-54	10.935	1.934	0.344		0.069	[d]	4.42	3.37	0.154	21.23
BP 2-55	16.400	2.604	0.270		0.059	[d]	7.38	3.15	0.121	29.98
BP 2-56	2.501	0.565	0.320		0.1178	[d]	1.439	2.092	0.177	7.21
BP 2-57	6.44	5.32	0.65		0.069	[d]	1.032	0.263	0.38	14.15
BP 2-58	11.38	3.87	0.46		0.258	[d]	3.99	3.53	0.116	23.60

[a] All values in this column represent combined yields of C_2H_6 and C_2H_4.

[b] Low sulfur content of the coal sample may have caused low H_2S yields.

[c] Possibly an inclusion of carbonate minerals may have caused high CO and CO_2 yields.

[d] NR = Not reported.

[e] Pyrite lenses may have been present, causing abnormally high H_2S yields; alternatively, significant hydrodesulfurization of sulfur that is normally refractory may have occurred.

[f] ND = None detected.

Table A-1.4. Effluent flow rates during experiment BP2-55, pyrolysis of Wilcox lignite in Ar at 3 K/min to 1330 K (1060°C).

Elapsed run time (h:min)	Reactor temperature (°C)	Gas evolution rates[a] (slpm)						
		H_2	CO_2	$C_2(s)$	H_2S	$C_3(s)$	CH_4	CO
1:10	336	0.006	0.008	0.0001	0.001			
1:30	410	0.024	0.050	0.001	0.005		0.002	0.008
1:50	490	0.068	0.153	0.012	0.020	0.005	0.019	0.075
2:10	573	0.157	0.326	0.054	0.035	0.022	0.078	0.202
2:30	634	0.454	0.521	0.111	0.039	0.042	0.174	0.307
2:50	706	1.549	0.979	0.169	0.043	0.062	0.329	0.473
3:10	780	3.363	1.457	0.168	0.035	0.043	0.558	0.832
3:30	828	4.522	1.514	0.137	0.029	0.010	0.789	1.381
3:50	873	5.930	1.639	0.115	0.027		1.091	2.130
4:10	903	5.459	1.238	0.063	0.019		1.040	2.262
4:30	929	4.665	0.838	0.029	0.016		0.909	2.141
4:50	953	4.410	0.668	0.017	0.016		0.881	2.189
5:10	976	3.653	0.423	0.008	0.011		0.706	1.901
5:30	1000	2.877	0.108	0.001	0.009		0.474	1.496
5:50	1023	1.913	0.021		0.010		0.272	0.975
6:10	1054	1.904	0.019		0.007		0.261	0.979
6:30	1061	1.121	0.010		0.004		0.148	0.580
6:50	1061	0.817	0.006		0.004		0.088	0.413
7:10	1062	0.355	0.003		0.003		0.038	0.224
7:30	1062	0.105	0.001		0.001		0.013	0.084
7:50	1062	0.125	0.002		0.002		0.016	0.104

[a]Flow rates in standard liters per minute (slpm); divide by 1344.6 to obtain mole/s. Flow of Ar purge gas was 2.921 slpm.

Table A-1.5. Effluent flow rates during experiment BP2-17, pyrolysis of Wyodak subbituminous coal in Inert purge gas (Ar) at 3 K/min to 1270 K (1000°C)

Sample No.	Reactor temperature (°C)	Time (h)	Volumetric flow rates[a] (slpm/kg maf coal)												Total, H_2O-free
			H_2	CH_4	H_2S	CO_2	$C_2(s)$	$C_3(s)$	$C_4(s)$	$C_5(s)$	Benzene	Toluene	CO	H_2O	
1	161	0.67	0.0	0.0	0.0	0.001	0.0	0.0	0.0	0.0	0.0	0.0	0.0	0.007	0.001
2	216	1.00	0.0	0.0	0.0	0.001	0.0	0.0	0.0	0.0	0.0	0.0	0.0	0.009	0.001
3	468	2.17	0.015	0.014	0.0	0.092	0.004	0.007	0.002	0.001	0.0	0.0	0.022	0.013	0.157
4	500	2.33	0.030	0.033	0.0	0.133	0.015	0.004	0.005	0.003	0.0	0.0	0.035	0.019	0.258
5	535	2.50	0.065	0.076	0.0	0.172	0.028	0.007	0.007	0.004	0.0	0.0	0.054	0.018	0.413
6	565	2.67	0.089	0.104	0.0	0.177	0.029	0.009	0.006	0.003	0.0	0.0	0.066	0.011	0.484
7	594	2.83	0.289	0.243	0.001	0.308	0.045	0.019	0.012	0.002	0.001	0.0	0.108	0.020	1.027
8	625	3.00	0.167	0.185	0.0	0.246	0.037	0.016	0.009	0.002	0.001	0.0	0.090	0.012	0.755
9	655	3.17	0.493	0.245	0.0	0.424	0.048	0.021	0.009	0.002	0.002	0.001	0.121	0.028	1.368
10	685	3.33	0.696	0.288	0.0	0.518	0.048	0.019	0.006	0.0	0.003	0.001	0.160	0.019	1.740
11	707	3.50	1.360	0.414	0.001	0.639	0.051	0.019	0.004	0.0	0.005	0.001	0.247	0.026	2.741
12	736	3.67	1.815	0.484	0.002	0.726	0.052	0.012	0.002	0.0	0.005	0.001	0.472	0.044	3.571
13	755	3.83	1.896	0.435	0.001	0.692	0.044	0.011	0.0	0.0	0.005	0.001	0.592	0.040	3.676
14	755	4.00	1.922	0.438	0.0	0.597	0.036	0.007	0.0	0.0	0.006	0.001	0.720	0.040	3.726
15	809	4.17	2.598	0.567	0.001	0.623	0.037	0.005	0.0	0.0	0.007	0.001	1.182	0.056	5.021
16	857	4.50	2.558	0.484	0.001	0.463	0.027	0.001	0.001	0.0	0.007	0.0	1.564	0.033	5.106
17	910	4.83	3.043	0.336	0.001	0.240	0.012	0.003	0.0	0.0	0.005	0.0	1.588	0.042	5.229
18	955	5.17	2.951	0.212	0.001	0.106	0.011	0.002	0.0	0.0	0.005	0.0	1.654	0.054	4.941
19	975	5.33	3.094	0.166	0.001	0.063	0.012	0.002	0.0	0.0	0.003	0.0	1.763	0.058	5.105
20	987	5.50	2.608	0.097	0.001	0.035	0.008	0.002	0.0	0.0	0.002	0.0	1.396	0.054	4.150
21	991	5.67	1.993	0.066	0.001	0.020	0.007	0.001	0.0	0.0	0.001	0.0	1.159	0.038	3.248
22	995	5.83	1.625	0.040	0.001	0.010	0.006	0.001	0.0	0.0	0.001	0.0	0.864	0.040	2.547
23	1000	6.17	1.023	0.010	0.0	0.003	0.002	0.0	0.0	0.0	0.0	0.0	0.257	0.030	1.295
24	1000	6.33	0.475	0.003	0.0	0.001	0.0	0.0	0.0	0.0	0.0	0.0	0.065	0.016	0.544
25	1000	6.67	0.175	0.001	0.0	0.001	0.0	0.0	0.0	0.0	0.0	0.0	0.027	0.012	0.204
Integrated total, sl/kg maf			414.9	62.2	0.2	76.5	6.4	2.0	0.7	0.2	0.8	0.12	195.2	10.4	759.2

[a]Flows in standard liters per minute per kg maf coal; divide by 1344.6 to obtain mole/s·kg.

Table A-1.6. Effluent flow rates during experiment BP2-24, pyrolysis of Pittsburgh bituminous coal in inert purge gas (Ar) at 3 K/min to 1257 K (984°C)

Reactor temperature (°C)	Time (h)	Volumetric flow rates[a] (slpm/kg maf coal)													Total, H_2O-free
		H_2	CH_4	H_2S	CO_2	C_2H_6	C_2H_4	C_3(s)	C_4(s)	C_5(s)	Benzene	Toluene	CO	H_2O	
71	0.25	0.0	0.0	0.0	0.0	0.0	0.0	0.0	0.0	0.0	0.0	0.0	0.0	0.005	0.0
440	2.08	0.014	0.046	0.0	0.005	0.009	0.0	0.014	0.006	0.002	0.0	0.0	0.001	0.009	0.096
490	2.42	0.053	0.132	0.0	0.009	0.030	0.004	0.021	0.011	0.004	0.0	0.0	0.009	0.008	0.275
539	2.67	0.111	0.243	0.001	0.012	0.023	0.034	0.035	0.019	0.005	0.001	0.0	0.021	0.010	0.503
595	3.00	0.207	0.355	0.001	0.019	0.060	0.032	0.047	0.019	0.003	0.002	0.001	0.024	0.012	0.771
650	3.33	0.360	0.476	0.003	0.031	0.064	0.059	0.046	0.004	0.001	0.003	0.0	0.052	0.021	1.099
700	3.67	0.470	0.494	0.003	0.034	0.046	0.077	0.029	0.007	0.0	0.005	0.002	0.065	0.027	1.241
750	4.00	0.683	0.589	0.003	0.035	0.045	0.105	0.011	0.004	0.0	0.008	0.002	0.090	0.024	1.575
809	4.33	0.894	0.571	0.003	0.032	0.026	0.093	0.001	0.002	0.0	0.012	0.002	0.107	0.032	1.741
863	4.58	1.221	0.574	0.003	0.028	0.016	0.061	0.0	0.001	0.0	0.015	0.002	0.122	0.037	2.042
915	4.83	1.553	0.548	0.003	0.025	0.009	0.033	0.0	0.003	0.0	0.020	0.001	0.138	0.053	2.334
958	5.08	1.735	0.448	0.002	0.018	0.004	0.0	0.0	0.001	0.0	0.013	0.0	0.133	0.033	2.354
984	5.25	1.578	0.327	0.001	0.012	0.002	0.004	0.001	0.0	0.0	0.011	0.0	0.120	0.039	2.056
975	5.50	0.934	0.017	0.001	0.002	0.001	0.0	0.0	0.001	0.0	0.003	0.0	0.050	0.024	1.009
972	5.67	0.337	0.003	0.0	0.001	0.0	0.0	0.0	0.0	0.0	0.001	0.0	0.023	0.014	0.366
972	6.00	0.128	0.002	0.0	0.001	0.0	0.0	0.0	0.0	0.0	0.001	0.0	0.012	0.009	0.144
Integrated total, sl/kg maf		158.69	84.71	0.44	4.91	6.83	9.25	4.60	1.76	0.34	1.50	0.16	15.60	6.59	288.80

[a]Flows in standard liters per minute per kg of maf coal; divide by 1344.6 to obtain mole/s·kg.

Table A-1.7. Effluent flow rates during experiment BP2-34, pyrolysis of Pittsburgh bituminous coal in H_2 at 3 K/min to 1273 K (1000°C)

	Temperature (°C)	Time (h)	Volumetric flow rates[a] (slpm/kg maf coal)													
			H_2	CH_4	H_2S	CO_2	C_2	C_3	C_4	C_5	C_6	Benzene	Toluene	N_2	CO	H_2O
1	245	1.00	0.0589	0.0005	0.0	0.0008	0.0004	0.0	0.0	0.0	0.0	0.0	0.0	0.0002	0.0	0.0037
2	395	2.00	0.0058	0.0100	0.0	0.0029	0.0002	0.0018	0.0008	0.0	0.0	0.0	0.0	0.0000	0.0019	0.0055
3	485	2.75	0.0093	0.0374	0.0006	0.0064	0.0136	0.0084	0.0035	0.0020	0.0010	0.0001	0.0002	0.0000	0.0057	0.0084
4	560	3.25	0.2782	0.1869	0.0009	0.0134	0.0596	0.0259	0.0102	0.0058	0.0033	0.0001	0.0003	0.0000	0.0358	0.0106
6	700	4.25	0.3719	0.3551	0.0137	0.0205	0.0900	0.0368	0.0137	0.0010	0.0	0.0028	0.0008	0.0000	0.0543	0.0112
7	760	4.75	0.5618	0.5758	0.0215	0.0307	0.1581	0.0233	0.0066	0.0	0.0	0.0055	0.0018	0.0000	0.0981	0.0312
8	830	5.25	1.1319	0.7722	0.0149	0.0368	0.1413	0.0046	0.0015	0.0	0.0	0.0128	0.0021	0.0000	0.1909	0.0362
9	890	5.50	1.4777	0.5655	0.0039	0.0255	0.0691	0.0027	0.0	0.0	0.0	0.0109	0.0009	0.0000	0.1533	0.0215
10	1000	6.00	1.8094	0.1321	0.0071	0.0068	0.0026	0.0021	0.0	0.0	0.0	0.0026	0.0003	0.0187	0.2047	0.0365
11	990	6.50	0.2491	0.0130	0.0027	0.0007	0.0008	0.0009	0.0	0.0	0.0	0.0004	0.0002	0.0210	0.0457	0.0093
12	1000	7.00	0.0817	0.0088	0.0023	0.0007	0.0009	0.0	0.0	0.0	0.0	0.0	0.0	0.0099	0.0324	0.0081
13	1000	7.50	0.0719	0.0078	0.0019	0.0006	0.0005	0.0	0.0	0.0	0.0	0.0002	0.0	0.0040	0.0255	0.0094
14	1000	8.50	0.0268	0.0056	0.0010	0.0003	0.0002	0.0007	0.0	0.0	0.0	0.0	0.0	0.0038	0.0113	0.0098
15	1000	9.50	0.0277	0.0051	0.0011	0.0002	0.0005	0.0006	0.0	0.0	0.0	0.0	0.0	0.0000	0.0156	0.0090
16	1000	10.50	0.003	0.0039	0.0014	0.0002	0.0003	0.0005	0.0	0.0	0.0	0.0	0.0	0.0000	0.0152	0.0078
Integrated total, sl/kg maf			179.14	79.57	2.41	4.60	16.98	4.29	1.48	0.38	0.19	0.94	0.19	1.91	27.23	7.67

[a]Flows normalized on basis of coal weight (maf) and having purge gas flow subtracted (2.95 slpm); divide by 1344.6 to obtain mol/s·kg.

Table A-1.8. Miscellaneous properties of gases from block heating experiments

Experiment	Average molecular weight[a]	Higher heating value (Btu/scf[b])	Cold gas efficiency (%)[c]
BP 1-4	14.50	420.1	42.50
BP 1-7	14.57	426.1	46.82
BP 1-10	16.42	571.5	47.42
BP 1-13	15.33	478.1	38.80
BP 2-2	14.70	416.6	31.97
BP 2-3	26.22	551.5	7.50
BP 2-4	29.24	603.7	10.86
BP 2-7	20.65	568.7	18.87
BP 2-8	23.26	593.0	16.52
BP 2-9	18.80	462.9	14.01
BP 2-10	18.31	528.7	17.80
BP 2-11	19.82	441.6	31.29
BP 2-12	15.40	429.3	35.83
BP 2-13	16.88	531.6	19.84
BP 2-14	17.03	508.8	21.86
BP 2-15	15.45	400.1	36.63
BP 2-16	15.62	495.0	22.55
BP 2-17	14.49	387.4	37.30
BP 2-18	15.80	459.1	20.46
BP 2-19	15.59	462.5	22.71
BP 2-20	22.19	580.3	16.39
BP 2-21	27.96	637.9	9.70
BP 2-23	9.71	616	20.0
BP 2-24	10.50	696	24.4
BP 2-25	11.65	701	18.5
BP 2-26	11.84	718	21.1
BP 2-27	17.00	984	15.8
BP 2-28	15.15	857	10.7
BP 2-29	14.19	826	15.6
BP 2-30	13.53	615	19.2
BP 2-31	10.86	640	15.1
BP 2-32	11.56	687	23.5
BP 2-33	20.38	1107	18.7
BP 2-34	10.93	647	25.6
BP 2-35	13.21	804	19.6
BP 2-37	12.45	735	20.8
BP 2-38	13.81	726	23.3
BP 2-39	17.98	853	15.4
BP 2-40	19.06	643	36.9
BP 2-41	*d*	*d*	42.4
BP 2-42	20.7	933	19.1
BP 2-43	16.9	839	18.0
BP 2-44	10.6	641	9.0
BP 2-45	13.9	805	10.5

Table A-1.8. (Continued)

Experiment	Average molecular weight[a]	Higher heating value (Btu/scf[b])	Cold gas efficiency (%)[c]
BP 2-46	16.75	449.3	30.11
BP 2-47	16.13	437.8	35.92
BP 2-48	20.90	526.6	22.87
BP 2-49	[d]	[d]	23.01
BP 2-50	17.99	447.5	29.98
BP 2-51	18.71	399.3	16.92
BP 2-52	16.49	442.0	23.20
BP 2-53	16.18	381.6	28.88
BP 2-54	16.19	387.0	24.78
BP 2-55	14.50	387.5	35.05
BP 2-56	23.17	410.0	8.92
BP 2-57	12.30	696	23.0
BP 2-58	16.14	464.6	33.07

[a]Molecular weight and higher heating values are reported as molar or volumetric averages.

[b]Standard cubic feet at 70°F, 1 atm (in comparison, standard liters are at 273 K, 1 atm).

[c]Computed from Btu of HHV in the product gas as a percentage of Btu of the starting coal and of any consumed H_2.

[d]Does not apply; H_2 yield is negative (i.e., purge H_2 was consumed).

Table A-1.9. Pyrophoricity data from charred blocks of Wilcox lignite, Wyodak subbituminous coal, and Hanna bituminous coal

Experiment	Coal	Initial temperature rise (K/min)	Maximum temperature (K)
BP2-3	Wyodak	2.30	>628
BP2-4	Wyodak	1.62	>543
BP2-5	Hanna	0.9	320
BP2-6	Hanna	0.7	322
BP2-7	Wyodak	2.10	>573
BP2-8	Wyodak	14.6	>548
BP2-9	Wyodak	20.1	522
BP2-10	Wyodak	4.4	533
BP2-11	Wyodak	3.3	404
BP2-12	Wyodak	2.6	>556
BP2-13	Wyodak		418
BP2-14	Wyodak		373
BP2-15	Wyodak		490
BP2-16	Wyodak	2.07	372
BP2-17	Wyodak	3.22	368
BP2-18	Wyodak	1.97	373
BP2-19	Wyodak	3.27	377
BP2-20	Wyodak	2.6	798
BP2-21	Wyodak	0.47	565
BP2-22	Wyodak	1.81	583
BP2-46	Wilcox	1.76	
BP2-47	Wilcox	[a]	
BP2-48	Wilcox	0.26	
BP2-49	Wilcox	[a]	
BP2-50	Wilcox	<0.1	
BP2-51	Wilcox	7.9	
BP2-52	Wilcox	12.8	
BP2-53	Wilcox	3.74	[b]
BP2-54	Wilcox	5.09	
BP2-55	Wilcox	0.73	
BP2-56	Wilcox	2.14	

[a] Block collapsed during removal from the reactor.

[b] Block could not be returned to the reactor to be quenched, so it burned extensively.

Table A-1.10. Consumption of water by block pyrolysis of Wilcox lignite in inert gas

Surface heating rate (K/min)	Water consumption[a] (kg H_2O/kg maf coal) at maximum temperature		
	873 K (600°C)	1073 K (800°C)	1273 K (1000°C)
0.3		0.033	
3	-0.001	0.179[b]	0.17-0.20[c]
10		0.228	

[a]Consumption was calculated by difference between water yield from powder and net yield from the blocks, as reported in Table A-1.2. Source of data on powder yields: J. B. Goodman, M. Gomez, and V. F. Parry, Laboratory Carbonization Assay of Low-rank Coals at Low, Medium, and High Temperatures, U.S. Bureau of Mines RI-5383, January 1958.

[b]Consumption was calculated to be 0.101 kg H_2O/kg maf coal from a predried block heated at 3 K/min. Other yields from that experiment indicated water yield was low, probably because of evaporation while the reactor was purged with dry inert gas during drying of the block.

[c]Approximate separation of water and organic liquids.

Appendix A-2

List of Publications, Presentations, and Data Notebooks Resulting from this Project

Appendix A-2. List of publications, presentations, and data notebooks resulting from this project

Outside publications and presentations

1. Monthly, Quarterly, and Annual Progress Reports of the ORNL Fossil Energy Program (Coal Technology Program), L. E. McNeese or J. P. Nichols (Ed.), August 1974 - July 1979.

2. P. R. Westmoreland and L. S. Dickerson, "Pyrolysis of Blocks of Lignite," In Situ 4 (4) (to be published in Fall 1980).

3. R. W. Lyczkowski and P. R. Westmoreland, "The Role of Drying in Underground Coal Conversion Processes," Keynote Lecture at 2nd International Symposium on Drying, McGill University, Montreal, Canada, July 6-9, 1980 (to be published in Advances in Drying).

4. P. R. Westmoreland, "Measurement of Thermal Diffusivity and Application to In Situ Coal Gasification," Proceedings of the 14th Intersociety Energy Conversion Engineering Conference, Boston, Mass., Aug. 5-10, 1979.

5. P. R. Westmoreland and L. S. Dickerson, "A Review of Supporting Research at Oak Ridge National Laboratory for Underground Coal Conversion," pp. 437-449 in Proceedings of the 5th Underground Coal Conversion Symposium, CONF-790630, U.S. Department of Energy, May 1979.

6. G. L. Alexander, B. V. Hu, and A. H. Kwai, Coal Block Pyrolysis: Effects of Changing Surface Characteristics, ORNL/MIT-294, Oak Ridge National Laboratory, Oak Ridge, Tenn., 1979.

7. P. R. Westmoreland and L. S. Dickerson, "Pyrolysis of Blocks of Texas Lignite," presented at the 86th National Meeting of AIChE, Houston, Tex., April 1-5, 1979.

8. P. R. Westmoreland, "Pyrolysis of Bituminous Coal Blocks," pp. 423-433 in Proceedings of the 4th Underground Coal Conversion Symposium, SAND 78-0941, Sandia National Laboratories, Albuquerque, N. Mex., June 1978.

9. P. R. Westmoreland, R. C. Forrester III, and A. P. Sikri, "In Situ Gasification: Recovery of Inaccessible Coal Reserves," vol. 7, pp. 3113-3132 in Proceedings of the International Conference on Alternative Energy Sources, Miami Beach, Fla., Dec. 1977.

10. R. C. Forrester, "Macroscopic Sample Effects on the Pyrolysis of Bituminous and Subbituminous Coals at Underground Coal Gasification Heating Rates," pp. 203-210 in Proceedings of the 3rd Annual Underground Coal Conversion Symposium, CONF-770652, Lawrence Livermore National Laboratory, Livermore, Calif., 1977.

11. P. R. Westmoreland and R. C. Forrester III, "Pyrolysis of Large Coal Blocks: Implications of Heat and Mass Transport Effects for In Situ Gasification," presented at the 173rd National Meeting of the American Chemical Society, New Orleans, La., March 21-25, 1977, Division of Fuel Chemistry Preprint 22 (1).

12. R. C. Forrester III and P. R. Westmoreland, "Two-Dimensional Pyrolysis Effects During In Situ Coal Gasification: Preliminary Results," paper SPE-6150, presented at the 51st Annual Fall Technical Conference of the Society of Petroleum Engineers, New Orleans, October 3-6, 1976; J. Pet. Technol. 31 571-573 (May 1979).

13. R. C. Forrester III, "Recovery of Inaccessible Coal Reserves by In Situ Gasification," in Proceedings of the 11th Intersociety Energy Conversion Engineering Conference, State Line, Nev., Sept. 1976.

14. R. C. Forrester, "Two-dimensional Studies of Coal Pyrolysis: Preliminary Results," pp. 402-410 in Proceedings of the 2nd Annual Underground Coal Gasification Symposium, MERC/SP-76-3, Morgantown Energy Research Center, Morgantown, W. Va., Aug. 1976.

15. P. R. Westmoreland, "Coal Pyrolysis in Underground Gasification," presented at the 11th Annual Southeastern Seminar on Thermal Sciences, University of Tennessee, Knoxville, Tenn., April 28-29, 1975.

Data Notebooks:

The following are the identification numbers of the registered data notebooks in which the original data are recorded.

Number	Contents
A-7262	Log for experiments BP1-1 through BP1-11
A-7523-G	Log for experiments BP1-12 through BP1-14
A-7443	Log of data reports for BP1 series
A-7514	Log of tar demister testing
A-7649-G	Logs for experiments BP2-1 through BP2-26
A-7973-G	Logs for experiments BP2-27 through BP2-55
A-8528-G	Log for experiments BP2-55 through BP2-58 and OB series

ORNL/TM-7313
Dist. Category UC-90d

INTERNAL DISTRIBUTION

1. R. E. Barker
2. C. H. Brown, Jr.
3. G. M. Caton
4. H. D. Cochran, Jr.
5. E. L. Fuller
6. W. R. Gambill
7. R. W. Glass
8-9. J. R. Hightower
10. J. K. Huffstetler
11. J. E. Jones, Jr.
12. R. P. Krishnan
13. K. H. Lin
14. L. E. McNeese
15. T. W. Pickel
16. L. W. Rickert
17. B. R. Rodgers
18. M. Siman-tov
19. I. Spiewak
20. M. G. Stewart
21. V. J. Tennery
22-26. P. R. Westmoreland
27. J. E. Wortman
28. E. L. Youngblood
29. W. H. Corcoran (Consultant)
30-31. Central Research Library
32. ORNL — Y-12 Technical Library Document Reference Section
33-34. Laboratory Records
35. Laboratory Records - RC
36. ORNL Patent Section

EXTERNAL DISTRIBUTION

37. Office of Assistant Manager for Energy Research and Development, DOE-ORO, Oak Ridge, Tenn. 37830.

38-42. R. C. Forrester III, Fluor Corporation, Irvine, Calif.

43-47. J. B. Gibson, Dow Chemical Company, Plaquemines, La.

49. B. B. Bader, Sandia Laboratories, Division 5732, Albuquerque, New Mexico 87115.

50. C. F. Brandenburg, Laramie Energy Technology Center, P. O. Box 3395, University Station, Laramie, Wyoming 82071

51. E. L. Burwell, Mailstop D-107, Germantown, Division of Fossil Fuels Extraction, Department of Energy, Washington, D.C. 20545.

52. D. L. Buskirk, Exxon Production Research Company, P. O. Box 2189, Houston, Texas 77001.

53. R. F. Chaiken, Pittsburgh Research Center, U.S. Bureau of Mines, 4800 Forbes Avenue, Pittsburgh, Pennsylvania 15213.

54. R. C. Corlett, University of Washington, Department of Mechanical Engineering, FU-10, Seattle, Washington 98195.

55. J. H. Daniel, Gulf Research and Development Company, P. O. Drawer 2038, Pittsburgh, Pennsylvania 15230.

56. C. W. Draffin, Mailstop D-107, Germantown, Division of Fossil Fuels Extraction, Department of Energy, Washington, D.C. 20545.

57. G. W. Douglas, Department of Mechanical Engineering, University of Alabama, P. O. Box 2908, University, Alabama 35486.

58. T. F. Edgar, Department of Chemical Engineering, University of Texas, Austin, Texas 78712.

59. V. S. Engleman, Science Application, Inc., P. O. Box 2351, La Jolla, California 92038.

60. H. C. Ganow, Lawrence Livermore Laboratory, P. O. Box 808, Livermore, California 94550.

61. J. F. Grant, Basic Resources, Inc., 2001 Bryan Tower, Dallas, Texas 75201.

62. M. Greenfeld, Alberta Research Council, 11315-87 Avenue, Edmonton, Alberta T6G 2C2, Canada.

63. R. D. Gunn, Department of Mineral Engineering, University of Wyoming, Laramie, Wyoming 82071.

64. R. Hertzberg, Director, Mailstop D-107, Germantown, Division of Fossil Fuels Extraction, Department of Energy, Washington, D.C. 20545.

65. R. W. Hill, Lawrence Livermore Laboratory, P. O. Box 808, Livermore, California 94550.

66. P. J. Hommert, Sandia Laboratories, Division 5732, Albuquerque, New Mexico 87115.

67. J. B. Howard, Department of Chemical Engineering, Building 66, Massachusetts Institute of Technology, Cambridge, Massachusetts 02139.

68. R. Jiacolletti, Project Manager, UCC, Laramie Energy Technology Center, P. O. Box 3395, University Station, Laramie, Wyoming 82071.

69. R. W. Lyczkowski, Department of Gas Engineering, Institute of Gas Technology, 3424 South State Street, IIT Center, Chicago, Illinois 60616.

70. J. W. Martin, Morgantown Energy Technology Center, P. O. Box 880, Morgantown, West Virginia 26505.

71. W. L. Noll, Denver Project Office, Department of Energy, Suite 211, 1075 South Yukon Street, Lakewood, Colorado 80226.

72. R. E. Pennington, Exxon Research and Engineering Company, P. O. Box 4255, Baytown, Texas 77520.

73. W. A. Peters, Room 66-240, Massachusetts Institute of Technology, Cambridge, Massachusetts 02139.

74. G. Savins, Mobil - MRDC, P. O. Box 900, Dallas, Texas 75221.

75. L. A. Schrider, Morgantown Energy Technology Center, P. O. Box 880, Morgantown, West Virginia 26505.

76. R. A. Schraufnagel, ARCO Oil and Gas Company, P. O. Box 2819, Dallas, Texas 75221.

77. S. H. Schwartz, Department of Mechanical Engineering and Mechanics, West Virginia University, Morgantown, West Virginia 26505.

78. J. W. Sibert III, ARCO Oil and Gas Company, P. O. Box 2819, Dallas, Texas 75221.

79. D. R. Stephens, Lawrence Livermore Laboratory, P. O. Box 808, Livermore, California 94550.

80. I. M. Stewart, University of Newcastle, Shortland, New South Wales, Australia.

81. L. D. Strickland, Morgantown Energy Technology Center, P. O. Box 880, Morgantown, West Virginia 26505.

82. R. Strickland, Petroleum Engineering Department, Texas A&M University, College Station, Texas 77843.

83. C. B. Thorsness, Lawrence Livermore Laboratory, P. O. Box 808, Livermore, California 94550.

84. N. E. Vanderborgh, Los Alamos Scientific Laboratory, P. O. Box 1663, Los Alamos, New Mexico 87544.

85. J. Wheeler, Exxon Production Research Company, P. O. Box 2189, Houston, Texas 77001.

86. J. E. Young, Argonne National Laboratory, 9700 South Cass Avenue, Argonne, Illinois 60439.

87-389. Given distribution as shown in TIC-4500 under Coal Conversion and Utilization — Liquefaction Category (25 copies - NTIS).

☆U.S. GOVERNMENT PRINTING OFFICE: 1981-740-062/96

CAL